

Ad-hoc Networks: Fundamental Properties and Network Topologies

Ramin Hekmat

 Springer

AD-HOC NETWORKS: FUNDAMENTAL
PROPERTIES AND NETWORK TOPOLOGIES

Ad-hoc Networks: Fundamental Properties and Network Topologies

by

RAMIN HEKMAT

*Delft University of Technology, The Netherlands
and
Rhyzen Information and Consulting Services,
Zoetermeer, the Netherlands*

 Springer

A C.I.P. Catalogue record for this book is available from the Library of Congress.

ISBN-10 1-4020-5165-4 (HB)
ISBN-13 978-1-4020-5166-1 (HB)
ISBN-10 1-4020-5166-2 (e-book)
ISBN-13 978-1-4020-5165-4 (e-book)

Published by Springer,
P.O. Box 17, 3300 AA Dordrecht, The Netherlands.

www.springer.com

Printed on acid-free paper

All Rights Reserved

© 2006 Springer

No part of this work may be reproduced, stored in a retrieval system, or transmitted in any form or by any means, electronic, mechanical, photocopying, microfilming, recording or otherwise, without written permission from the Publisher, with the exception of any material supplied specifically for the purpose of being entered and executed on a computer system, for exclusive use by the purchaser of the work.

To Mandana

Contents

List of Figures	xi
List of Tables	xv
Preface	xvii
Acknowledgement	xix
1 Introduction to Ad-hoc Networks	1
1.1 Outlining ad-hoc networks	1
1.2 Advantages and application areas	3
1.3 Radio technologies	4
1.4 Mobility support	5
2 Scope of the book	9
3 Modeling Ad-hoc Networks	15
3.1 Erdős and Rényi random graph model	18
3.2 Regular lattice graph model	21
3.3 Scale-free graph model	25
3.4 Geometric random graph model	25
3.4.1 Radio propagation essentials	26
3.4.2 Pathloss geometric random graph model	30
3.4.3 Lognormal geometric random graph model	31
3.5 Measurements	35
3.6 Chapter summary	38
4 Degree in Ad-hoc Networks	41
4.1 Link density and expected node degree	41
4.2 Degree distribution	44
4.3 Chapter summary	49

5	Hopcount in Ad-hoc Networks	51
5.1	Global view on parameters affecting the hopcount	51
5.2	Analysis of the hopcount in ad-hoc networks	52
5.3	Chapter summary	56
6	Connectivity in Ad-hoc Networks	57
6.1	Connectivity in $G_p(N)$ and $G_{p(r_{ij})}(N)$ with pathloss model ...	58
6.2	Connectivity in $G_{p(r_{ij})}(N)$ with lognormal model	60
6.3	Giant component size	66
6.4	Chapter summary	68
7	MAC Protocols for Packet Radio Networks	71
7.1	The purpose of MAC protocols	71
7.2	Hidden terminal and exposed terminal problems	72
7.3	Classification of MAC protocols	74
7.4	Chapter summary	75
8	Interference in Ad-hoc Networks	77
8.1	Effect of MAC protocols on interfering node density	78
8.2	Interference power estimation	82
8.2.1	Sum of lognormal variables	83
8.2.2	Position of interfering nodes	87
8.2.3	Weighting of interference mean powers	89
8.2.4	Interference calculation results	91
8.3	Chapter summary	93
9	Simplified Interference Estimation: Honey-Grid Model	95
9.1	Model description	95
9.2	Interference calculation with honey-grid model	100
9.3	Comparing with previous results	103
9.4	Chapter summary	105
10	Capacity of Ad-hoc Networks	107
10.1	Routing assumptions	107
10.2	Traffic model	108
10.3	Capacity of ad-hoc networks in general	109
10.4	Capacity calculation based on honey-grid model	111
10.4.1	Hopcount in honey-grid model	111
10.4.2	Expected carrier to interference ratio	114
10.4.3	Capacity and throughput	117
10.5	Chapter summary	122
11	Book Summary	125
A	Ant-routing	131

B Symbols and Acronyms 135

References 139

List of Figures

1.1	Comparison of wireless cellular and wireless ad-hoc network concepts.	2
1.2	BMW talking cars	4
2.1	Positioning our work in the filed of ad-hoc networks research . . .	10
2.2	Scope of the research and the relation between research topics. .	12
3.1	Snapshot of an ad-hoc network	16
3.2	Example of clustering coefficient for a node.	18
3.3	Comparison of hopcount formulas with simulated values	20
3.4	Growth of the giant component size	21
3.5	2-dimensional lattice graphs	22
3.6	Hopcount along a one-dimensional lattice.	23
3.7	Simplified indication of small scale and medium scale radio signal power fluctuations	28
3.8	Schematic view showing the nondeterministic nature of radio links	31
3.9	Shift in views for modeling ad-hoc networks.	32
3.10	Link probability in lognormal geometric random graphs	34
3.11	Coverage of a node	36
3.12	Measured power as function of the distance between receiver and transmitter	37
3.13	Probability density function for measured data	37
4.1	Link density for square-sized areas and different values of ξ	44
4.2	Distribution and nodes falling inside an irregular shape area . . .	45
4.3	Links between nodes with and without toroidal distances	46
4.4	Degree distribution for different values of N	48
4.5	Degree distribution for different values of ξ	49

5.1 Nodes and links in an ad-hoc network for different values of ξ . . . 53

5.2 Hopcount for different values of ξ 54

5.3 Effects of the changes in ξ on the hopcount 55

5.4 Hopcount for $\xi = 0$ and different number of nodes. 55

6.1 Simulated results showing applicability of connectivity theorems to ad-hoc networks 62

6.2 Simulated results showing applicability of connectivity theorems to ad-hoc networks with toroidal distances 64

6.3 Mean hopcount as function of the mean degree for different values of ξ 65

6.4 Mean node degree for 500 nodes uniformly distributed over areas of different sizes for different values of ξ 66

6.5 Mean size of components other than the giant component for different values of ξ 67

6.6 Comparison of the giant component size in a random graph with the values found for ad-hoc networks. 68

6.7 Simulated and calculated values for the giant component size in ad-hoc networks for different values of ξ 69

7.1 Sending, Receiving, Hidden and Exposed terminals in packet radio communication networks 72

7.2 The working of the three MAC protocol classes 74

8.1 Example of the working of MAC classes 1, 2 and 3 on randomly distributed nodes 79

8.2 Density of interfering nodes found by simulations for MAC classes 1, 2 and 3 81

8.3 2-dimensional plots of interfering nodes densities found by simulations 81

8.4 Plots for the estimated interfering nodes densities 82

8.5 Test of the FW and SY interference power estimation methods . 86

8.6 Probability density function of the distance of interfering nodes to the center node in an ad-hoc network 90

8.7 Weighted and non-weighted area mean power coming from interfering nodes in ad-hoc networks 90

8.8 Simulated and calculated PDF and CDF of interference powers 92

8.9 Expected mean interference power for $\eta = 3.0$ and $\sigma = 4.0$ 93

8.10 Expected mean interference power for $\eta = 6.0$ and $\sigma = 8.0$ 94

9.1 Constellation of interfering nodes around node 0 with maximum number of interferers 96

9.2 Regular lattice forms in the 2-dimensional plane 98

9.3 The honey-grid model showing all nodes. 99

9.4 Relay rings and relay nodes in honey-grid model 100

9.5	Interfering rings in honey-grid with $a = 1$	101
9.6	Comparison of interference upper bound with lognormal summation method for $\xi = 0$	104
9.7	Comparison of interference upper bound with lognormal summation method for $\xi = 2$	105
10.1	Hopcount distribution in honey-grid model	113
10.2	Mean and variance of the hopcount in the honey-grid model.	113
10.3	Mean value of hopcount in honey-grid model for different values of N and a	115
10.4	Expected value of C/I in honey-grid model for different values of λ	117
10.5	Expected value of C/I in honey-grid model for different values of a	118
10.6	Effect of traffic increase due to routing overhead on expected C/I	119
10.7	Comparing the capacity and the output bit rate per node in honey-grid model for $a = 1$	120
10.8	Comparing the capacity and the output bit rate per node in honey-grid model for $a = 2$	121
10.9	Throughput per node for different values of input data bit rate per node	121
10.10	Portion of the throughput per node assigned to a node's own traffic	122
A.1	The principle of ant-routing.	132
A.2	Routing table and local traffic statistics in ant-routing.	132
A.3	Simulated results with Ant-net	133

List of Tables

1.1	Technical characteristics of wireless technologies	6
3.1	Comparison of network models.	39
4.1	Calculated versus simulated values of the link density	44
7.1	Prohibited and allowed transmission/reception possibilities for different classes of the MAC protocols.	75
8.1	Calculated and simulated interference power statistics	92

Preface

Wireless mobile ad-hoc networks are formed by mobile devices that set up a possibly short-lived network for communication needs of the moment.

Ad-hoc networks are decentralized, self-organizing networks capable of forming a communication network without relying on any fixed infrastructure. Each node in an ad-hoc network is equipped with a radio transmitter and receiver which allows it to communicate with other nodes over wireless channels. All nodes can function, if needed, as relay stations for data packets to be routed to their final destination. In other words, ad-hoc networks allow for multi-hop transmission of data between nodes outside the direct radio reach of each other.

Ad-hoc networks have distinct advantages over traditional communication networks. For example, ad-hoc networks can be more economical as they eliminate fixed infrastructure costs, and they can be more robust because of their non-hierarchical distributed control and management mechanisms. Ad-hoc networks increase mobility and flexibility, as they can be brought up and torn down in a very short time.

Ad-hoc networks form a relatively new and very diverse field of research. In this book we focus our attention on the fundamental properties of ad-hoc networks. For an ad-hoc network to function properly in the first place it must be connected, or mostly connected. Otherwise the network would consist of scattered isolated islands and could not support networking applications. Secondly, the ad-hoc network must have enough capacity to transport the required amount of data between network nodes. By fundamental properties we mean those properties of the network that directly and substantially affect the connectivity or the capacity of the network.

In this book we have introduced a new mathematical model for ad-hoc networks which is based on realistic assumptions for radio propagation. By using this model we were able to modify connectivity theorems for wireless ad-hoc networks, and have contributed substantially to a better understanding of degree distribution and hopcount in ad-hoc networks. Another novel aspect in this book is a new method proposed for the calculation of interference

statistics. Also, we have shown that interference in ad-hoc networks is upper bounded and have derived a mathematical formula for this upper bound. Our interference calculation methods have allowed us to investigate the capacity of ad-hoc networks. We have found capacity limits for ad-hoc networks and have established that in multi-hop ad-hoc networks there is a trade-off between the network size and the maximum input bit rate possible per node. Large ad-hoc networks, consisting of thousands of nodes, can only support low-bit-rate applications.

Delft, The Netherlands

Ramin Hekmat
March 2006

Acknowledgement

This book is mainly based on research conducted from 2001 to 2005 at the faculty of Electrical Engineering, Computer Science and Mathematics of the Delft University of technology in The Netherlands. I would like to thank my colleagues there who were supportive throughout this whole period.

Introduction to Ad-hoc Networks

We start this book with a brief introduction into ad-hoc networks. The purpose of this short introductory chapter is to familiarize the reader with the concept of ad-hoc networking before describing the fundamental research topics considered in this book in Chapter 2.

In this chapter we will outline ad-hoc networks by comparing them with wireless cellular communication systems. Some advantages and application possibilities of ad-hoc networks are mentioned as well. Like any other wireless communication system, ad-hoc networks are restricted in their capabilities by radio technology limitations on data transmission speeds and range. In order to get a fair idea of these restrictions, we will summarize in this chapter basic characteristic features of some radio technologies commonly used at the physical layer in ad-hoc networks. Further, because mobility support is a challenge in ad-hoc networks, we will evaluate two methods for resolving this issue.

1.1 Outlining ad-hoc networks

Ad-hoc networks are formed in situations where mobile computing devices require networking applications while a fixed network infrastructure is not available or not preferred to be used. In these cases mobile devices could set up a possibly short-lived network for the communication needs of the moment, in other words, an ad-hoc network. Ad-hoc networks are decentralized, self-organizing networks and are capable of forming a communication network without relying on any fixed infrastructure. A high-level description of ad-hoc networks and related research topics can be found in [1] and [2].

In Figure 1.1 wireless ad-hoc networks are conceptually compared to traditional wireless cellular networks. Wireless multi-hop ad-hoc networks are formed by a group of mobile users or mobile devices spread over a certain geographical area. We call the users or devices forming the network *nodes*. The *service area* of the ad-hoc network is the whole geographical area where

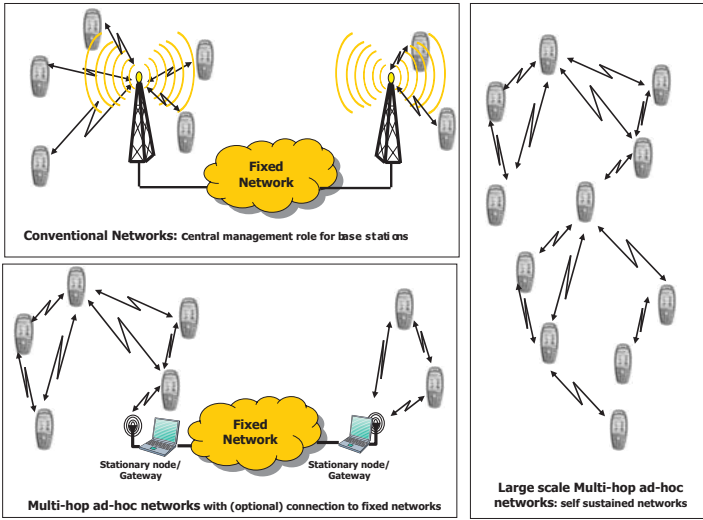


Fig. 1.1. Comparison of wireless cellular and wireless ad-hoc network concepts.

nodes are distributed. Each node is equipped with a radio transmitter and receiver which allows it to communicate with the other nodes. As mobile ad-hoc networks are self-organized networks, communication in ad-hoc networks does not require a central base station. Each node of an ad-hoc network can generate data for any other node in the network. All nodes can function, if needed, as relay stations for data packets to be routed to their final destination. A mobile ad-hoc network may be connected through dedicated gateways, or nodes functioning as gateways, to other fixed networks or the Internet. In this case, the mobile ad-hoc network expands the access to fixed network services.

Although single-hop ad-hoc networks are often used in practice¹, when we refer to ad-hoc networks in this book we always mean multi-hop ad-hoc networks. The multi-hop support in ad-hoc networks, which makes communication between nodes out of direct radio range of each other possible, is probably the most distinct difference between mobile ad-hoc networks and other wireless communication systems.

¹ For example, a laptop communicating with devices like a PDA, a memory storage device and a video camera by using Bluetooth forms a single-hop ad-hoc network.

1.2 Advantages and application areas

Mobile ad-hoc networks have certain advantages over the traditional communication networks. Some of these advantages are:

- Use of ad-hoc networks can increase mobility and flexibility, as ad-hoc networks can be brought up and torn down in a very short time.
- Ad-hoc networks can be more economical in some cases, as they eliminate fixed infrastructure costs and reduce power consumption at mobile nodes.
- Ad-hoc networks can be more robust than conventional wireless networks because of their non-hierarchical distributed control and management mechanisms.
- Because of multi-hop support in ad-hoc networks, communication beyond the Line of Sight (LOS) is possible at high frequencies.
- Multi-hop ad-hoc networks can reduce the power consumption of wireless devices. More transmission power is required for sending a signal over any distance in one long hop than in multiple shorter hops. It can easily be proved that the gain in transmission power consumption is proportional to the number of hops made.
- Because of short communication links (multi-hop node-to-node communication instead of long-distance node to central base station communication), radio emission levels can be kept low. This reduces interference levels, increases spectrum reuse efficiency, and makes it possible to use unlicensed unregulated frequency bands.

Examples of potential applications of mobile ad-hoc networks are only limited by imagination. We may think of a group of people with laptop computers at a conference that wish to exchange files and data without mediation of any additional infrastructure. We also can think of deploying ad-hoc networks in homes for communication between smart household appliances. Ad-hoc networks are suitable to be used in areas where earthquakes or other natural disasters have destroyed communication infrastructures. Ad-hoc networks perfectly satisfy military needs like battlefield survivability, operation without pre-placed infrastructure and connectivity beyond the line of sight. Figure 1.2 shows an interesting commercial application of ad-hoc networks for local hazard warning on the road. Real-time hazard warning is just one possible commercial application of ad-hoc communication networks.

A specific kind of ad-hoc network is the sensor network (see e.g. [3]), where the nodes forming the network do not or rarely move. Sensor networks have received much attention in recent years because they have huge potential applications. A sensor network is composed of a large number of sensor nodes, which are densely deployed either inside the phenomenon to be observed or very close to it. The position of sensor nodes need not to be engineered or pre-determined. This allows random deployment in inaccessible terrains or in disaster relief operations. The physical dimensions of sensor nodes, which can

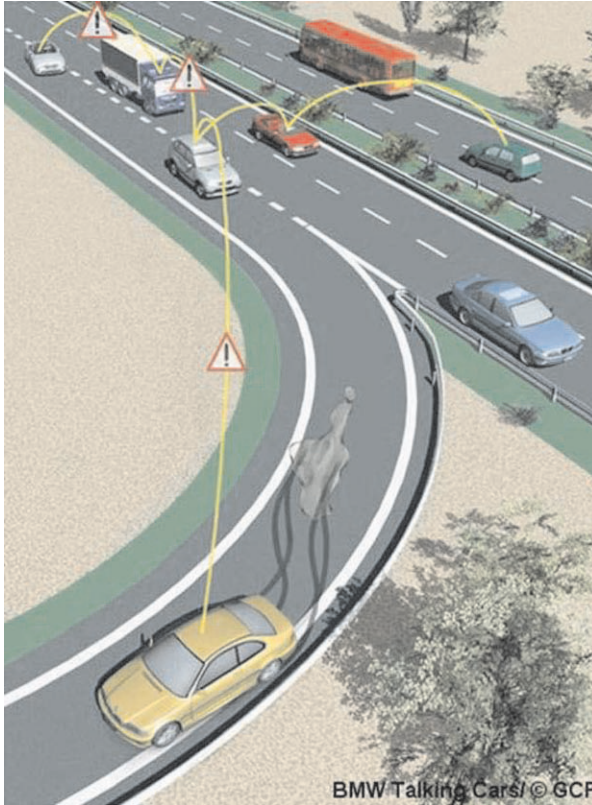


Fig. 1.2. BMW talking cars for local hazard warning: a working example of a commercial application of ad-hoc networks. The car's on-board computer uses data coming from the brakes and ABS monitoring systems to decide whether and when to transmit a hazard warning to other vehicles in its vicinity. This hazard warning can then be relayed up to a predefined number of hops to other cars.

be in the order of a few cubic millimeters, along with their low costs due to mass production, makes them suitable for many applications. Weather and seismological monitoring, inventory control, chemical and biological monitoring, and defense-related networks are just a few examples.

1.3 Radio technologies

In wireless ad-hoc networks, communication between nodes takes place over radio channels. The radio technology used for this purpose can be any of a wide range of systems and standards. Details of such radio communication technologies used in ad-hoc networks are beyond the scope of this book. However, in order to get an impression regarding possibilities and restrictions imposed

by radio communications we provide an overview of basic characteristics of some radio technologies suitable for ad-hoc networks.

Depending on the service area size, a radio technology developed for Wireless Personal Area Networks (WPAN), Wireless Local Area Networks (WLAN), or Wireless Metropolitan Area Networks (WMAN) may be adopted for ad-hoc networks [4]. The coverage radius of a WPAN is roughly in the order of a few meters up to 20 meters. WLAN coverage radius is limited to about 100 meters, while WMAN coverage is in the order of a few kilometers. For each network type various wireless technologies have been proposed. Some examples are:

- WPAN: Bluetooth, UWB
- WLAN: IEEE 802.11a, IEEE 802.11b, IEEE 802.11g
- WMAN: IEEE 802.16e

Basic characteristic features of these technologies are given in the Table 1.1 along with GPRS and UMTS cellular radio systems for comparison reasons. This table serves only for rough quality and performance comparison between technologies. The maximum supported bit rate, frequency allocation and typical ranges are important features that determine the appropriateness of each technology for applications to be provided by the ad-hoc network. For example, dense low-bit-rate sensor networks may be built based on a WPAN technology, while for communication between moving cars at distances in the order of tens of meters a WLAN technology like IEEE 802.11b may be more suitable. It is also worth mentioning that ISM frequency bands are license-exempt frequency bands. This makes deployment of ad-hoc networks in these frequency bands commercially attractive.

A look at the last column of Table 1.1 reveals that, in contrast to cellular systems, the WPAN, WLAN and WMAN radio technologies have not been designed specifically to support mobility or only allow very moderate forms of mobility. However, wireless ad-hoc networks can consist of (fast) moving nodes. How mobility is catered for when these radio technologies are used at the link layer is briefly discussed in the next section.

1.4 Mobility support

The main advantage of wireless mobile communication systems is the support of mobility, which frees the users from restrictions of being attached to a fixed location. Cellular systems like GSM/GPRS and UMTS support mobility through handover and roaming procedures. Handover is applied when a user moves through the coverage areas of various cells in a wireless network and crosses cell boundaries. To support handover, cellular systems depend on dedicated signaling systems in parallel to the content transmission part of their network. In cellular systems the handover between wireless cells of the same type is often referred to as Horizontal Handover, and the handover between

Table 1.1. Technical characteristics of wireless technologies

	Maximum data rate (17)	Frequency allocation	Channel bandwidth	Number of RF Channels	Multiple Access technology	Typical range	Mobility support
Bluetooth	1 Mbps	2.4 GHz (ISM)	1 MHz	79	FHSS	10 m	(1)
UWB	110 Mbps (at 10m)	3.1-10.6 GHz	Min. 500 MHz Max. 7.5 GHz	1-15	THSS OFDM (11)	10-15 m	(1)
IEEE 802.11b	11 Mbps	2.4-2.497 GHz (ISM)	25 MHz	3	DSSS	50-80 m (9)	(2)
IEEE 802.11g	54 Mbps	2.4-2.497 GHz (ISM)	(10)	(10)	(10)	50-80 m (9)	(2)
IEEE 802.11a	54 Mbps	various bands in 5 GHz region	20 MHz	US: 12 EU: 8 Japan: 4	OFDM	40-60 m (9)	(2)
IEEE 802.16e	75 Mbps	2-11 GHz 10-66 GHz (3)	1.5 – 20 MHz (3)	(3)	(15)	30 km (4) 4 km (5)	(6)
GPRS	171 kbps (12)	800, 900 and 1800 MHz bands (13)	200 kHz (13)	(13)	TDMA with FDD	1-5 km (14)	Handover possible also at high speeds
UMTS(W-CDMA) (8)	2 Mbps	1920-1980 MHz 2110-2170 MHz	5 MHz	(7)	DSSS	1-3 km (16)	Handover possible also at high speeds

Notes:

- (1) Technology by itself does not support handover.
- (2) Movement within a cell is possible. Technology by itself does not support handover.
- (3) IEEE 802.16 is designed for a wide range of licensed and license-exempt frequencies with flexible bandwidth allocation to accommodate easier cell planning throughout the world.
- (4) With line of sight condition.
- (5) Without line of sight condition.
- (6) Mobility is only supported in the 2-6 GHz band. At walking speeds, handoff between adjacent cells is possible.
- (7) Number of frequency bands depends on the operator's license.
- (8) Of different variants of UMTS, here we only consider the European W-CDMA.
- (9) Lower bound corresponds to 11 Mbps data rate, and upper bound corresponds to 2 Mbps data rate.
- (10) For data rates 1, 2, 5.5 and 11 Mbps the same channel spacing, bandwidth and modulation is used as in IEEE 802.11b (for backwards compatibility). Other supported bit rates use OFDM.
- (11) UWB can be implemented using several spreading technologies. Most implementations use OFDM or THSS.
- (12) This is the maximum data rate using 8 time slots and Coding Scheme 4 (CS-4).
- (13) Same as in GSM.
- (14) With Coding Scheme 1 (CS-1), the coverage radius of GSM voice and GPRS data is the same, with CS-2, CS-3 and CS-4 the coverage radius reduces. Typical range in this table is for urban areas. Theoretically the maximum range could be as much as 30 km.
- (15) IEEE 802.16 physical layer supports three access technologies: 1. Single Carrier Modulation (SC), 2. OFDM in combination with TDMA and 3. OFDMA. OFDM and OFDMA are mainly proposed for no line of sight operation.
- (16) Typical range in this table is for urban areas. Theoretically the maximum range could be as much as 20 km.
- (17) Figures given here are for a single user. In the case of shared use of the radio channel, the capacity is divided amongst all users.

wireless cells of different network types (e.g., GPRS and UMTS) as Vertical Handover [5]. Roaming can be considered as a special case of handover that requires traffic handling agreements between operators and network providers across country borders.

WLAN, WMAN and WPAN networks were designed for portable terminals, often in a single-cell configuration. They cover specifications for the Physical Layer and the Data Link Layer of the OSI model. These systems can handle mobile stations but with serious restrictions. For example in IEEE 802.11, station mobility is handled within the MAC sub-layer, which implies that a station may move, but maintenance of upper layer connections cannot be guaranteed when a station moves across different LAN segments [6]. Therefore mobility needs to be managed at higher OSI layers. Because ad-hoc networks are designed with cost efficiency and simplicity in mind, they tend to be based entirely on the IP protocol suit. It seems then logical to attempt an IP based solution for mobility support in ad-hoc networks. However, since IP was not designed with mobility in mind, there are several problems that need to be solved before "all-IP" wireless networks can be deployed for moving users. Looking at the ad-hoc network developments and the research in the past few years, we distinguish two basic methods for solving the mobility issue in ad-hoc networks:

Mobile IP: The Mobile IP [7], with two flavors Mobile IPv4 and Mobile IPv6 ([8] and [9]), is a well-known approach for mobility support in "all IP" networks and an accepted standard by the IETF community [10]. Mobile IP offers a pure network layer architectural solution for mobility support and isolates the higher layers from the impact of mobility. However, an inter-domain Mobile IP solution for handover can take up to a few seconds to complete. This is certainly an adequate solution for nomadic users², but for fast and frequent handover of delay-sensitive voice and multimedia applications, better solutions are required. For this purpose, various adjustments and enhancements to Mobile IP have been proposed. Examples are Hierarchical Mobile IP, Cellular IP (CIP) and Handoff-aware Wireless Access Internet Infrastructure (Hawaii) for local handover control [11]. However, none of these proposals has been implemented and proved to work on a large-scale basis yet.

Fast routing protocols: Routing protocols are designed to cope with changes in the network topology. In fixed networks, when a router or a link becomes unavailable, the routing mechanism finds an alternative route from source to destination [12]. In ad-hoc networks, movement of nodes continuously changes the topology of the network. Some nodes become unreachable while new nodes become available, old links are broken while new

² A nomadic user moves from location to location requiring access to the network at each location but not while on the move. An example of a nomadic user is a person with a laptop who logs into a cooperate network to read his emails either at the office or at home.

ones are established at a fast rate. Theoretically, a routing protocol could still trace network changes and allow nodes to find each other. In other words, the mobility issue can be seen as a routing problem. However, the routing protocols developed for fixed networks (like RIP or OSPF [13]) cannot handle rapid changes in the network and create a relatively large routing overhead. Therefore, for ad-hoc networks special routing protocols are needed. These protocols, provided that they are fast and efficient, do solve the mobility problem. Routing in ad-hoc networks is basically a compromise between the method of dealing with fast topology changes and keeping the routing overhead minimal. There are proactive and reactive protocols, and protocols that use a hybrid solution ([2], [4]). Proactive methods maintain routes to all nodes, including nodes to which no packets are to be sent. These protocols react to topology changes, even if no traffic is affected by the changes. Reactive methods, on the other hand, find a route between a source and a destination only when there is a demand for data transmission. Reactive protocols are also called on-demand protocols. Reactive routing protocols can significantly reduce routing overhead in situations where the traffic load is low and the topology changes are fast. However, proactive protocols suffer less from delay because a route between the source and the destination is already known and needs not to be found when the need arises. Hybrid methods try to combine the best of both proactive and reactive methods [14], [15]. There is a huge amount of research dedicated to routing protocols for ad-hoc networks (see e.g. [16]). Although a single standard has not emerged yet, the IETF working group MANET [17] is working intensively on a number of promising solutions like TBRPF [18], AODV [19], and OLSR [20]. These protocols have already been tested in various realistic settings with good results [21].

To summarize, there are two distinct methods for mobility support in wireless ad-hoc networks: mobile IP, and fast routing protocols. Research in both areas is still progressing. At this moment it seems that a solution based on fast routing protocols is more widely accepted.

Scope of the book

Despite their evident advantages and potential application possibilities, ad-hoc networks are yet far from being deployed on a large-scale basis. Some fundamental ad-hoc networking problems remain unsolved or need optimized solutions. Here we give a few examples. Robustness of ad-hoc networks in highly dynamic environments with changing loads and variable speeds of the nodes has not been investigated thoroughly yet. Although various routing protocols have been suggested and tested for mobile ad-hoc networks, performance metrics like throughput, delay and protocol overhead in relation to successfully transmitted data need better understanding and optimization. This optimization would depend on the application type and on whether the throughput is to be maximized or the delay to be minimized. One single protocol would probably not work efficiently across the entire range of design parameters and operating conditions. An additional complexity factor in ad-hoc network design is that the different layers of the system are highly interdependent. Therefore, layers one, two, and three of the standard OSI model probably could not be separated and optimized independent of the other layers. To the list of research areas we can certainly add searching for a suitable position determination system and position upgrade mechanisms. One other major research topic is the interaction between ad-hoc networks and the existing telecommunication systems and networks.

In addition to these technical points, there are various commercial, social and ethical topics that require attention. For example, it is still unclear whether large-scale deployment of mobile ad-hoc networks can be seen as complementary to existing cellular networks or as a threat to mobile operators. Further, it is conceivable that public use of ad-hoc networks would require specific regulations and charging mechanisms that are not clear yet. In multi-hop ad-hoc networks, the willingness of general public to share their communication device and its resources (as a relay station) with the total community of ad-hoc network users is far from trivial. Although simple incentives like call credits could prove to be commercial motivating factors, it is questionable whether these incentives would be sufficient from an ethical point of view to

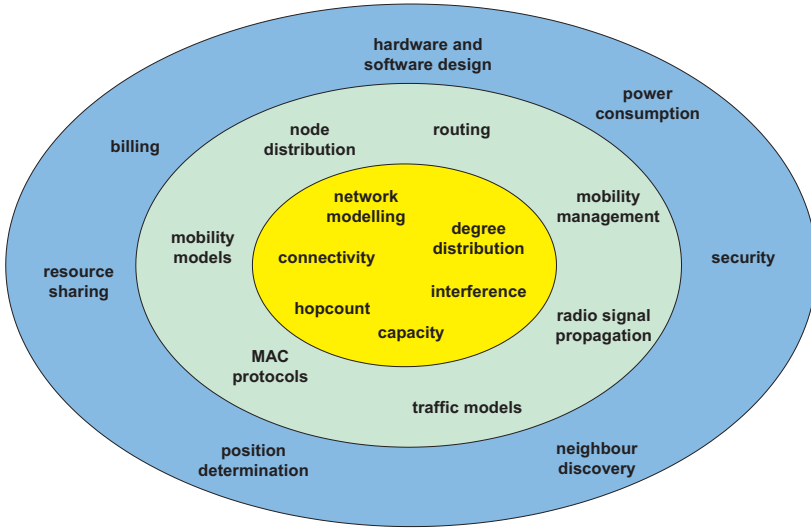


Fig. 2.1. Positioning our work in the field of ad-hoc and sensor networks research: The inner zone shows topics in our main research and focus area. The second zone, around the inner zone, includes topics about which we have made assumptions or have performed light research. The third zone shows topics that have not been included in our study.

motivate ad-hoc network users to function as relay stations for someone else's data.

From the short discussion above it may be evident that ad-hoc networking is a vast research area. It is not surprising then to see that many aspects of wireless ad-hoc networks are under investigation or have already been studied by the international research community.

On the technical front, which is the focus of our work, various aspects of ad-hoc networking have been studied in the past few years. For example, extensive work has been done in the development and optimization of ad-hoc network routing protocols ([17], [16]). Others have investigated the capacity and the scalability of wireless ad-hoc networks ([22], [23], [24], [25]). The effect of selfish nodes or misbehaving nodes on the stability of ad-hoc networks is an interesting topic that has also received the necessary attention [26]. Due to the complexity of ad-hoc networks, many of the study results in this field are based on simulation models ¹. However, in comparison to mathematical

¹ In particular simulations based on ns-2 [27] are widespread and commonly used. Network Simulator version 2 (ns-2) is a discrete-event simulator targeted at networking research. The source code of the program in C++ is open for adjustments and additions. Many routines and modules in ns-2 are contributed by researchers worldwide. ns-2 is often used for the simulation of routing protocols and MAC

models, simulation models could be less suitable to provide an in-depth understanding of the system dependency on various parameters. Fortunately, literature survey reveals that mathematical modeling of ad-hoc networks is gaining increased attention ([29], [30], [31]). Furthermore, many publications are emerging that analyze ad-hoc networks based on measurements rather than on pure theoretical models ([32], [33]). We see this latter point as a positive development and a clear indication that ad-hoc networking is moving from an academic concept towards a practical real-life solution.

Considering the diversity of research, it is important to outline the contours of our work precisely and to formulate clearly the scientific contribution of this book. In this book we have investigated fundamental properties of multi-hop ad-hoc networks through realistic mathematical modeling of the network. We explain what we mean by fundamental properties. For an ad-hoc network to function properly, in the first place it must be connected (or mostly connected). Otherwise the network would consist of scattered isolated islands of nodes and could not support networking applications between most of the nodes. Secondly, the ad-hoc network must have enough capacity to transport the required amount of data between the nodes. By fundamental properties we mean those properties of the network that directly affect the connectivity or the capacity of the network. One novel aspect in our work is the use of a realistic mathematical model for ad-hoc networks. By using this model we believe that we have contributed substantially to a better understanding of connectivity, degree distribution, and hopcount in ad-hoc networks. Another novel aspect in this book is a new method for calculation of interference statistics. Further, we have been able to show that interference in ad-hoc networks is upper bounded and have derived a mathematical formula for this upper bound. Our interference calculation methods have allowed us to investigate the capacity of ad-hoc networks. We have found capacity limits for ad-hoc networks and have shown that the maximum supported data transmission speed per node in ad-hoc networks is inversely proportional to the mean hopcount. In other words, in ad-hoc networks there is a trade-off between the network size and the maximum bit rate possible per node. For example, only ad-hoc networks of small size with few hops can support high-bit-rate multimedia applications.

To position our main focus areas in relation to other possible technical research topics we refer to Figure 2.1. In this figure², the core topics of our study are shown in the inner zone in the middle of the figure. We will call these topics the *primary* research topics of this book. For the study of primary research topics we have made assumptions with respect to the topics depicted in the second zone (the zone immediately around the inner zone). The topics in

protocols in wireless ad-hoc networks. However, this tool needs numerous improvements, especially regarding the physical layer and MAC modeling, in order to provide results fitting realistic scenarios [28].

² We don't claim the list of topics depicted in Figure 2.1 to be exhaustive.

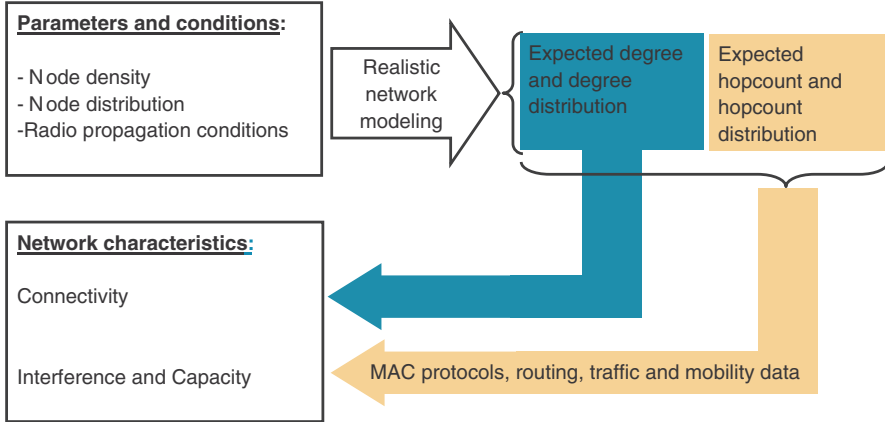


Fig. 2.2. Scope of the research and the relation between research topics.

this zone have not been studied in depth. However, when needed we obtained information available in the literature and projected it in a way suitable for the study of the primary research topics. We will call the topics in the second zone the *secondary* research topics. The third zone (the outer zone) shows topics of research that although very valuable to the study of ad-hoc networks in general, are not relevant to our study.

The way that the primary and the secondary research topics are related to each other is shown in Figure 2.2. Throughout this book we will see that connectivity is affected by degree distribution and capacity by factors like the hopcount distribution, Medium Access Control (MAC) protocols, and interference.

Figure 2.2 can also be used to understand the structure of this book and the way in which different topics are ordered. We present in Chapter 3 our method for realistic modeling of wireless ad-hoc networks. The degree distribution and the hopcount, based on our model for ad-hoc networks, are discussion topics in Chapters 4 and 5, respectively. The connectivity of ad-hoc networks, which can be seen as a first indicative parameter for the robustness of the network, is handled in Chapter 6. For the study of interference in ad-hoc networks it is necessary to have a good model for effects of the MAC protocols on simultaneously allowed transmissions. MAC protocols are the topic of Chapter 7 and interference is studied subsequently in Chapter 8. For the study of interference we have proposed a simplified model that facilitates mathematical analysis. This model is described in Chapter 9. The capacity of ad-hoc networks is studied in Chapter 10. In that chapter we also explain our assumption regarding the routing protocols and traffic patterns. Finally, our overall conclusions are summarized in Chapter 11.

It needs to be mentioned here that our study covers not only ad-hoc networks but also sensor networks, which can be considered as a specific case of ad-hoc networking with fixed nodes. Therefore, all results are also applicable to sensor networks. We mention this point here and avoid persistent repetition of the applicability of our results to sensor networks in the rest of the book.

Modeling Ad-hoc Networks

In wireless multi-hop ad-hoc networks, any node may have direct radio links with some other nodes in its vicinity and each node can, if needed, function as a relay station routing traffic to its final destination. Regardless of the radio technology used or the movement pattern of nodes, from the topology point of view, at any instant in time an ad-hoc network can be represented as a graph with a set of vertices consisting of the nodes of the network and a set of edges consisting of the links between the nodes (see Figure 3.1). We assume that links between nodes are two-way, undirected links. There is a link between two nodes if a signal transmitted from one node is received at the other node above a minimum required power threshold (for more details see Section 3.4.1). Two nodes are connected if there is a link between them. It needs to be emphasized that we look at the network topology based on the above-mentioned requirement for connectivity between nodes. Whether two connected nodes can communicate with each other at the desired data communication speed at all times is a matter of interference and capacity calculation that are considered in Chapters 8 and 10. In other words, we have chosen to separate network topology from network capacity. Whenever, due to interference, communication between two connected nodes drops to lower speeds or even becomes impossible we say that the link capacity is reduced, instead of saying that the probability of connectivity between these two nodes has decreased.

In this book we focus on fundamental properties of ad-hoc networks, including the connectivity, the degree distribution and the hopcount. These properties can be studied using a graph representation of the ad-hoc network. The study of graphs is known as graph theory (see e.g. [34], [35], [36]). A graph, G , is defined as a set of vertices V and a set of edges E and can be denoted as $G = (V, E)$. The sets V and E are always assumed to be finite. An edge is a link between two vertices. An edge that joins the vertices i and j is denoted by (i, j) . The vertices i and j are the *end-vertices* of this edge. If an edge exists between two vertices, then these two vertices are called *adjacent* or *neighboring* vertices of G . Two edges are called *adjacent* if they have

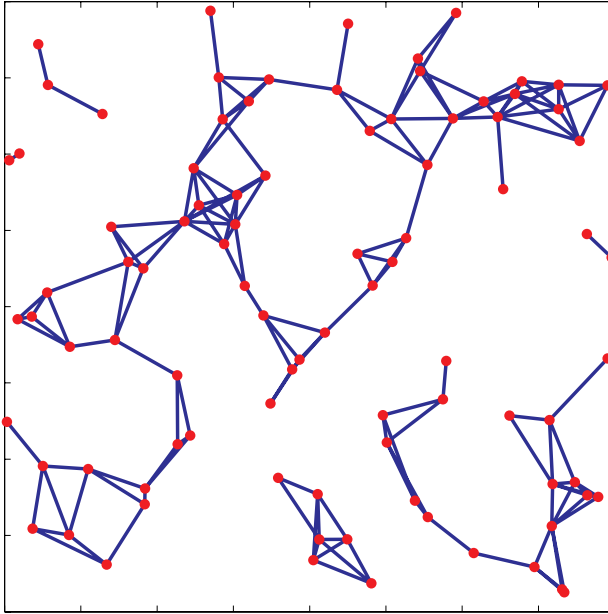


Fig. 3.1. Snapshot of an ad-hoc network. In this graph, dots represent nodes forming the network and lines indicate links between nodes. Links are assumed to be established over wireless channels.

exactly one common end-vertex. To the edges of a graph specific values or weights may be assigned, in which case the graph is called a *weighted* graph. The edges of graphs may also be accommodated with directedness, in which case each edge is given a unique direction. A *simple graph*, also called a *strict graph* [37], is an unweighted, undirected graph containing no self-loops¹ and at most one edge connecting any two vertices. Unless stated otherwise, the unqualified term "graph" in this book will refer to a simple graph.

When graph theory is used to describe a network, the nodes in the network correspond to the vertices in the graph and the links between the nodes correspond to the edges of the graph.

Before proceeding with the description of graph models for ad-hoc networks we describe here a few general terms and definitions that will frequently be used throughout this chapter.

Complete graph A complete graph has an edge between every pair of vertices.
Adjacency matrix When a network is presented as a graph, the topological structure of a network with N nodes can be described by the *adjacency matrix* A . Adjacency matrix is a $N \times N$ matrix where each element a_{ij} of A is either zero or one: $a_{ij} = 1$ if there is a link between node i and node

¹ An edge having same vertex as both its end-vertices is called a self-loop.

j , else $a_{ij} = 0$. Hence, the adjacency matrix expresses how the nodes in the network are interconnected.

Degree The degree of node i is the number of direct neighbors of that node in the network: $d_i = \sum_{j=1}^N a_{ij}$.

Connectedness A graph G is connected if there exists a path $\{i, \dots, j\}$ between any pair of vertices i and j . To achieve a fully *connected* network, there must be a path from any (source) node to any other (destination) node. The path between the source and the destination may consist of one hop (when source and destination are neighbors) or several hops. When there is no path between at least one source-destination pair, the network is said to be *disconnected*. A disconnected network may consist of several disconnected islands or clusters.

Giant component The largest connected cluster in the network is called the *giant component*. In a fully connected network the giant component covers the entire network. When the network is not fully connected, we only speak of a giant component when a single cluster clearly dominates in size all other clusters.

Hopcount The hopcount specifies the number of hops on the path between a source and a destination. The average hopcount in a network is the average value of the hopcount between all possible source-destination node pairs.

Shortest path The shortest path between two nodes is the one having the shortest length (shortest number of hops).

Diameter Let \mathcal{S} be the set of the lengths of the shortest paths between all pairs of nodes in the network. The diameter of the graph is the maximum of \mathcal{S} .

Clustering coefficient For node i with $d_i \geq 2$, an edge (u, v) is *opposite* to node i if there exist edges (i, v) and (i, u) . The clustering coefficient of node i is defined as:

$$c_i = \frac{\text{number of opposite edges of } i}{d_i(d_i - 1)/2}.$$

The clustering coefficient is thus the ratio between the actual number of links between the neighbors of node i and the maximum possible number of links between these neighbors. In other words, the clustering coefficient is the ratio between the number of triangles that contain i and the number of triangles that would contain i if all neighbors of i were interlinked (see Figure 3.2). The clustering coefficient of G , denoted by C_G , is the average of c_i for all nodes with $d_i \geq 2$.

Local correlation Let node i be connected to node j . If the probability of node i being connected to the neighbors of node j is higher than the probability of node i being connected to other nodes in the network (all nodes except node i 's one-hop and two-hop neighbors), we say that edges are *locally correlated*. If edges are *independent*, the probability of node i being connected to any node in the network is the same. It is obvious that

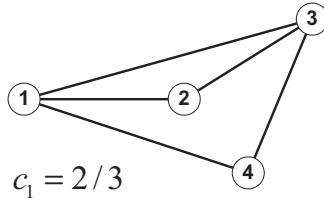


Fig. 3.2. Example of clustering coefficient for a node.

local correlation increases the clustering coefficient. However, a high clustering coefficient value does not necessarily mean strong local correlation between nodes. For example, a complete graph has the highest clustering coefficient value while all edges may still be independent.

Small-world property A network is said to have the *small-world property* when the hopcount in that network is not strongly affected by an increase in the network size. Please note that we use the term "strongly" in a rather loose sense. This phenomenon is addressed very often in the literature (see e.g. [38]). In a network with the small-world property, there is a high probability that there is a relatively short path between any two nodes, despite the large size of the network. The small-world property has already been observed in social networks as well as neural networks [39]. Even the World Wide Web pages seem to possess the small world property [40]. The most famous manifestation of the small-world property has been formulated as "six degrees of separation", uncovered by the social psychologist Stanley Milgram in 1967 [41]. It refers to the concept that everyone is connected to everyone else in the world by only six degrees of separation, or six sets of acquaintances.

For the study of network characteristics in general, different graph models may be proposed. In this chapter we consider the Erdős and Rényi random graph model, the regular lattice model, the scale-free model, and the geometric random graph model. Although knowledge of all these models is essential for our study, it will become clear that not all of these models are equally suitable to characterize wireless multi-hop ad-hoc networks.

3.1 Erdős and Rényi random graph model

The random graph of Erdős and Rényi [42] is one of the best studied models of a network [43]. This model is exactly solvable for many of its average properties [34]. Unless stated otherwise, the term "random graph" in this book will refer to the Erdős and Rényi random graph.

A random graph with N vertices and L edges can be constructed by starting with N vertices and zero edges. Then L edges are chosen randomly

and independently from the $N(N-1)/2$ possible edges. In total, there are $\binom{N(N-1)/2}{L}$ equiprobable random graphs with N vertices and L edges. Another way of looking at random graphs is the assumption that any pair of vertices in a random graph is connected with the probability p . The number of edges L in the random graph is then a random variable with the expectation $E[L] = p \frac{N(N-1)}{2}$.

It should be obvious by now that the random graph model is not a realistic representation of a wireless ad-hoc network. After all, in ad-hoc networks two nodes at close range have a higher probability of being connected than nodes at farther distances. However, we will proceed with a description of some of the properties of the random graphs in this section, because these results are required for a better understanding of the model of ad-hoc networks presented later in this chapter.

We denote a random graph by $G_p(N)$, where N is the number of nodes in the graph and p is the probability of having a link (edge) between any two nodes [34]. The fundamental assumption in random graphs is that the presence or absence of a link between two nodes is *independent* of the presence or absence of any other link. As mentioned before, the degree of a node i , denoted as d_i , is defined as the number of nodes connected directly to node i . In other words, the degree of a node is the number of neighbors of that node. In a random graph, d_i has by definition a binomial distribution [34]:

$$\Pr [d_i = k] = \binom{N-1}{k} p^k (1-p)^{N-1-k} \simeq \frac{z^k e^{-z}}{k!}, \quad (3.1)$$

where z is the mean (average) node degree: $z = E[d_i] = (N-1)p$. The variance of the node degree is $(N-1)p(1-p)$. The second term in (3.1) is the Poisson approximation for large N .

As each node in the random graph is connected to about z other nodes, after h hops, z^h nodes have been reached (assuming a tree-like graph structure with no short loops, which is a correct assumption when z is sufficiently small compared to N). All nodes are reached typically when $z^h \simeq N$. This implies that the typical average hopcount $E[h]$ in random graphs is

$$E[h] \simeq \frac{\log(N)}{\log(E[d])}. \quad (3.2)$$

This formula for the expected hopcount in random graphs is also given by Albert and Barabasi [44]. Although (3.2) is a rough approximation, it indicates clearly that the average hopcount in random graphs scales with the logarithmic value of the number of nodes. A better approximation is provided by Newman, Strogatz and Watts in [29]:

$$E[h] \simeq \frac{\log(N/E[d])}{\log(E[d(d-1)]/E[d])} + 1. \quad (3.3)$$

There exists a very close approximation for the mean hopcount given by Hooghiemstra and Van Mieghem ([45], [46]). Although an explanation of the

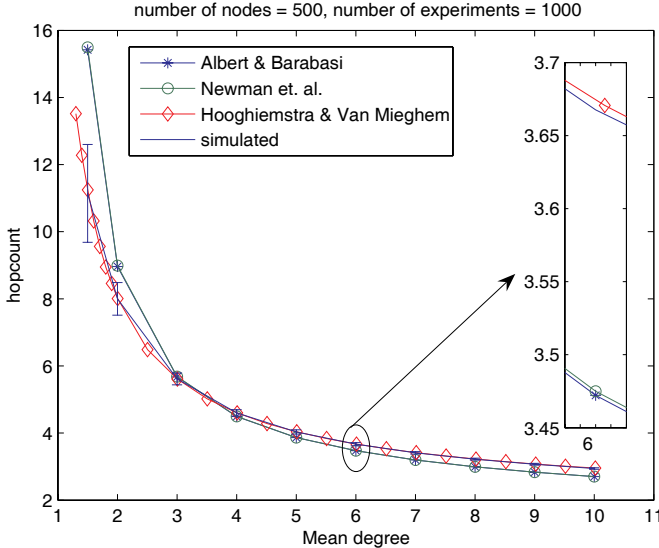


Fig. 3.3. Comparison of three hopcount formulas with simulated values for a random graph of 500 nodes. Simulation results are average values for 1000 experiments, with standard deviation shown as error bars. For better visibility, we have blown up the section around the mean degree of 6.

latter formula is beyond the scope of this book, we have compared these three formulas with simulated values of the hopcount in Figure 3.3. As we can see from this figure, the simulation results match best with the Hooghiemstra and Van Mieghem estimate, however, despite its simplicity, (3.2) seems to be a good approximation of the hopcount as well.

An interesting aspect of random graphs is the existence of a critical probability at which a giant cluster forms. This means that at low values of p , the random graph consists of isolated clusters. When the value of p increases, above a threshold value a giant cluster emerges that spans almost the entire network. This phenomenon is similar to the percolation transition, a topic much studied in both mathematics and statistical mechanics (see e.g. [47]). If S is the fraction of the graph occupied by the giant component, for large N in random graphs, S is the solution to the following equation [29], [48]:

$$S = 1 - \exp(-zS), \quad (3.4)$$

where $z = E[d]$ is the mean degree of the graph. Fast converging series have been found [49] to solve (3.4), but a standard zero finding algorithm like the Newton-Raphson method can also be used to find S as function of z . Figure 3.4 shows the values of S found as function of the mean degree by solving 3.4.

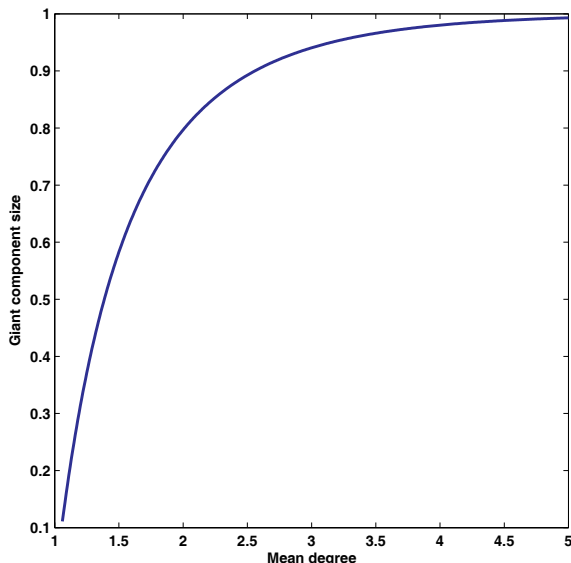


Fig. 3.4. Growth of the giant component size as function of the mean nodal degree in a random graph.

Because clustering coefficient is the percentage of neighbors of a node that are connected to each other, and in a random graph links between nodes are established independently with probability p , we may expect the clustering coefficient in a random graph to be:

$$C_G = p.$$

This result has been proved in both [50] and [44].

3.2 Regular lattice graph model

A regular lattice graph is constructed with nodes (vertices) placed on a regular grid structure. Adjacent nodes on the grid are all equidistant (although this distance can be defined to be non-metric). The probability that two adjacent nodes on the grid are connected is p . Non-adjacent nodes cannot be linked directly. Links (edges) are then created independently and are all equiprobable. Figure 3.5 shows an example of a 2-dimensional lattice graph on a square grid of size 10×20 for two different values of p .

Let us see how suitable the lattice graph model is to represent ad-hoc networks. In wireless ad-hoc networks, nodes use radio communications to form links with other nodes. Because radio signal powers decay with increasing distance between nodes, the link probability is bound to be a function of the

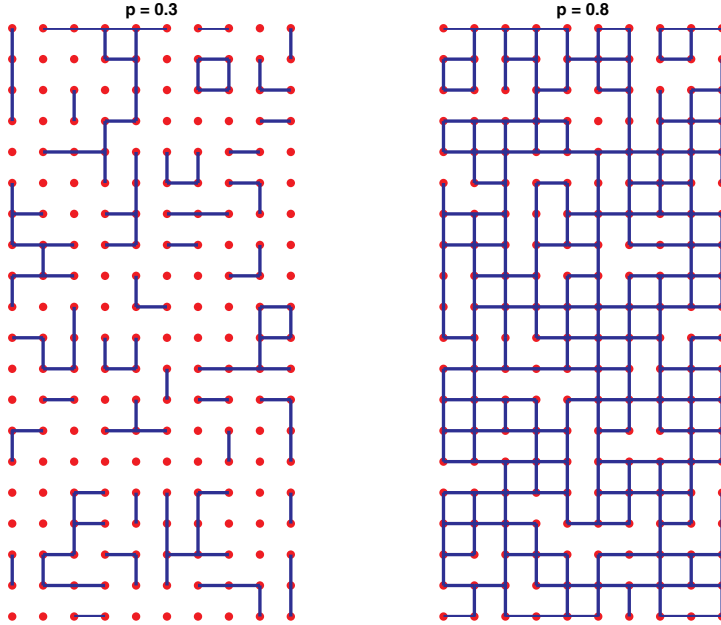


Fig. 3.5. A 2-dimensional lattice graph on a 10×20 square grid with $p = 0.3$ (figure on the left) and $p = 0.8$ (figure on the right).

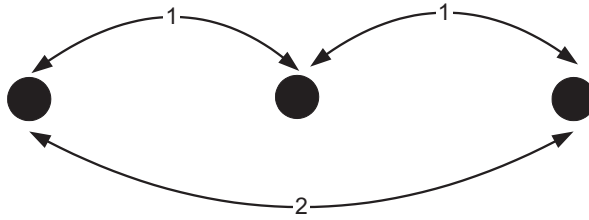
distance between nodes. We see that the lattice model and ad-hoc networks share the notion that the distance between nodes influences the link probability. From this point of view, the lattice model is more suitable to represent an ad-hoc network than the random graph model discussed previously. However, the position of nodes in an ad-hoc network (or even a sensor network) is generally not fixed to a regular lattice. Further, in radio communication the distance over which nodes can "see" each other is not a fixed value. Despite these differences, we will here study some basic characteristics of lattice graphs in more detail to gain a better understanding of the properties of our model for ad-hoc networks, which is described later in Section 3.4.3.

We denote a 2-dimensional lattice graph on a square grid of size $m \times n$ with $G_{m,n}$. The number of nodes in this lattice graph is $N = m \times n$. For a dense lattice graph with $p \simeq 1$, it is easy to verify that the mean degree is

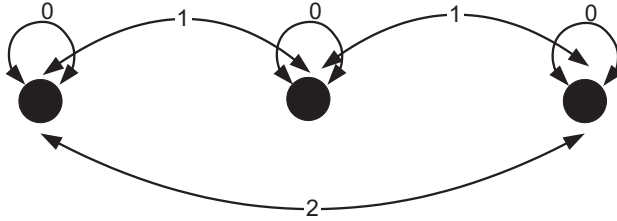
$$E[d_{m \times n}] = 4 - \frac{2(m+n)}{m \times n}. \quad (3.5)$$

The expected value of the hopcount is

$$E[h_{m \times n}] = \frac{m+n}{3} \stackrel{\text{if } m \simeq n}{\simeq} O(\sqrt{N}). \quad (3.6)$$



Possible hops along one dimension with 3 nodes



Possible hops with zero-length hops along one dimension

Fig. 3.6. Hopcount along a one-dimensional lattice.

where $O(\cdot)$ is the *big-O* asymptotic order notation [51]².

To prove (3.6), we start with a one-dimensional lattice of $1 \times n$ nodes. In this lattice, there are always $n - k$ node combinations with hopcount k , where $1 \leq k \leq n - 1$ (see Figure 3.6, top part). Based on this distribution:

$$\Pr[h = k] = \frac{n - k}{\sum_{i=1}^{n-1} i} = \frac{2(n - k)}{n(n - 1)},$$

and

$$E[h_{k=1 \dots n-1}] = \sum_{k=1}^{n-1} k \Pr[h = k] = \sum_{k=1}^{n-1} \frac{2k(n - k)}{n(n - 1)} = \frac{n + 1}{3}.$$

In a 2-dimensional lattice, any hopcount from one node to another can be projected to a corresponding number of one-dimensional horizontal and vertical hops. However, it is possible that either the horizontal or vertical hopcount is zero. For a one-dimensional lattice of $1 \times n$ nodes, if we consider the possibility of zero-length hops, there are always $n - k$ node combinations

² Notation $f(N) = O(\varphi(N))$ where N is an integer which tends to infinity means that asymptotically $|f(N)| < c\varphi(N)$ for some constant c .

hopcount k where $0 \leq k \leq n - 1$ (see Figure 3.6, bottom part). Based on this distribution:

$$\Pr [h = k] = \frac{n - k}{\sum_{i=1}^n i} = \frac{2(n - k)}{n(n + 1)},$$

and

$$E [h_{k=0\dots n-1}] = \sum_{k=0}^{n-1} k \Pr [h = k] = \sum_{k=0}^{n-1} \frac{2k(n - k)}{n(n + 1)} = \frac{n - 1}{3}.$$

In the 2-dimensional lattice of size $n \times m$, that has n nodes in horizontal direction and m nodes in vertical direction, we have:

$$\begin{aligned} h_{n \times m} &= h_{\text{horizontal}} + h_{\text{vertical}} \\ E [h_{n \times m}] &= E [h_{\text{horizontal}}] + E [h_{\text{vertical}}] \end{aligned}$$

For each occurrence of $h_{n \times m}$, either $h_{\text{horizontal}}$ or h_{vertical} can be 0 but not both simultaneously. Either way for the mean hopcount value we can write:

$$\begin{aligned} E [h_{n \times m}] &= E [h_{k=1\dots n-1}] + E [h_{k=1\dots m-1}] - \frac{2}{3} \\ &= \frac{n + m}{3}, \end{aligned}$$

which proves (3.6).

When we compare the hopcount in lattice graphs (3.6) with that in random graphs (3.2) we note that in lattice graphs the hopcount growth is polynomial with respect to increasing network size N , while in random graphs the expected hopcount is only logarithmic in N . We can thus say that lattice networks do not have the small-world property while random graphs do. The question is then which of these two more closely resembles the behavior of ad-hoc networks. In other words, do wireless ad-hoc networks possess the small-world property? Because radio signals have limited range, when the size of the service area of an ad-hoc network increases, to reach farther nodes, the hopcount needs to increase as well. From this point of view, ad-hoc networks seem to be like lattice graphs and can be expected not to have the small-world property. However, radio signal powers always fluctuate and are unpredictable. As a result, depending on the strength of the power fluctuations and the actual service area size, as we will see later on in this chapter, ad-hoc networks may show some degree of the small-world property. A different matter is when ad-hoc networks increase in size (number of nodes) while the service area does not change. In this situation, the diameter of the network is not expected to change by the increase in network size.

3.3 Scale-free graph model

Various authors have observed ([29], [52], [53]) that real-world networks such as the Internet, social networks and biological networks cannot be modeled as random graphs. The binomial degree distribution in random graphs seems to be an unrealistic assumption for these network types. Further, the clustering coefficient in these networks is typically much larger than in random graphs of equal number of vertices and edges [39]. Based on experimental studies, a more realistic model is suggested for the presentation of real-world networks which assumes that the degree distribution has a power-law tail [54]. In other words,

$$\Pr [d = k] \simeq k^{-\gamma}, \quad (3.7)$$

where γ is a constant independent of the size of the network. Because of the independence of the degree distribution from the network size, these networks are referred to as scale-free networks. The value of γ is found to be different for various network types. For experimentally found values of γ in ecological networks, movie actor collaboration network, science collaboration graph and the Internet we refer to [44]. A specific method for generating a scale-free network is a process in which vertices are added to a graph one at a time and joined to a fixed number of earlier vertices, selected with probabilities proportional to their degrees. This process creates a scale-free network with $\gamma = 3$ [55].

The power-law degree distribution influences the way in which the network operates, including how it responds to catastrophic events. A scale-free graph, where a very small number of network nodes (called *hubs*) are far more connected than other nodes, shows striking resilience against random breakdowns. In scale-free networks, in spite of large sizes of the networks, the distances between most vertices is short because these paths usually go through the hubs. The small-world property is more strongly present in scale-free networks than in random graphs.

Despite the suitability of the scale-free network model for many social and man-made networks, we argue here that the scale-free network model is not appropriate for ad-hoc networks. In an ad-hoc network where nodes are uniformly distributed over the service area, and radio propagation conditions as well as radio transmit power and receiver sensitivity are the same for all nodes, there is no reason to assume that some nodes may have a much higher number of neighbors than other nodes.

3.4 Geometric random graph model

Having considered the random graph, the lattice and the scale-free graph models, we discuss in this section the geometric random graph model and will

show how this model can be adapted to become a realistic model for ad-hoc networks.

A wireless ad-hoc network consists of a number of nodes (radio devices) spread over a certain geographical area. Each node may be connected to other nodes in its vicinity. In wireless ad-hoc networks, because of node movements and radio signal fluctuations, the topology of the network can change from time to time. However, as mentioned before, at any instant in time, an ad-hoc network can be considered as a graph with a certain number of nodes and links between nodes.

Ad-hoc networks cannot be modeled as pure random networks. As discussed in previous sections, in a wireless ad-hoc network the actual set of connections, in contrast to random graphs or scale-free networks, depends on the geometric distance between nodes. A direct consequence of the dependency of the links on the distance between nodes is that in wireless ad-hoc networks there is an increased probability of two nodes to be connected when they have a common neighbor. In other words, in a wireless ad-hoc network links are *locally correlated*. In the literature, graphs with distance-dependent links between nodes and correlated links are referred to as geometric random graphs (see e.g. [30]). Local correlation between nodes increases the clustering coefficient [44].

We denote an undirected geometric random graph with N nodes by $G_{p(r_{ij})}(N)$, where $p(r_{ij})$ is the probability of having a link between two nodes i and j (or j and i) at metric distance r_{ij} . We assume in a geometric random graph N nodes are uniformly distributed over the entire service area. This is not an obligatory requirement for the model in general, but it is always assumed to be the case in our study. The reliability of a geometric random graph model depends directly on the accuracy of $p(r_{ij})$. In other words, for a reliable model we need to have an accurate description of radio propagation characteristics that determine the link probability between nodes in wireless environments. In Section 3.4.1 we provide an incomplete overview of radio propagation theory. This theory will be used to describe two different geometric random graphs models for ad-hoc networks in Sections 3.4.2 and 3.4.3.

3.4.1 Radio propagation essentials

Radio propagation characterization and modeling the radio channel has always been one of the most difficult parts of the design of terrestrial wireless communication systems. A mobile wireless ad-hoc network is no exception. Stronger yet, good modeling of the radio channel could be more important in the design of ad-hoc networks than in the traditional wireless communication systems. In ad-hoc networks not only the service quality but also the whole routing and network topology is affected by the impairments over the radio links.

Radio channel is generally hostile in nature and it is very difficult to predict its behavior. Any model for a radio link is bound to be a simplification of the reality. In general the radio channel is modeled in statistical way using real propagation measurement data. A lot of measurements have been done to obtain information concerning propagation loss and signal power variations (fading) in classical radio communication systems ([56], [57], [58], [59]). These measurements have shown that generally the signal fading over a radio channel between a transmitter and a receiver can be decomposed into 3 components ([60], [61]):

1. a large scale pathloss power component,
2. a medium scale slow varying power component having a lognormal distribution, and
3. a small scale fast varying amplitude component with a Rayleigh (Rician) distribution without (with) a Line-of-Sight connection between the transmitter and the receiver.

The large scale pathloss indicates the dependency of the expected received signal mean power to the distance between the transmitter and the receiver. The small scale fading is used to describe rapid fluctuations of the amplitude of a radio signal experienced by a mobile user over a short period of time (in the order of a few milliseconds up to seconds) or travel distance (in the order of a few wavelengths) [61]. The medium scale component captures variations in the radio signal power over distances much larger than a few wavelengths. It is related to the fact that the signal power measured at two different locations having the same transmitter-receiver separation may vastly be different from each other. Figure 3.7, although a rough simplification of reality, relates the large scale, medium scale and small scale propagation effects to each other. As indicated in this figure, when a nodes moves, in the order of a few wavelengths, in the vicinity of each of the locations 1 to 5 or when the radio channel characteristics change overtime, the received radio signal level fluctuates according to the small scale model. The mean received signal power values at locations 1 to 5 are, respectively, p_1 to p_5 . These values are different from each other and are, when expressed in dBm or dBW, normally distributed according to the medium scale propagation model. The mean values of all p_i 's taken at many positions with the same distance to the receiver is the large scale pathloss component.

Attenuation of radio signals due to the pathloss effect has been modeled by averaging the measured signal powers over long times and over many distances around the transmitter. The averaged power at any given distance to the transmitter is referred to as the *area mean power* \mathbf{P}_a (in Watt or milliwatt). The pathloss model states that \mathbf{P}_a is a decreasing function of the distance r between the transmitter and the receiver, and can be represented by a power law [60]:

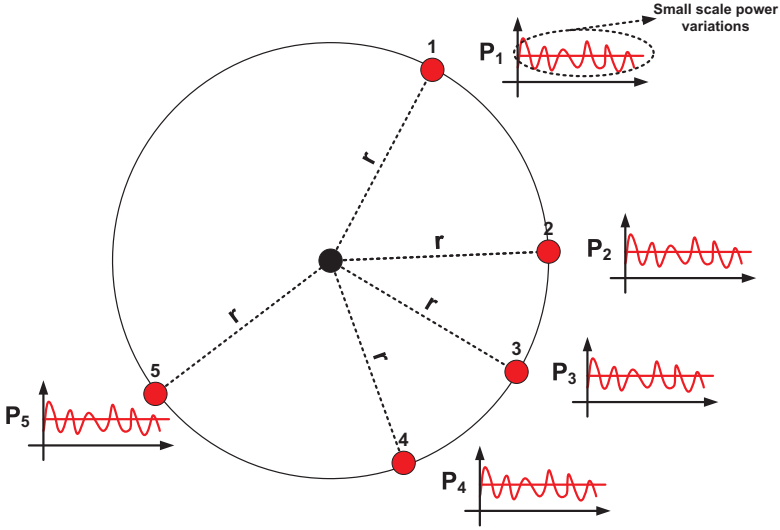


Fig. 3.7. Simplified indication of small scale and medium scale (p_i 's) power fluctuations. The mean of many p_i values, corresponds to the large scale area mean power at distance r .

$$\mathbf{P}_a(r) = c \left(\frac{r}{r_0} \right)^{-\eta}. \quad (3.8)$$

In this formula r_0 is a reference distance³. Parameter η is the pathloss exponent which depends on the environment and terrain structure and can vary between 2 in free space to 6 in heavily built urban areas. In indoor environments with line-of-sight condition, pathloss exponent values of about 1.6 to 1.8 have been measured as well [61]. The constant c depends on the transmitted power, the receiver and the transmitter antenna gains and the wavelength [61].

The medium scale power variations are modeled with a lognormal distribution. In the lognormal radio model the mean received power taken over all possible locations that are at distance r to the transmitter is equal to the area mean power, similar to the pathloss model. However it is further assumed that the average received power varies from location to location in an apparently random manner [56]. More precisely, the lognormal radio model assumes that the logarithmic value of the received signal power at distance r is normally distributed with standard deviation σ around the logarithm of the area mean power. The magnitude of the standard deviation indicates the severity of signal

³ This distance for low-gain antennas in 1-2 GHz region is typically chosen to be 1 m in indoor environments and 100 meter or 1 km in outdoor environments [61].

fluctuations caused by irregularities in the surroundings of the receiving and transmitting antennas. The lognormal model allows then for random power variations around the area mean power. The medium scale power variation is often referred to as lognormal shadowing model [61]. However, in our opinion the term "shadowing" used in the name of this model is somehow confusing because shadowing may imply that the model considers correlated fading in the received power at two locations blocked from the transmitter by means of a physical obstruction. This however is not the case. Variations in radio signal power at different locations with the same distance to the receiver are assumed to be random and independent. The dependent reduction in radio signal powers due to obstruction by buildings is better referred to by the term "blocking" and is not included in the model.

Let the received power at distance r from the transmitter be denoted by $\mathbf{P}(r)$. In the lognormal model the basic assumption is that the logarithm of $\mathbf{P}(r)$ is normally distributed around the logarithmic value of the area mean power:

$$10 \log_{10} (\mathbf{P}(r)) = 10 \log_{10} (\mathbf{P}_a(r)) + x. \quad (3.9)$$

In this expression x is a zero-mean normal distributed random variable (in dB) with standard deviation σ (also in dB). The standard deviation is larger than zero and, in case of severe signal fluctuations due to irregularities in the surroundings of the receiving and transmitting antennas, measurements [61] indicate⁴ that it can be as high as 12. We notice that when $\sigma = 0$, the lognormal model reduces to the pathloss model. So, the pathloss model can be seen as a specific case of the more general lognormal model.

The small scale signal fluctuations without Line-of-Sight component⁵ are represented with a Rayleigh distribution, and therefore are also referred to as Rayleigh fading. Rayleigh fading, named after Lord Rayleigh [62], is the fading of a communications channel generated by the combination of different out-of-phase signals traveling along different paths. The probability density function of a signal amplitude subject to Rayleigh fading is [63]:

$$f_\alpha (\alpha/\bar{p}) = \begin{cases} \frac{2\alpha}{\bar{p}} \exp\left(-\frac{\alpha^2}{\bar{p}}\right) & 0 \leq \alpha < \infty \\ 0 & \alpha < 0 \end{cases}$$

where α is the signal amplitude and \bar{p} is the average power of the signal. The instantaneous power of Rayleigh faded signal is $p = \alpha^2$. Using the transformation [64]:

⁴ It should be noted the measurements that we refer to have been done on lower frequencies than frequencies used in WLAN networks. If a wireless ad-hoc network is making use of WLAN radio modules, the range of variation in σ could be different.

⁵ In this book we will not describe the small scale fading model with Line-of-Sight component which is presented with a Rician distribution. For more information about Rician fading we refer to [60, Chapter 2].

$$\varphi(z) = f(x) \left| \frac{dx}{dz} \right| \quad \text{if } z = h(x),$$

we obtain the following expression for the instantaneous power of a Rayleigh faded signal:

$$f_p(p/\bar{p}) = \frac{1}{\bar{p}} \exp\left(-\frac{p}{\bar{p}}\right). \quad (3.10)$$

3.4.2 Pathloss geometric random graph model

Geometric random graphs have been proposed to model wireless ad-hoc networks before (see e.g. [65], [66], [67], [68]). As we mentioned in the beginning of this section, for realistic modeling of ad-hoc networks it is essential to have an accurate model for the link probability between nodes. All geometric random graph models proposed in the literature prior to our model suggestion (see [69]) were based on the pathloss radio propagation model. Due to the dependency of the link probability in this geometric random graph model on the pathloss radio propagation model, we call this model throughout this book the *pathloss geometric random graph model*.

Let us assume that for correct reception of radio signals it is required that the received power at the receiver is more than a certain threshold value \mathcal{P} . The *coverage area* of node i in a wireless ad-hoc network is the collection of all the points j in the 2-dimensional space where the received signal power from i is more than \mathcal{P} . A node can communicate directly with nodes that fall inside its coverage area but not with other nodes. If the pathloss radio model is used, based on (3.8) all nodes within the range $R = r_0 \left(\frac{c}{\mathcal{P}}\right)^{1/\eta}$ can communicate with each other. This means that the necessary and sufficient condition for two nodes to be connected is that the distance between them is less than R . Depending on the value of R graphs representing ad-hoc networks can be dense or sparse, connected or not connected.

The pathloss geometric random graph model results into a perfect circular coverage area around each node with radius R . In this model the link probability between two nodes $p(r_{ij})$ is a simple step function:

$$p(r_{ij}) = \begin{cases} 1 & 0 < r_{ij} \leq R \\ 0 & r_{ij} > R \end{cases}. \quad (3.11)$$

The pathloss geometric random graph model resembles a highly clustered lattice network with the difference that in the pathloss geometric random graphs, due to strict distance dependency, links between nodes are locally correlated.

Although used extensively in the literature, the pathloss geometric random graph model is in our opinion not a realistic model for ad-hoc networks. In reality the received power levels may show significant variations around the area mean power. Due to these variations, the coverage area will deviate from

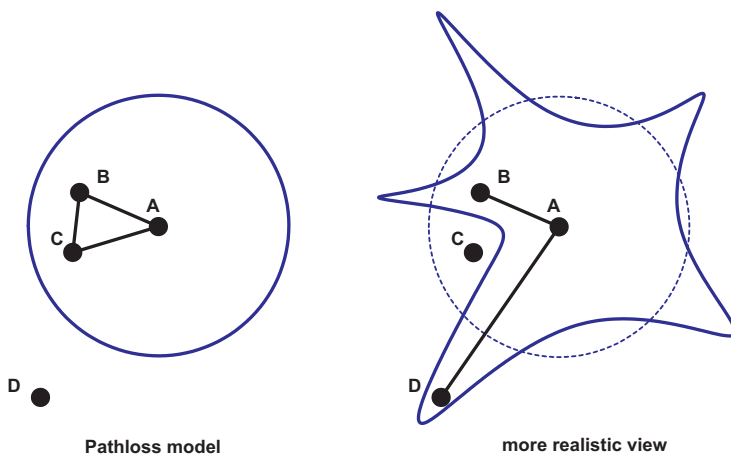


Fig. 3.8. Schematic view showing the nondeterministic nature of radio links where in reality short distance links may not exist while longer distance links do.

a perfect circular shape and consequently, some short links could disappear while long links could emerge (see Figure 3.8). In the next section we propose a more realistic model for ad-hoc networks than the pathloss geometric random graph model. Our model allows for random signal power variations and is described by us in [69] and [70].

3.4.3 Lognormal geometric random graph model

We discussed earlier that the random graph model is not a suitable model for ad-hoc networks, because in random graphs there is no correlation between links and any two nodes have the same probability of being connected. When researchers realized that random graphs are not suitable to model ad-hoc networks, they shifted en masse towards the pathloss geometric random graph model, with very strict and deterministic view, implying that every node within a circle must be connected to the center node. The pathloss geometric random graph model is an attempt towards better modeling of ad-hoc networks. It indeed introduces the notion of distance dependency and adds correlation between links, but it oversimplifies the reality by assuming a perfect circular coverage area for all nodes. Because the nature of radio propagation is nondeterministic and to some degree random, we argue here that the best model for representation of wireless ad-hoc networks lies probably in-between a random graph approach and the pathloss geometric random graph approach. Therefore we propose a model with more relaxed local correlation between links. In this regard we suggest a shift back towards (but not com-

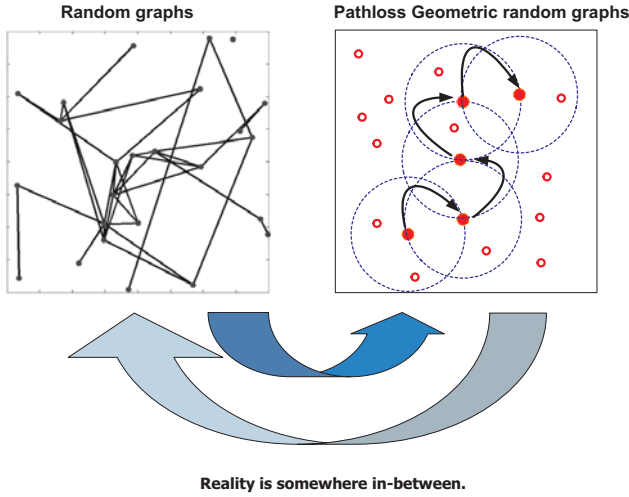


Fig. 3.9. Shift in views for modeling ad-hoc networks.

pletely back to) the random graphs that have no notion of local correlation (see Figure 3.9).

The approach used in this book to make a more realistic geometric random graph model is by taking the medium scale radio signal power variations into account. Medium scale power fluctuations are assumed to have lognormal distribution, as described in Section 3.4.1. Due to the dependency of the link probability in our model on the lognormal radio propagation, we call our model throughout this book the *lognormal geometric random graph model*. In the rest of this book whenever the term geometric random graph is used without explicit mentioning of pathloss or lognormal, we always mean the lognormal geometric random graph.

In our modeling we have not considered the small scale fluctuation of signal amplitudes (the Rayleigh or Rician fading). If we may assume that during the life time of a link the small scale fading effects are averaged-out (over time or over distance), then including small scale fading effects is not sensible. However, we do not exclude the possibility of adding more accuracy to the model by taking the small scale fading into account as well. As a matter of fact, we believe that radio modeling for better understanding of ad-hoc network characteristics is a research area where a lot needs to be done yet. Our approach here should therefore be seen as an attempt towards this goal. Shortly after the publication of our geometric random graph model [69], the lognormal model of medium scale power variations appeared to be suggested for modeling ad-hoc networks by Bettstetter as well [71]. This naturally strengthened our belief in

our model and encouraged us to continue the study of fundamental properties of ad-hoc networks based on the lognormal radio model.

The power received at node j from node i with distance r_{ij} between them according to the lognormal radio model is found using (3.9):

$$10 \log_{10} (\mathbf{P}(r_{ij})) = 10 \log_{10} (\mathbf{P}_a(r_{ij})) + x.$$

To eliminate parameters not relevant to our study, we normalize variables as follows. In Section 3.4.2 we already defined R as the distance where the area mean power $\mathbf{P}_a(r_{ij})$ is equal to \mathcal{P} , the receiver sensitivity. In other words, $\mathcal{P} = c(R/r_0)^{-\eta}$. By dividing powers by \mathcal{P} and using (3.8) we find:

$$\begin{aligned} 10 \log_{10} \left(\frac{\mathbf{P}(r_{ij})}{\mathcal{P}} \right) &= 10 \log_{10} \left(\left(\frac{r_{ij}}{R} \right)^{-\eta} \right) + x \\ 10 \log_{10} \hat{\mathbf{P}}(\hat{r}_{ij}) &= 10 \log_{10} (\hat{r}_{ij}^{-\eta}) + x, \end{aligned} \quad (3.12)$$

where we define $\hat{r}_{ij} \triangleq r_{ij}/R$ as the normalized distance and $\hat{\mathbf{P}}(\hat{r}_{ij}) \triangleq \mathbf{P}(r_{ij})/\mathcal{P}$ as the normalized power. From this formula we see that the logarithm of normalized power has normal distribution with the mean $10 \log_{10} (\hat{r}_{ij}^{-\eta})$ and the variance σ^2 (variance of x). The condition for correct reception of signals at normalized distance \hat{r}_{ij} is that the normalized power at this distance is more than 1 (or zero dB). The probability that two nodes are connected (link probability) is then [70]:

$$\begin{aligned} p(\hat{r}_{ij}) &= \Pr \left[10 \log_{10} (\hat{\mathbf{P}}(\hat{r}_{ij})) > 0 \right] \\ &= \frac{1}{\sqrt{2\pi}\sigma} \int_0^\infty \exp \left[-\frac{(t - 10 \log_{10} (\hat{r}_{ij}^{-\eta}))^2}{2\sigma^2} \right] dt \\ &= \frac{1}{2} \left[1 - \operatorname{erf} \left(v \frac{\log (\hat{r}_{ij})}{\xi} \right) \right], \quad \xi \triangleq \sigma/\eta \end{aligned} \quad (3.13)$$

where $v = 10/(\sqrt{2} \log 10)$, and ξ is defined as the ratio between the standard deviation of radio signal power fluctuations, σ , and the pathloss exponent, η . Low values of ξ correspond to small variations of the signal power around the area mean power and high values of ξ correspond to stronger power variations. Based on the aforementioned range of possible values for η and σ in Section 3.4.1, we note that theoretically ξ may vary between 0 and 6 [70], although values higher than 3 seem to be unrealistic [72], because high values of σ correspond to heavily built and irregular areas where the pathloss exponent is high as well. The best way to determine the most probable value range for ξ is through extensive measurements. To our knowledge reliable and extensive measurements of this type for typical wireless ad-hoc network environments are not available yet. We have performed ourselves some limited measurements that will be discussed in Section 3.5.

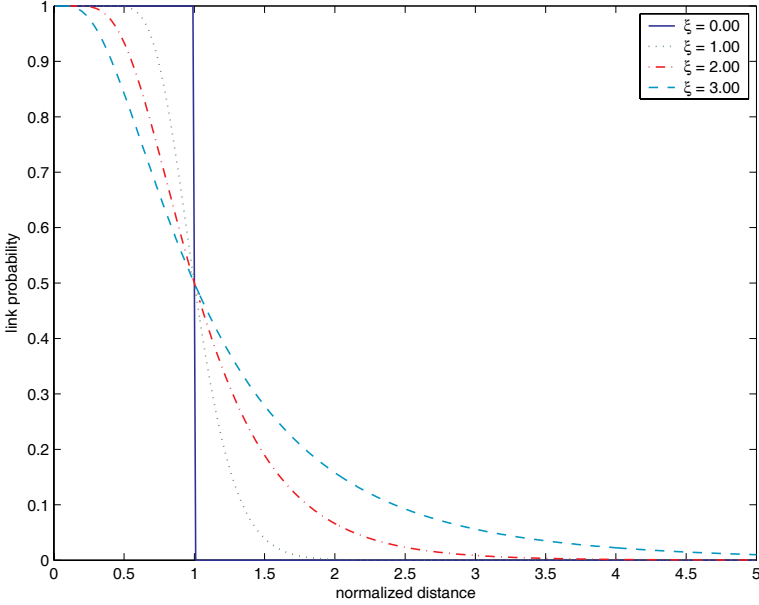


Fig. 3.10. Link probability in lognormal geometric random graph model for different ξ values. In the case $\xi = 0$ the lognormal model reduces to the pathloss model with circular coverage per node.

In the case of $\xi \rightarrow 0$, our model is equivalent to the pathloss model (3.11) with a simple step function as link probability:

$$\lim_{\xi \rightarrow 0} p(\hat{r}_{ij}) = \begin{cases} 1 & \text{if } \hat{r}_{ij} < 1 \\ 0 & \text{if } \hat{r}_{ij} > 1 \end{cases}.$$

This means that our lognormal geometric random graph model is a more general case of the pathloss geometric random graph model. Figure 3.10 shows for different values of ξ the link probability calculated with (3.13). It should be noticed that the normalized distance 1 depends directly on pathloss exponent η . So, the actual length of the normalized distance 1 for any of the lines in Figure 3.10 need not to be the same.

With the lognormal radio model for $\xi > 0$ there is a nonzero probability that nodes at a distance larger than 1 are connected, while there is a nonzero probability that nodes at distances less than 1 are disconnected. In Figure 3.10 we see that as signal fluctuations become more severe (as the value of ξ increases), the link probability at short distances reduces, while at large distances the link probability increases. We mention here briefly that especially the long-distance connectivity probability will affect the hopcount and connectivity in the network; similar to the small world networks extended with a

few "long" links [38]. This matter will be investigated extensively in Chapters 5 and 6.

Figure 3.11 shows results where we used (3.13) to located points in a squared area of normalized size 10×10 that at a certain instant in time are connected to a node in the center of this area at coordinates $(0, 0)$. The points shaded in this figure represent the connected points to the center node. This collection of points can be considered as the coverage area around the center node for different values of ξ . It should be noticed that the area of coverage is not an area with fixed boundaries. It can change according to the distribution function of the lognormal model. When $\xi = 0$ (upper left subplot in Figure 3.11), variance of the received power around the area mean power is zero, and the coverage area is a perfect circular area with normalized radius 1. As the value of ξ increases, variations in the received power increase as well. Consequently we will have more nodes at normalized distances larger than 1 that may have a link with the center node. From the reduced density of shaded points at close distances to the center node, we conclude that there are nodes at distances less than the normalized distance 1 that do not have a link with the center node.

3.5 Measurements

We mentioned before that there are not enough measurement results in the literature to verify the lognormal radio propagation model for wireless ad-hoc networks in indoor and outdoor environments. We have performed our own limited measurements. In this section we describe general set up of the measurements and discuss final results.

We have used WLAN (IEEE 802.11b) access points installed in three railways stations in The Netherlands to perform measurements on the received signal powers⁶. In these three railway stations in total ten WLAN access points were installed at convenient locations, varying in height between 2.5 to 14 meters. Using a WLAN receiver card with a laptop, we have measured the received signal powers from the access points while moving in and around these train stations at walking speed. We logged on the laptop the received signal power and the distance to the access point at the rate of 1 sample per second. After filtering unreliable data we had 9 hours of measurement data. For position determination we used a GPS receiver with 10 meters position accuracy⁷.

⁶ WLAN equipment used in these measurements was installed within the frame work of an cooperative research project by ProRail, a company responsible for reliability, security and capacity of railways in The Netherlands.

⁷ We may expect that the measured position falls with 68% probability (one sigma confidence interval) within the stated distance from the actual position. This accuracy is achieved with the civilian code of GPS without selective availability

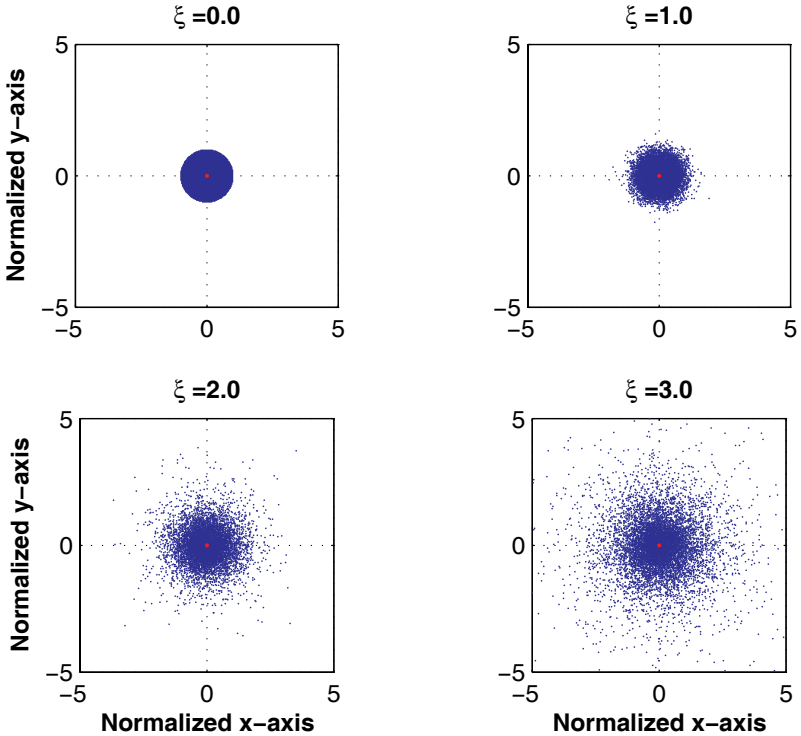


Fig. 3.11. Coverage of a node in the center of a service area of size 10×10 , for different values of ξ .

Figure 3.12 shows as function of the distance to the access points the measured signal powers. In this figure we have smoothed the data by taking the average of the measured signal powers for all distances that fall within intervals of 10 meters to the access points. We notice that there is a good match between the measured area mean power values and the pathloss propagation model, with the pathloss exponent value given in the figure.

We have also noticed that measured power values have an approximately normal distribution around the expected power area mean values for each distance, as the lognormal propagation model predicts. This can be seen from Figure 3.13.

(S/A). S/A is an intentional degradation in the accuracy of GPS introduced originally for civilian users. In the year 2000 the United States Department of Defense decided to switch off selective availability.

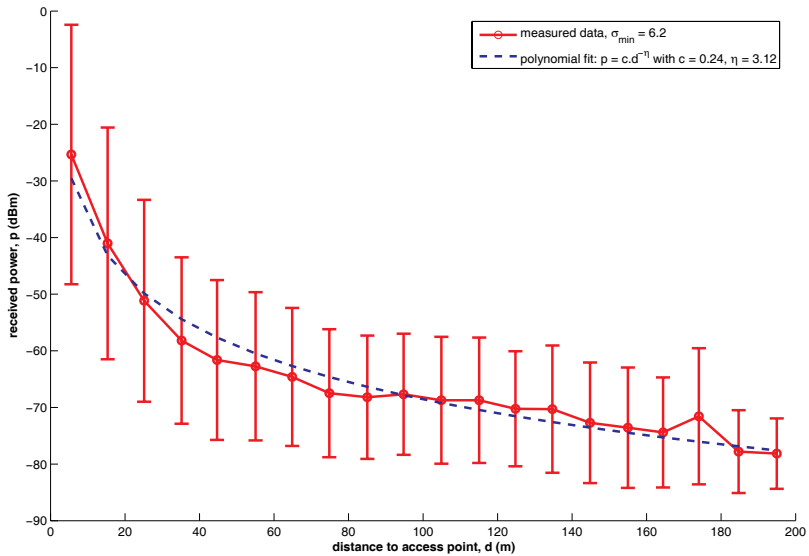


Fig. 3.12. Power as function of the distance to access points. Error bars show the standard deviation of measured data.

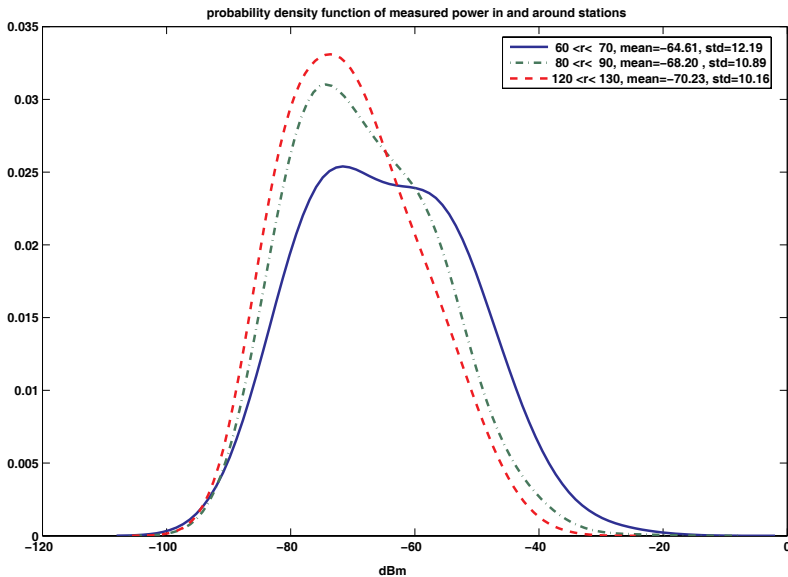


Fig. 3.13. Probability density function for some range of measured data. Lines in this figure show the contour of the PDF's.

Our measurements roughly agree with the theoretical lognormal radio propagation model. However, despite this match, based on these measurements alone we may not conclude with certainty that radio propagation in ISM bands for wireless ad-hoc networks can be modeled with a lognormal radio model. Our measurements are unfortunately not extensive enough and, foremost, not very reliable. There are several reasons for the unreliability of the data:

1. The position determination method used by us is inaccurate. For reliable measurements we need a position determination accuracy in the order of 1 meter or better. However due to budget restriction we were not able to achieve this goal. One direct consequence of position inaccuracy is the high values of the standard deviation for measured powers at close distances to the access points (see Figure 3.12).
2. We have aggregated the data from all access points, without any correction for the height of the antenna at each access point.
3. The WLAN card and the software used to log the data were unable to measure beyond about -94 dBm power levels. Consequently, we were not able to perform measurements at relatively longer distances to the access points.
4. The structure of the areas where we have performed the measurements has been very diverse, from heavily obstructed indoor environments without line-of-sight to vast open spaces with line-of-sight. Putting measured data from all these different areas together is a very crude way of statistical analysis. Our measurement data is not extensive enough for statistical analysis of each area type separately.

3.6 Chapter summary

In this chapter we described important characteristics of random graphs, lattice graphs, scale-free graphs and the pathloss geometric random graphs to position our model for ad-hoc networks. Our model for ad-hoc networks is based on the medium scale signal power fluctuations in radio communications and assumes that these power fluctuations have a lognormal distribution. We have discussed why our lognormal geometric random graph model can be a realistic way of modeling ad-hoc networks. For easy comparison we have summarized some of the important characteristics of wireless ad-hoc networks and different graph models discussed in this chapter in Table 3.1. As it can be seen from this table, our lognormal geometric random graph model matches the characteristics of wireless ad-hoc networks better than other models.

We have argued that our modeling of ad-hoc networks, based on the lognormal assumption of power variations, is a step in the right direction for better and more realistic modeling of ad-hoc networks. However, we emphasized at the same time that more measurements are needed for better understanding of radio channel characteristics in typical ad-hoc network environments

Table 3.1. Comparison of network models.

	link probability	local correlation	small-world property
ad-hoc networks	depends on the distance and fading	yes, grows weaker as fading increases	(1)
random graph	distance independent, same for any two nodes	no	yes
regular lattice graph	distance dependent, same for any two adjacent nodes	no	no
scale-free graph	distance independent, higher for links to "hubs"	(2)	yes (strongly)
pathloss geometric random graph	distance dependent, same for any two nodes at the same distance	yes	(3)
lognormal geometric random graph	distance dependent, a probabilistic function of distance and ξ (4)	yes, grows weaker as ξ increases	depends on ξ (5)

Notes:

(1) If the increase in number of nodes is combined with an increase in the size of the service area, network diameter increases and small-world property is not present. If only node density is increased, network diameter does not change and ad-hoc network shows small-world property. In both cases, with strong power fluctuation of radio signals (fading), the network diameter and the mean hopcount tend to reduce due to the appearance of occasional long links.

(2) Scale-free graphs show strong clustering, but this is not necessarily because of local correlation. For example, on the Internet two pages may have a link to the same popular website, while there is no increased probability of these two pages to be linked as well. However, in social networks, two acquaintances of a popular person may be introduced to each other by that person. Only in the latter case, local correlation is present.

(3) Same as (1), except that there is no way to reflect effects of the fading.

(4) ξ is the ratio between the standard deviation of radio signal power fluctuations and the pathloss exponent.

(5) Same as (1). Parameter ξ in this model reflects effects of the fading. For each number of nodes and node density, network diameter and the mean hopcount reduce as ξ increases.

and frequencies. A set of measurements performed by us supports so far the lognormal model, but has limited extend and accuracy.

Degree in Ad-hoc Networks

In Chapter 3 is mentioned that random graphs have binomial (Poisson) degree distribution (see (3.1)) and in scale-free networks degree distribution has a power-law form, according to (3.7). In this chapter we focus on the mean degree and degree distribution in wireless ad-hoc networks. As indicated in Figure 2.2, the degree and the degree distribution in ad-hoc networks directly affects connectivity of the networks.

4.1 Link density and expected node degree

In wireless ad-hoc network the actual set of connections, in contrast to random graphs or scale-free networks, depends on the geometric distance between nodes. An undirected geometric random graph with N nodes is denoted as $G_{p(r_{ij})}(N)$, where $p(r_{ij})$ is the probability of having a link between two nodes i and j (or j and i) at distance r_{ij} from each other. In this graph the expected number of edges or links between nodes is by definition:

$$L = \sum_{i=1}^N \sum_{j=i+1}^N p(r_{ij}).$$

Let us assume that N nodes are uniformly distributed over a 2-dimensional area with size Ω . To derive the average number of links over all possible configurations, $E[L]$, we have used a dissection technique and assumed that area Ω is covered with $m > N$ small squares (or placeholders) of size $\Delta\Omega$. Assuming that $\Delta\Omega$ is small enough to include only one node, the total number of configurations that can be formed with N nodes over the whole area is $\binom{m}{N}$. We denote these configurations by $G_1, G_2, \dots, G_{\binom{m}{N}}$ and the expected number of links in these configurations by $L_1, L_2, \dots, L_{\binom{m}{N}}$. The average number of links over all possible configurations is by definition the number of links in each configuration multiplied by the probability of occurrence of that configuration:

$$\begin{aligned}
E[L] &= \Pr[G_1] L_1 + \Pr[G_2] L_2 + \dots + \Pr[G_{\binom{m}{N}}] L_{\binom{m}{N}} \\
&= \sum_{k=1}^{\binom{m}{N}} \Pr[G_k] \left[\sum_{i=1}^N \sum_{j=i+1}^N p(|\Delta\Omega_{k,i} - \Delta\Omega_{k,j}|) \right].
\end{aligned}$$

Here $\Delta\Omega_{k,x}$ indicates the position of the placeholder containing node x in configuration k , and $|\Delta\Omega_{k,i} - \Delta\Omega_{k,j}|$ is the distance between two nodes i and j in configuration k . This formula can be simplified and rearranged by taking the following into account:

- N nodes can be placed in m possible placeholders in $\binom{m}{N}$ distinct ways. If nodes are uniformly distributed over area Ω , all configurations are equally probable with probability $\binom{m}{N}^{-1}$.
- In the summation over all possible configuration possibilities, each node could be positioned in any of the m possible positions. Therefore, the sum of the link probabilities $p(\cdot)$ over all possible links between N nodes over all possible configurations, can be written as summation of link probabilities $p(\cdot)$ over all combination of placeholders themselves. Further, we notice that in placing N nodes in m placeholders, a link between any two placeholders i and j occurs exactly in $\binom{m-2}{N-2}$ configurations (if positions i and j are occupied, there are $N-2$ nodes to be positioned in $m-2$ places, and this can be done in $\binom{m-2}{N-2}$ ways). Considering these points, the formula for $E[L]$ can be rewritten as:

$$\begin{aligned}
E[L] &= \binom{m-2}{N-2} \sum_{i=1}^m \sum_{j=i+1}^m p(|\Delta\Omega_i - \Delta\Omega_j|) \binom{m}{N}^{-1} \\
&= \frac{N(N-1)}{m(m-1)} \sum_{i=1}^m \sum_{j=i+1}^m p(|\Delta\Omega_i - \Delta\Omega_j|) \\
&= \frac{N(N-1)}{m(m-1)} \sum_{i=1}^m \sum_{j=i+1}^m p(r_{ij}),
\end{aligned}$$

where r_{ij} is the distance between two placeholders i and j . We mention here that the above double summation can be simplified in several ways to make numerical computations faster. One method is to rearrange and regroup terms so that summations will be over the number of nodes, rather than number of placeholders. An integral expression is also possible [73].

Link density \mathcal{L} is the ratio between $E[L]$ and $E_{\max} = N(N-1)/2$, the maximum number of links in a full-mesh network:

$$\mathcal{L} = \frac{E[L]}{E_{\max}} = \frac{2}{m(m-1)} \sum_{i=1}^m \sum_{j=i+1}^m p(r_{ij}). \quad (4.1)$$

From this formula we see that link density is independent of the number of nodes in the network. The link density depends only on the "strength of connectivity" (defined by the function $p(r)$) over the area of consideration. In other words, the link density is a measure that indicates how well different parts of the area can be reached from other parts. Knowing the expected number of links in the network, the mean degree, $E[d]$, over all nodes is by definition:

$$E[d] = \frac{2E[L]}{N} = (N-1)\mathcal{L}. \quad (4.2)$$

Formulas (4.1) and (4.2) are valid for any geometric random graph $G_{p(r_{ij})}(N)$. For our lognormal geometric random graph model $p(r_{ij})$ is given by (3.13). Assuming normalized distances and substituting $p(r_{ij})$ in (4.1) with (3.13) provides the formula for link density with lognormal radio model, \mathcal{L}_{lg} :

$$\mathcal{L}_{\text{lg}} = \frac{1}{m(m-1)} \sum_{i=1}^m \sum_{j=i+1}^m \left[1 - \operatorname{erf} \left(3.07 \frac{\log(\hat{r}_{ij})}{\xi} \right) \right], \quad (4.3)$$

where \hat{r}_{ij} is the normalized distance between two placeholders i and j in the service area of the ad-hoc network. The service area of the ad-hoc network is the whole area where nodes are uniformly distributed. Figure 4.1 shows the calculated values¹ of the link density found using (4.3) for different sizes of square-shaped service areas and for different values of ξ . Important is to notice that when the size of the service area increases, the link density tends to zero. Further, we see that the link density is higher for larger values of ξ . From a radio propagation point of view, a higher value of ξ means more signal power fluctuations that results into higher probability of having occasional links with nodes at farther distances. As expected, this translates itself into a higher value of the link density over the service area.

Having a formula for the link density; the expected node degree in an ad-hoc network with lognormal radio model follows directly from (4.2):

$$E[d]_{\text{lg}} = (N-1)\mathcal{L}_{\text{lg}} \quad (4.4)$$

Table 4.1 shows some values of the link density and the mean node degree found using (4.3), respectively, (4.4); and compares them with values found through simulations. The simulation program used for verification of computed results, spreads N nodes uniformly over a square-shaped area of given size, and establishes links between node pairs using (3.13). The simulated value of the link density in each case is the ratio of the established links

¹ Wherever the link density is numerically calculated for an area of size Ω , we have assumed that $\Delta\Omega$ is an area of normalized length 0.1 by normalized width of 0.1.

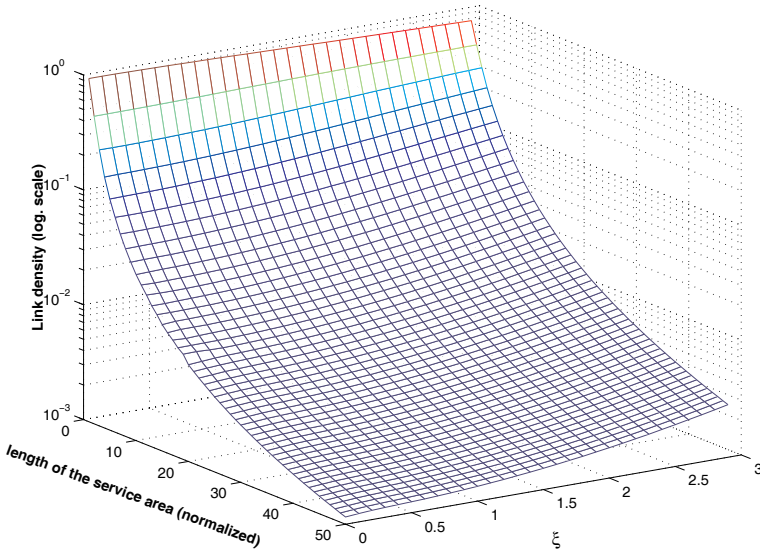


Fig. 4.1. Link density for square-sized areas and different values of ξ .

Table 4.1. Calculated versus simulated values of link density and average node degree based on the lognormal geometric random graph model. In all simulations $N = 2000$.

area	ξ	calculated \mathcal{L}_{lg}	calculated $E[d]_{lg}$	simulated L_{lg}	simulated. $E[d]_{lg}$
5×5	0	0.1046	209.04	0.1051	210.02
5×5	3	0.1820	363.73	0.1823	364.42
10×10	0	0.0288	57.57	0.0287	57.41
10×10	3	0.0606	121.14	0.0610	122.00
20×20	0	0.0074	14.72	0.0074	14.85
20×20	3	0.0175	34.98	0.0178	35.52
50×50	0	0.0012	2.34	0.0012	2.45
50×50	3	0.0030	6.00	0.0030	6.08

to the maximum number of possible links. The simulated value of the mean node degree is the mean value of the degree found for all nodes. It can be seen from Table 4.1 that there is a good match between the simulated and the calculated results.

4.2 Degree distribution

In the previous section we calculated the link density and the expected node degree with the lognormal geometric random graph model and verified by sim-

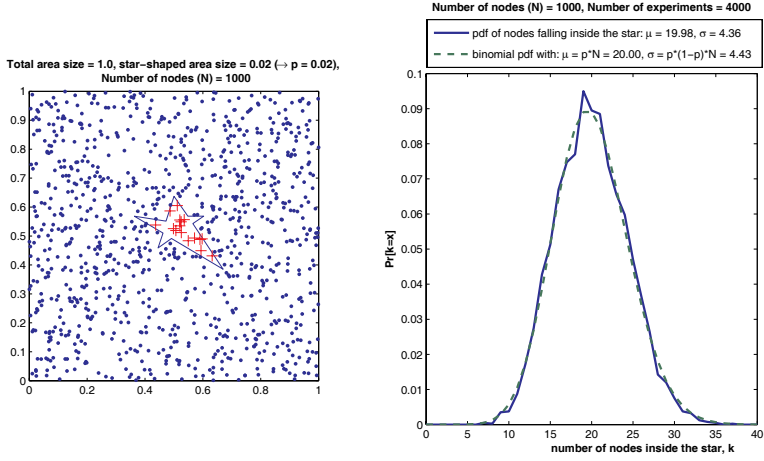


Fig. 4.2. When N nodes are uniformly distributed over an area, the number of nodes falling inside any subsection of irregular shape, like a star in this case, has a binomial distribution, with a mean value directly depending on the ratio of the subsection surface to the surface of the whole area.

ulation that (4.3) and (4.4) provide accurate results, regardless of the size of the service area. In this section we concentrate on the degree distribution. For random graphs we know that by definition the degree distribution is binomial. The question considered in this section is whether the degree distribution in ad-hoc networks is binomial as well.

When nodes are uniformly distributed over the service area, for any node i with an arbitrary but fixed shape of coverage area the degree distribution is binomial with a mean value that depends on the size of the coverage area of node i . This property follows directly from the uniform distribution of nodes and can be verified easily. An example with a star-shaped coverage area is shown in Figure 4.2.

This observation implies that degree distribution in an ad-hoc network must be binomial as well, even if the shape of the coverage area of any node may be very irregular. However, in an ad-hoc network there are two factors that make the situation more complex. At the first place because the coverage area is determined by a probability function, the coverage area of each node does not have a fixed shape and can vary from node to node. Secondly, for nodes close to the borders of the service area, the coverage area is truncated physically by border limits of the service area. We will call the first factor *coverage fluctuations*, and the second factor *border effect*. The border effect reduces the expected number of neighbors for nodes in the border area in

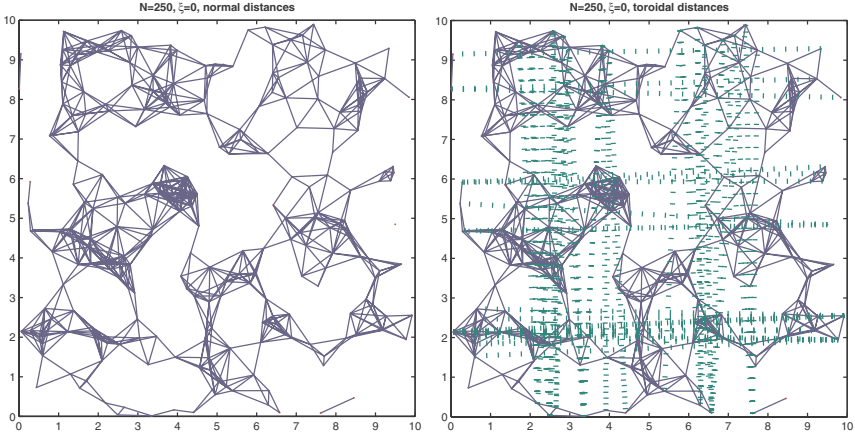


Fig. 4.3. Links between nodes in a rectangular area (figure on the left), and new links that appear when toroidal distances are considered (figure on the right).

comparison to nodes situated more towards the center of the service area. Taking these two aspects into account, what is the distribution of node degree in an ad-hoc network when we look at all nodes collectively?

We have investigated this question through simulations, using our geometric random graph model, for different network sizes, network densities and ξ . The simulation method is straightforward. In each simulation we distribute N nodes over an area of $x \times y$ (normalized values). Then we establish links between nodes using $p(\hat{r}_{ij})$ according to (3.13) and calculate the degree distribution for all nodes. Our main conclusion based on these simulations is that in wireless ad-hoc networks the node degree can be considered to be binomially distributed, with a mean value given by (4.4), when the border effect is negligible. The coverage fluctuations do not seem to distort the binomial distribution of the node degree. In the following two paragraphs we elaborate this conclusion.

Effect of coverage fluctuations

To be able to investigate the effect of coverage fluctuations separate from the border effect, the area can be considered as a torus with toroidal distances between the nodes. This eliminates all borders, and consequently the border effects. A torus can be constructed from a rectangle by gluing both pairs of

opposite edges together with no twists. The resulted torus is embedded in three-dimensional space and is shaped like a donut. Figure 4.3 compares the possible links between nodes when toroidal distances are assumed with the case that only Euclidian distances over the rectangular area are allowed. In the former case there exist simply no border nodes. Our simulation results showed consistently that regardless of the network size, the network density and the value of ξ , the degree distribution is binomial when toroidal distances are used.

Another way of canceling the border effects is to focus on degree distribution for nodes in the inner region of the service area. The inner region of a rectangular service area of size $x \times y$ is a rectangle with size $(x - 2l) \times (y - 2l)$. The service area and the inner region are co-centered rectangles. To exclude the border effect, l should be chosen in such a way that only a negligible portion of the coverage area of any node in the inner region could fall outside the service area. In our simulation for each value of ξ we chose l to be the distance where the link probability drops to 5% (see (3.13)). Our simulation results showed that regardless of the network size, the network density and the value of ξ , the degree distribution for inner nodes is binomial.

The border effect

When we look at all nodes in the service area with some nodes in the border regions and Euclidian distances between nodes, under certain circumstances the border effect could be considered negligible. When the border effect is negligible, the degree distribution is by good approximation binomial. The border effect is negligible if:

1. the service area is much larger than coverage area of a single node, and
2. the node density is low.

A relatively large service area is equivalent to a low link density. Therefore, the combined effect of conditions 1 and 2 is reflected in the product of the link density and the number of nodes; in other words, in the value of the mean node degree (see (4.4)). Considering this, we can say that the border effect is negligible and the degree distribution is binomial when the mean node degree is low. In the remainder of this section we justify this statement and try to quantify conditions for its validity through simulations.

Figure 4.4 shows the degree distribution found through simulations for $\xi = 3$ and different number of nodes uniformly distributed over an area of 20×20 . Figure 4.5 shows another set of simulation results found for $N = 1000$ and different values of ξ . In both figures the solid lines represent the actual degree distribution, while in each case a dotted line shows a binomial distribution with the same mean value as the actual degree distribution. We have used the Kolmogorov-Smirnov test with 5% significance level [74] to verify the hypothesis that the actual degree distribution is binomial. The

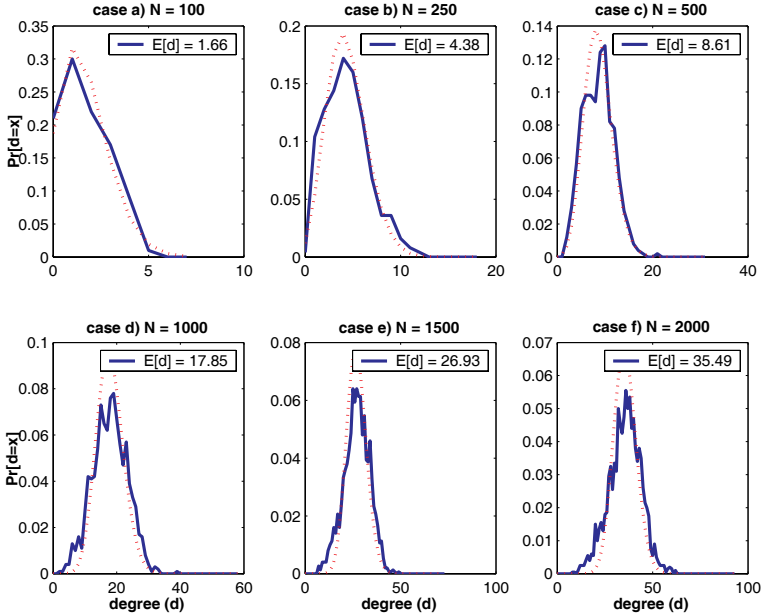


Fig. 4.4. Degree distribution found through simulation for different values of N , compared with a binomial distribution having the same mean value. Service area in all cases is 20×20 and $\xi = 3$.

Kolmogorov-Smirnov tests show that for the low values of mean node degree, $E[d]$, the degree distribution is binomial with high probability. As the mean node degree increases, the probability of accepting the hypothesis reduces. However, only in cases e , f , k and l in Figures 4.4 and 4.5, where the mean node degree is higher than 18, the hypothesis of binomial distribution could be rejected. Other simulation results for different sizes and shapes of the service area (not presented here) are consistent with this result: in all cases where nodes are uniformly distributed over the service area, the distribution of the node degree can be considered to be binomial if the mean node degree is low (lower than 18 for square-shaped areas).

In Chapter 6 we will discuss that knowing the exact degree distribution is relevant in the study of connectivity in ad-hoc networks. Without going into details at this stage we mention that the transition from disconnected to connected networks takes place at low values of the mean node degree ([70], [75], [65]). Therefore, in the regions close to the transition between connected and disconnected networks, it is safe to assume that the degree distribution is binomial. In practice too, the mean node degree is unlikely to be high in wireless ad-hoc networks, personal area networks or sensor networks. At the first place the transmission power of nodes forming these networks is low which limits the geographical size of the coverage area, and consequently the

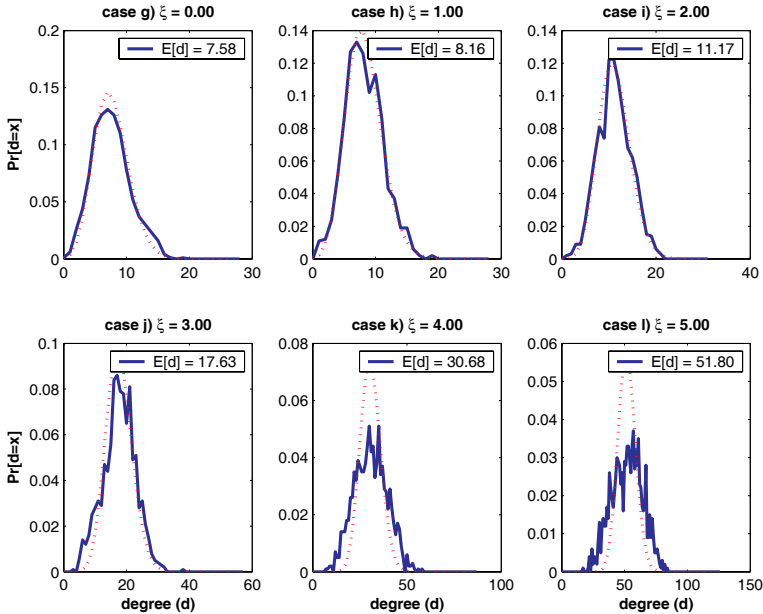


Fig. 4.5. Degree distribution found through simulation for different values of ξ , compared with a binomial distribution having the same mean value. Service area in all cases is 20×20 and $N = 1000$.

number of neighboring nodes. Secondly, because of medium sharing in these networks, a high node degree would result into a very low throughput per node which is an undesired situation and would be avoided.

4.3 Chapter summary

We have studied three topics in this chapter, link density, expected node degree and degree distribution. Main results regarding these topics are summarized below.

Link density: It has been shown that link density is a function of the area size and the parameter ξ . When area size tends to ∞ , link density tends to 0, which is a direct consequence of that fact that in ad-hoc networks links are distance dependent. Further, it has been shown that the link density is higher for larger values of ξ . The minimum link density value for each area size appears for $\xi = 0$, which corresponds to the pathloss model of radio propagation. We have found an analytic expression for the link density in ad-hoc network (see (4.3)).

Expected node degree: Expected node degree in ad-hoc networks is found by multiplying the link density with the number of nodes forming the

network (see (4.2) and (4.4)). Because link density is minimum for the pathloss radio model, we may conclude the pathloss model is the most pessimistic model for estimation of the mean degree in ad-hoc networks.

Degree distribution: In ad-hoc networks degree distribution can be considered to be binomial when the density of nodes is low and the area size is large in comparison to the *maximum link distance*. By the maximum link distance we mean the length of the distance over which two nodes could be connected with a non-negligible probability (for example, $p(\hat{r}_{ij}) \geq 0.05$). Both conditions are required to avoid the so-called border effect. The combined effect of these two conditions is a low value for the mean degree. We have shown that when $E[d] \lesssim 18$, the degree distribution can be considered to be binomial. We recall from Chapter 3 that degree distribution is also binomial in random graphs. It is interesting to see that despite the totally different forms of behavior, both the random graph and the geometric random graph have binomial degree distribution. It should be noticed however that binomial degree distribution in geometric random graphs is conditional on uniform distribution of nodes over the service area. If nodes are not uniformly distributed over the service area, degree distribution will not be binomial. In this book we are always assuming uniform distribution of nodes.

Hopcount in Ad-hoc Networks

In this chapter we focus on the mean hopcount and hopcount distribution in ad-hoc networks. Hopcount is a measure for the number of relay stations that a data packet or a routing message is expected to pass through while traveling between arbitrary source and destination nodes. Therefore understanding the hopcount is important for estimation of the relay traffic, routing overhead and delay in ad-hoc networks. As indicated in Figure 2.2, hopcount is needed for the study of the capacity in ad-hoc networks. Details of the influence of the hopcount on the network capacity are considered in Chapter 10.

In this chapter we will use our geometric random graph model of ad-hoc networks to study the effects of radio propagation conditions, area size and the number of nodes on the expected hopcount and the hopcount distribution in ad-hoc networks. It is obvious that in a sparse network or a network consisting of a few isolated clusters, the mean hopcount and hopcount distribution are not descriptive and meaningful values for the entire network. In this chapter whenever hopcount is calculated or expressed in formulas it is assumed that the underlying network is connected or almost connected¹.

5.1 Global view on parameters affecting the hopcount

In the description of our geometric random graph model for ad-hoc networks we mentioned already that when $\xi = 0$ an ad-hoc network tends to behave like a regular 2-dimensional lattice network. When the value of ξ increases, ad-hoc network starts to deviate from a regular lattice model. Links over larger distances may appear and links over short distances may disappear. In other words, for higher values of ξ an ad-hoc network tends to show stronger small world property, resembling to some degree a random graph. Based on this observation we expect that the hopcount in ad-hoc networks is directly affected by the value of ξ .

¹ Mathematical definition of "almost connected" is given in Chapter 6.

The mean hopcount is the average distance between any pair of nodes, or the average path length in the network. The mean hopcount in a random graph $G_p(N)$ is by approximation $E[h] \simeq \log(N)/\log(E[d])$, where N is the number of nodes and $E[d]$ is the expected node degree in the random graph (see (3.2)).

In contrast to random graphs where links are completely uncorrelated and relative node positions irrelevant, an extremely regulated graph in two dimensions is a rectangular lattice. In a dense 2-dimensional rectangular lattice graph, apart from border nodes, each node has a constant degree of 4 (see (3.5) for the mean degree taking all nodes into account). Further, neighboring nodes are all at the same distance from each other. We call the distance between neighboring nodes the *granularity* of the lattice. The size of the lattice is the number of nodes in the lattice. The mean hopcount in a 2-dimensional rectangular lattice of the size $N = m \times n$ is $\frac{m+n}{3}$ (see (3.6)). We see that for connected graphs, the mean hopcount in a lattice is higher than the mean hopcount in a random graph of the same size. In this chapter we show that the mean hopcount in an ad-hoc network can vary between the expected values for a lattice network and a random graph, depending on the value of ξ and the size of the service area.

5.2 Analysis of the hopcount in ad-hoc networks

For study of the hopcount in ad-hoc networks we have used simulations. In each simulation scenario N nodes are uniformly distributed over a service area with a certain length and width. Then we have formed links between nodes using the link probability (3.13). In the resulted graph we have calculated the hopcount between any two connected node pairs and have derived the hopcount distribution from it. In all simulation cases the size of the service area and the number of nodes have been chosen in such a way that the entire network of nodes has a high probability of connectivity. Connectivity and conditions for that are studied in detail in Chapter 6. At this stage it suffice to mention that the value of N has been chosen high enough for a giant component [65] to appear. This condition is required when we want to relate the calculated hopcount values to the provided value of N . If the node density is so low that the network consists of scattered small clusters, the hopcount calculation is not reliable. Our findings about the hopcount in ad-hoc networks are listed below.

- Hopcount in ad-hoc networks is strongly affected by ξ . Figure 5.1 visualizes the effect of the variation in ξ on the topology of an ad-hoc network. When $\xi = 0$, only nodes at distances less than the normalized distance 1 are connected. As ξ increases, the probability of having a link between two nodes at farther distances increases as well. Consequently, the mean hopcount reduces. Figure 5.2 shows the hopcount distribution corresponding to the subplots in Figure 5.1. At low values of ξ , the mean hopcount

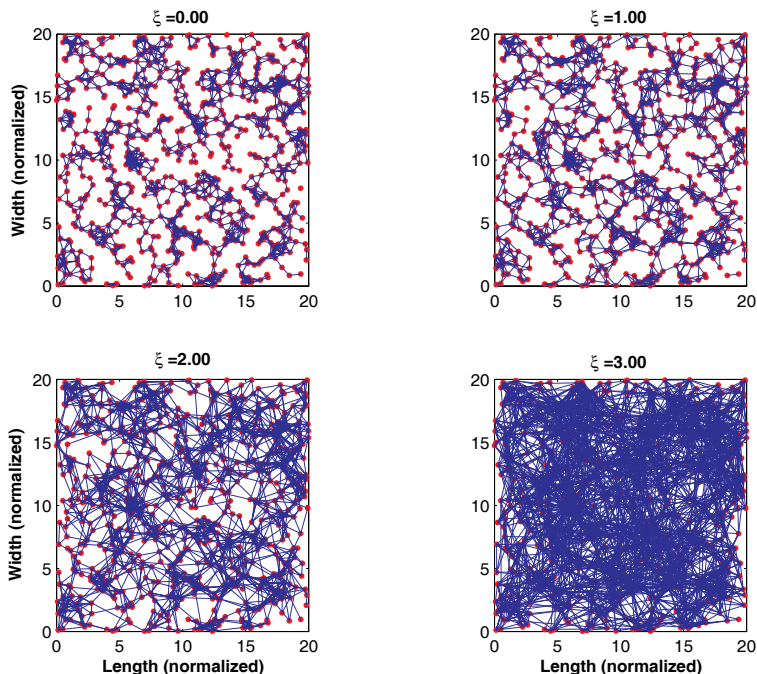


Fig. 5.1. Nodes and links in an ad-hoc network for different values of ξ . In all subplots $N = 1000$, and service area is 20×20 .

is close to the mean hopcount in a lattice with the same length and the same width as the service area **and granularity** 1. When ξ increases, the mean hopcount tends more towards the mean hopcount in a random graph with the same number of nodes and the same link probability. Of course even for the highest value of ξ (about 3 as discussed in Section 3.4.3) we may not expect a hopcount value exactly the same as in random graphs, because in ad-hoc networks the distance dependency of links is always a fact. Only when the length and the width of the service area are in the same order of magnitude as the *maximum link distance* (the metric length of the distance over which two nodes could be connected with a non-negligible probability), we may observe a low mean hopcount value close to the mean hopcount in a random graph.

- Despite the strong effect of ξ on the hopcount in ad-hoc networks, it should not be forgotten that the mean hopcount and hopcount distribution also depend on the area size. For any value of ξ , the mean hopcount increases when the size of the service area increases as well (see Figure 5.3). In other words, when the increase in the network size is combined with an increase in the size of the service area, the diameter of the networks increases.

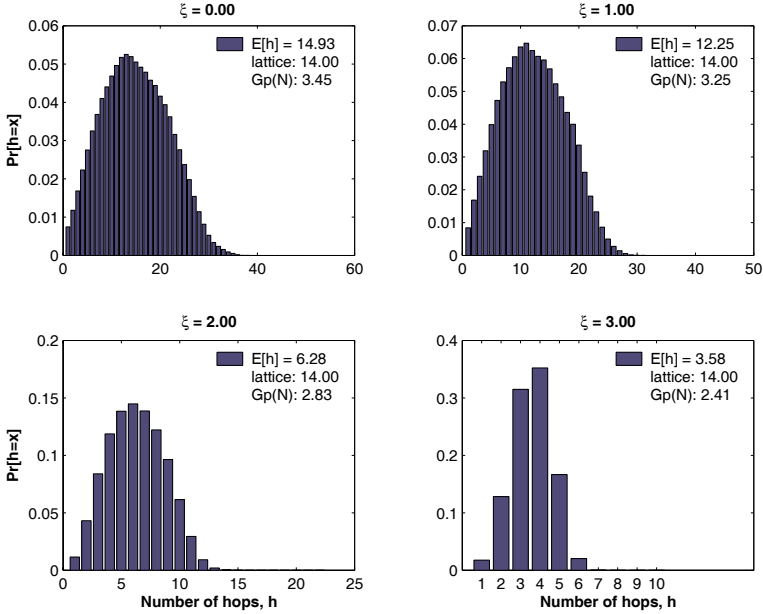


Fig. 5.2. Hopcount for different values of ξ . In all subplots $N = 1000$, and service area is 20×20 . The mean hopcount is indicated on each subplot, for the ad-hoc network, a lattice of size 21×21 , and a random graph with 1000 nodes and the same link probability as in the ad-hoc network.

Under this condition the ad-hoc network does not show the small-world property.

- The hopcount in ad-hoc networks for low values of ξ depends only on the size of the service area and not on the number of nodes. In Figure 5.4 we have plotted the hopcount distribution over the same area size with different number of nodes. We see that the hopcount distribution and the mean hopcount is not affected by changes in the number of nodes. Under this condition we see that an increase in the network size does not increase the hopcount (or diameter) of the network. This means that ad-hoc networks show the small-world property, when only the node density increases.

We had some discussions in Chapter 3 about the small-world property in ad-hoc networks. We said that wireless ad-hoc networks are expected to show small-world property, like random graphs, when the node density increases but the service area size does not change. On the other hand, wireless ad-hoc networks are similar to lattice graphs and do not show small-world property when an increase in the network size (number of nodes) is the result of increasing the service area size (see also Table 3.1). We see here how our lognormal geometric random graph model with parameter ξ captures this dual behavior

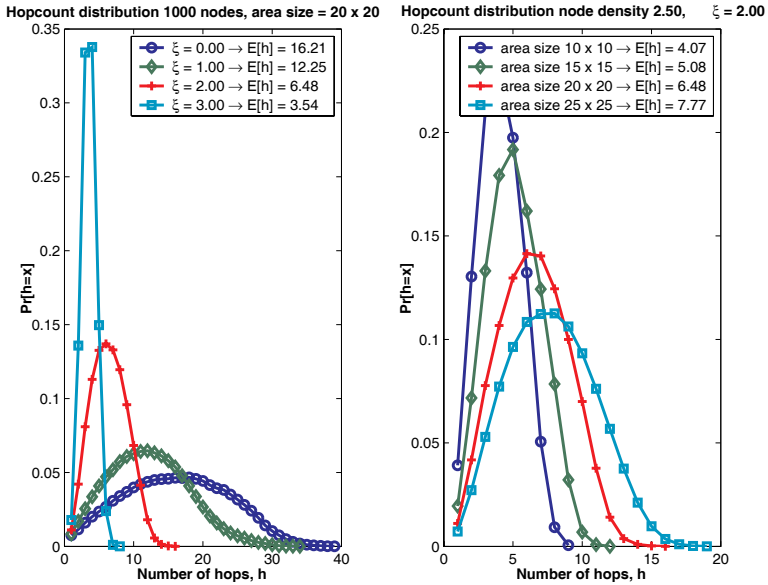


Fig. 5.3. Effects of the changes in ξ (figure on the left) and the area size (figure on the right) on the hopcount in ad-hoc networks.

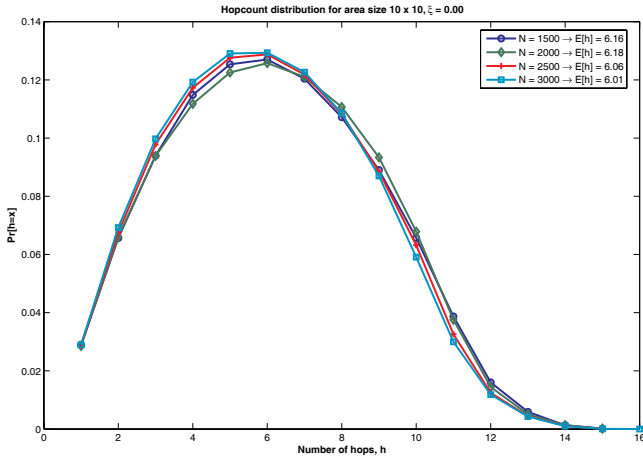


Fig. 5.4. Hopcount in an ad-hoc network for $\xi = 0$, service area is 10×10 and different number of nodes.

5.3 Chapter summary

In this chapter we have shown that the hopcount behavior in ad-hoc networks for low values of ξ is similar to the hopcount in rectangular lattice networks with the same length and the width as the service area of the ad-hoc network. When ξ increases, the mean hopcount and the network diameter are reduced due to the presence of occasional "long links" between nodes. The hopcount in ad-hoc networks increases when the service area increases in size. Further, hopcount is independent of the number of nodes in the network (small-world property) when we increase node density over a given service area.

We have observed that the hopcount in ad-hoc networks is a function of the parameters ξ , N , and the service area size. We have clear picture of how the hopcount is affected by a change in each of these parameters. This is sufficient for the rest of our research concerning interference and capacity determination of ad-hoc networks. Finding an exact analytic formula showing the dependency of the hopcount on ξ , N and the service area size is certainly useful, although we expect this to prove to be a challenging task. However, for a simplified model of ad-hoc networks where position of nodes are fixed to the vertices of a hexagonal lattice, we have found an algorithm to produce the exact hopcount distribution. This model is described in Chapter 9. The algorithm to produce the exact hopcount distribution is given in Section 10.4.1 of Chapter 10.

Connectivity in Ad-hoc Networks

This chapter is about mathematical modeling and better understanding of one of the most important fundamental properties in ad-hoc networks, the connectivity. From a practical point of view, connectivity is a prerequisite to providing reliable applications to the users of a wireless ad-hoc network. To achieve a fully connected ad-hoc network there must be a path from any node to any other node. The path between the source and the destination may consist of one hop (when the source and the destination are neighbors) or several hops. When there is no path between at least one source-destination pair the network is said to be disconnected. A disconnected network may consist of several disconnected islands or clusters. The largest cluster in the network is called the giant component [34]. It should be mentioned that there are two ways of looking at connectivity in a graph or a network: vertex connectivity and edge connectivity. To give a simple example, consider a telephone network. The vertex connectivity is related to the smallest number of switching stations that must be damaged in order to separate the network. The edge connectivity is related to the smallest number of wires that need to be cut to accomplish the same thing.

Connectivity in ad-hoc networks has been studied previously in various papers (see e.g. [66]). However, in this book we have used for the first time the lognormal radio propagation model and our geometric random graph model (see Section 3.4.3) to study connectivity. Our radio model takes statistically into account the dynamics of radio signal power variations. These variations are unavoidably caused by obstructions and irregularities in the surroundings of the transmitting and the receiving antennas. Therefore, this radio model is more realistic than the static and solely on distance dependent models that are commonly used to model wireless ad-hoc networks. We show here that these variations strongly affect the connectivity behavior of the network.

We regard connectivity to be independent of traffic load in the network, although some authors (see e.g. [76]) have preferred to see connectivity as a condition related to the total traffic load in the network. In our approach, on the physical layer connectivity between nodes is predicted by the radio

model. Whether two connected nodes can communicate with each other at any given moment in time depends of course on interference conditions which are directly linked to the traffic load and simultaneous communications between other nodes in the network. Due to interference, communication between two connected nodes may drop to lower speeds or even become impossible at certain times. However, in these cases we say that the link capacity is reduced, instead of saying that the probability of connectivity between these two nodes is decreased. In other words, we consider interference as a capacity-affecting factor and not as a connectivity issue.

In this chapter we will first provide an overview of theoretical published results for the connectivity in random graphs, and in pathloss geometric random graphs. Subsequently, we will show that our lognormal geometric random graph model allows us to refine these connectivity theorems for wireless ad-hoc networks.

6.1 Connectivity in $G_p(N)$ and $G_{p(r_{ij})}(N)$ with pathloss model

For the study of connectivity we consider a wireless ad-hoc network at any instant in time as a graph with fixed topology. Two paths in a graph are said to be independent if any node common to both paths is an end-node of both paths. A graph is said to be k -vertex-connected if for each pair of nodes there exist at least k mutually independent paths connecting them [66]. Another equivalent definition [35] is that a graph is k -vertex-connected if and only if there is no set of $k-1$ vertices whose removal would disconnect the graph. The vertex-connectivity $\kappa(G)$ of a graph is the maximum k such that the graph is k -vertex-connected. Similarly, a graph is k -edge-connected if and only if there is no set of $k-1$ edges whose removal would disconnect the graph [35]. The edge-connectivity $\varkappa(G)$ of a graph is the maximum k such that the graph is k -edge-connected. There is a close relationship between the vertex-connectivity, edge-connectivity and the minimum degree d_{\min} in a graph [35]:

$$\kappa(G) \leq \varkappa(G) \leq d_{\min}.$$

In the literature, as well as in this book, by the term connectivity always vertex-connectivity is meant.

Connectivity has been studied in many publications for random graphs as well as pathloss geometric random graphs. Here we give an overview of two main theorems with relation to the connectivity.

Theorem 6.1. *If we start with a graph on N vertices and an empty edge set and add edges randomly and independently one by one until having m edges, the graph almost surely¹ becomes 1-connected when $m \geq \frac{N \log(N)}{2} +$*

¹ We say that a graph has some property Q *almost surely* (a.s.) or *with high probability* (whp) if the probability it has Q tends to one as N tends to infinity.

$O(N)$. Considering that in $G_p(N)$ two nodes are connected with probability $p \triangleq m/\binom{N}{2}$, we can say that for a random graph to be 1-connected there must hold:

$$p \geq \frac{\log(N)}{N} \quad a.s. \quad (6.1)$$

Theorem 1 dates from the pioneering work of Erdős and Rényi [42] on random graphs where they considered the $G_p(N)$ model to study the threshold for connectivity in graphs. While (6.1) holds for random graphs, in [65] and [66] it is shown that this result is also valid for pathloss geometric random graphs, in any dimension higher than one (but not for one-dimensional graphs).

Intuitively one may see that the connectivity in wireless ad-hoc networks depends on the number of nodes per unit area and on the transmission range of wireless devices. Increasing the density of nodes or increasing the transmission power of a radio node will increase the node degree. Based on this deduction, it is not surprising to see that the second theorem of connectivity relates connectivity to the node degree.

Theorem 6.2. *In a random graph of N nodes if edges are added one by one to the empty graph in an order chosen uniformly at random from the $\binom{N}{2}!$ possibilities, then almost surely the resulting graph becomes k -connected when it achieves a minimum degree of k . In other words, for large N ,*

$$\Pr[G \text{ is } k\text{-connected}] = \Pr[d_{\min} \geq k] \quad a.s. \quad (6.2)$$

where d_{\min} is the minimum degree per node.

Theorem 2 is proved for random graphs in [34]. In [67] and [66] it is proved that this theorem is also valid for the pathloss geometric random graphs, in any dimension higher than one when $\Pr[d_{\min} \geq k]$ is almost 1.

These two theorems of connectivity are not conflicting theorems for random graphs. Here we prove for random graphs, that for large N , $\Pr[G_p(N)$ is 1-connected] $\simeq 1$ if $p > \log(N)/N$, and $\Pr[G_p(N)$ is 1-connected] $\simeq 0$ if $p < \log(N)/N$.

Denote by $f(p) = \Pr[G_p(N)$ is 1-connected]. Because of binomial degree distribution in random graphs and independence of the links, this probability is computed as (see (3.1)):

$$\begin{aligned} f(p) &= \Pr[d_{\min} \geq 1 \text{ in } G_p(N)] \\ &= \left[\sum_{k=1}^{N-1} \binom{N-1}{k} p^k (1-p)^{N-1-k} \right]^N \\ &= [1 - \Pr[d_{\min} = 0]]^N \\ &= [1 - (1-p)^{N-1}]^N. \end{aligned} \quad (6.3)$$

According to (6.3), $f(p)$ is always one for fixed $0 < p < 1$ and large N . Therefore, the asymptotic behavior of $\Pr[G_p(N) \text{ is 1-connected}]$ requires to investigate the influence of p as function of N . The order of $f(p_N)$ for large N is:

$$\begin{aligned} f(p_N) &= \exp\left(N \log\left(1 - (1 - p_N)^{N-1}\right)\right) \\ &= \exp\left(-N \sum_{j=1}^{\infty} \frac{(1 - p_N)^{jN-j}}{j}\right) \\ &= \exp\left(-N(1 - p_N)^{N-1} - N \sum_{j=2}^{\infty} \frac{(1 - p_N)^{jN-j}}{j}\right) \\ &= e^{-N(1-p_N)^{N-1}} \left(1 + O\left(N \sum_{j=2}^{\infty} \frac{(1-p_N)^{(N-1)j}}{j}\right)\right). \end{aligned}$$

If we define $c_N \triangleq N \cdot (1 - p_N)^{N-1}$, then the order term $O\left(N \sum_{j=2}^{\infty} \frac{(1-p_N)^{(N-1)j}}{j}\right) = O\left(N \sum_{j=2}^{\infty} \frac{c_N^j}{jN^j}\right)$ vanishes for large N provided we choose $c_N = O(N^\beta)$ with $\beta < \frac{1}{2}$. For large N , we thus have that $f(p_N) = e^{-c_N} \sim e^{-AN^\beta}$ which tends to 0 for $0 < \beta < \frac{1}{2}$ and to 1 for $\beta < 0$. Hence, the critical exponent where a sharp transition occurs is $\beta = 0$. In that case, $c_N = c$ (a real positive constant) and

$$p_N = 1 - \exp\left(\frac{\log c}{N-1} - \frac{\log N}{N-1}\right) = \frac{\log N}{N} + O\left(\frac{\log c}{N}\right).$$

In summary,

$$f(p) \longrightarrow \begin{cases} 0 & \text{if } p < \log(N)/N \\ 1 & \text{if } p > \log(N)/N \end{cases},$$

with a transition region around $\frac{\log N}{N}$ of width of $O(\frac{1}{N})$.

In the next section we will investigate connectivity in wireless ad-hoc networks by using our geometric random graph model explained in Section 3.4.3. As mentioned before, this model is more realistic than the pathloss geometric random graph model. We present results obtained through simulations. We believe that our simulation results provide new insights into the theory of connectivity in wireless ad-hoc networks.

6.2 Connectivity in $G_{p(r_{ij})}(N)$ with lognormal model

Our focus will be on 1-connectivity. Higher orders of connectivity are not considered at this moment. For the study of connectivity in ad-hoc networks

based on our geometric random graph model we have used simulations. The simulation program distributes N nodes uniformly over a square area and establishes links between node-pairs using the probability function (3.13). The *service area* of the ad-hoc network is the whole area where nodes are uniformly distributed. In the resulting graph for each simulation run we check the 1-connectivity and store information regarding the number of clusters (components) in the graph, the mean component size, the total number of components and the degree distribution. We have performed simulations with $N = 250, 500$ and 1000 . For each value of N , results are gathered for $\xi = 0, 1, 2, 3$ and different values of the area size. Changing the area size changes the expected values for the node degree and allows us to study connectivity as function of the mean degree. For each unique combination of the area size, ξ and N we have repeated simulations with 500 independent network configurations.

Two different procedures can be used for checking 1-connectivity [31]:

1. The first procedure chooses a node at random and uses a simple flooding algorithm to tag all nodes belonging to the same cluster. This procedure is repeated for all untagged nodes until no untagged nodes remain in the graph. If the largest cluster found in this way contains all nodes, the network is 1-connected. In the process of checking for 1-connectivity, this procedure provides us the exact size of all clusters in the graph. By definition the largest cluster in the graph is called the *giant component*. The *size* of each cluster is defined as the ratio of the number of nodes in that cluster to the total number of nodes in the network. Similarly, the *giant component size* is the ratio of the number of nodes in the giant component to the total number of nodes forming the network.
2. The second procedure for checking 1-connectivity uses the $N \times N$ Laplacian of G . The Laplacian [35] is the difference between the diagonal node degree matrix, in which element (i, i) is degree of the node i ; and the adjacency matrix, in which element (i, j) is one or zero depending on whether a link does or does not exist between nodes i and j (diagonal elements of the adjacency matrix are zeros). Eigenvalues of the Laplacian are real positive numbers. The number of zero eigenvalues of the Laplacian is equal to the number of cluster in G [35]. This is a fast and powerful method for checking connectivity of a graph. For a connected graph we have only one zero eigenvalue. The second smallest eigenvalue of the Laplacian, although not considered further in this book, is a beautiful representative of the strength of the connectivity and robustness in G . The larger this number, the more difficult it is to disconnect the graph by taking out edges or vertices [35, section VIII.2].

We have used the first procedure to gather simulation results, while the second procedure is applied consistently to verify reliability of the first procedure. Results of both procedures matched always perfectly with each other.

Figure 6.1 shows a part of the simulated results for 500 nodes. Each subplot corresponds to a different value of ξ . In each subplot in this figure we have

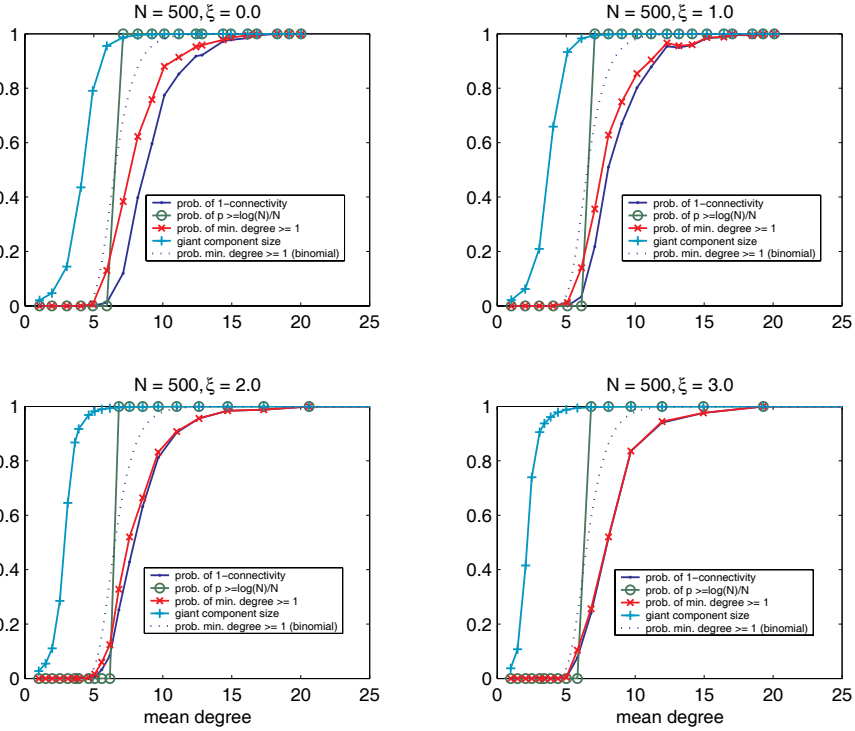


Fig. 6.1. Simulated results for different values of ξ showing: the probability of 1-connectivity, the probability of p exceeding the $\log(N)/N$ threshold, the probability of the minimum node degree being more than or equal to one, and the giant component size as fraction of the total number of nodes. For comparison reasons, we have drawn on each graph the probability of minimum degree being more than or equal to one for a binomial degree distribution.

shown as function of the node’s mean degree the following data obtained through simulations:

1. The probability of 1-connectivity.
2. The probability of p exceeding the $\log(N)/N$ threshold, which allows us to check the accuracy of the first theorem of connectivity by comparing this data with the first set of data mentioned above.
3. The probability of the minimum node degree being more than or equal to 1, which allows us to check the accuracy of the second theorem of connectivity by comparing this data with the first set of data mentioned above.
4. The giant component size.

The dotted line without markers in each subplot is added for comparison reasons and shows, as function of the mean node degree, the probability of

1-connectivity (or the probability of the minimum degree being more than or equal to 1) in a random graph with N nodes, according to (6.3).

The first conclusion we can draw after analyzing simulation data is that our results indeed comply with both theorems of connectivity for the pathloss geometric random graph model (in other words, when $\xi = 0$). However we can add more important additional details to refine the connectivity theorems:

- In all simulated cases, the first theorem of connectivity based on $\log(N)/N$ threshold predicts an almost surely connected network at those values of the mean degree where the actual probability of 1-connectivity is rather low (about 0.2 or less in subplots of Figure 6.1). Is this theorem too optimistic? We can examine this question by looking at the size of the giant component. For example, in Figure 6.1 for $\xi = 0$ the giant component size at the threshold where p exceeds $\log(N)/N$ is 0.987. In another set of simulation with 1000 nodes (not shown in this chapter), the giant component size at this threshold point for $\xi = 0$ was 0.998. This means that from the 1000 nodes, only 2 nodes did not belong to the giant component. The giant component size at the threshold point where this theorem predicts "almost surely" connectivity increases as $N \rightarrow \infty$, and this is exactly what the theorem stands for.
- In simulated cases with the low values of ξ the actual probability of connectivity coincides with the probability of $d_{\min} \geq 1$ only when $\Pr[d_{\min} \geq 1]$ is almost 1. This complies with the second theorem of connectivity for the pathloss geometric random graphs. However, when the ξ increases, these two lines merge at lower values of $\Pr[d_{\min} \geq 1]$. For example, for $\xi = 3$ these two lines are overlapping each other virtually for the entire range of the mean degrees. This behavior was expected from the second theorem of connectivity only for random graphs. We can conclude that when ξ increases, the increase in the long-distance connectivity probability together with the reduction of the short-distance connectivity probability reduces the correlation between links. As a result, the geometric random graph approaches the random graph behavior, and the probability of 1-connectivity equals the probability $d_{\min} \geq 1$ for all values of $\Pr[d_{\min} \geq 1]$.
- Comparing the $\Pr[d_{\min} \geq 1]$ in ad-hoc networks with the $\Pr[d_{\min} \geq 1]$ in random graphs (the dotted line in subplots of Figure 6.1) suggests that ad-hoc networks need a higher value of the mean degree to achieve the same probability of not having any isolated nodes. This is due to the existence of nodes around the borders of the service area. If we eliminate the border effect by considering toroidal distances rather than Euclidian distances (as described in Chapter 4) this difference diminishes. Figure 6.2 shows one set of simulated data gathered with toroidal distances. In this figure, the line indicating $\Pr[d_{\min} \geq 1]$ in random graphs overlaps with the line for $\Pr[d_{\min} \geq 1]$ in ad-hoc networks.
- As mentioned in Chapter 5, the increase in long-distance connectivity probability affects the hopcount in the network. In that chapter we al-

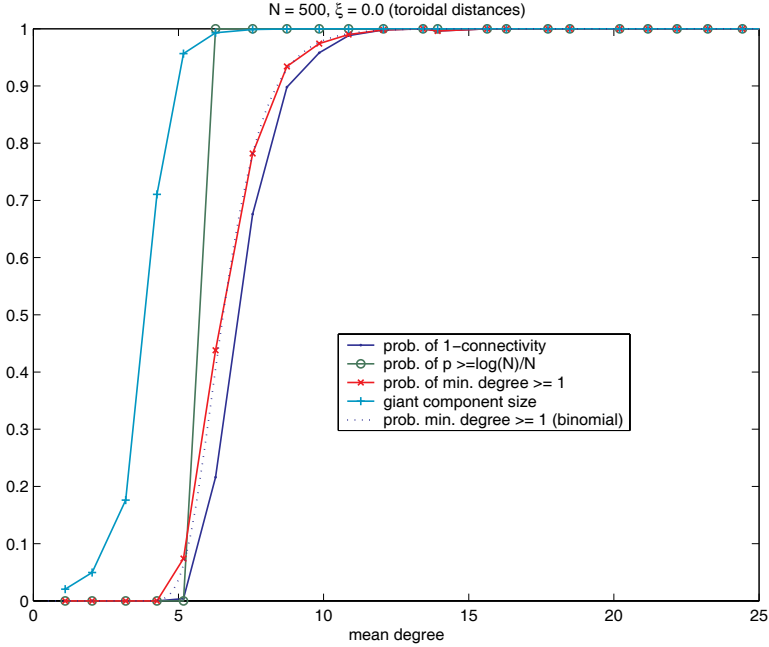


Fig. 6.2. One set of simulated results similar to Figure 6.1 but with toroidal distances.

ready stated that the mean hopcount in an ad-hoc network can vary between the expected values of the hopcount in a lattice network and in a random graph, depending on the value of ξ . As ξ increases, the probability of having a link between two nodes at farther distances increases as well. Consequently, the mean hopcount reduces and gets closer to the expected hopcount in random graphs. This behavior is investigated as function of the mean node degree in Figure 6.3. This Figure shows the mean hopcount found for $\xi = 0$ and $\xi = 3$. When the mean degree is high enough for a giant component to appear, at low values of ξ the mean hopcount is close to the mean hopcount in a lattice network with the same length and width as the service area of the ad-hoc network. When ξ increases, the mean hopcount tends more towards the mean hopcount in a random graph with the same number of nodes and the same link probability.

- For the same area size and for the same number of nodes the average node degree increases with increasing value of ξ (see Figure 6.4). From the radio propagation point of view, a higher value of ξ means a higher probability of having links with nodes at farther distances. This translates itself into a higher value of the mean node degree over the service area. This phenomenon was addressed previously in [69] and in Chapter 4. The increase

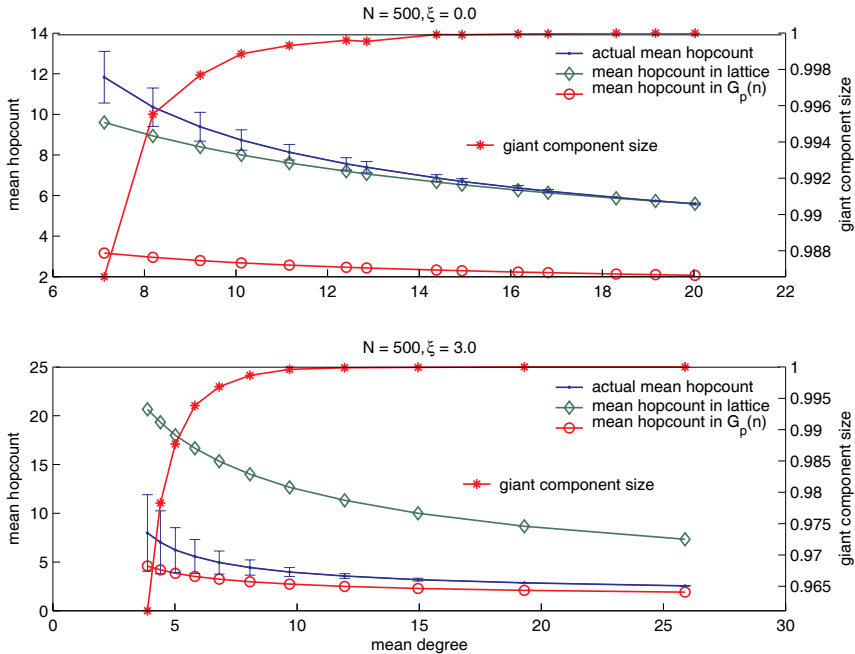


Fig. 6.3. Simulated results showing the mean hopcount as function of the mean degree for different values of ξ in ad-hoc networks in comparison to the mean hopcount in lattice networks and random graphs. Error bars on the line for actual hopcount indicate the standard deviation of the simulated hopcount.

in the mean node degree directly enhances the probability of connectivity.

- In all simulated cases we see that the giant component size is growing steeply towards 1 for those values of the mean degree that the probability of 1-connectivity is very low. For a relatively large span of the mean degree values the giant component is already covering most of the network but 1-connectivity is not achieved yet. This is due to only a few isolated nodes or small node clusters outside the giant component. This fact is demonstrated in Figure 6.5 that shows the mean size of components other than the giant component for different values of ξ . Starting from small values of the mean degree, as the mean degree increases, the mean size of the giant component as well as the mean size of other components increase. However, soon the giant component will "swallow" smaller clusters and causes their mean size to drop rapidly. In [77] it is proved that the size of the components other than the giant component is $O(\log N)$, to which our simulated results comply. We believe for practical use of ad-hoc networks 1-connectivity is a too stringent condition to satisfy. Therefore, we suggest to use the giant component size as a measure for connectivity in wireless ad-hoc networks.

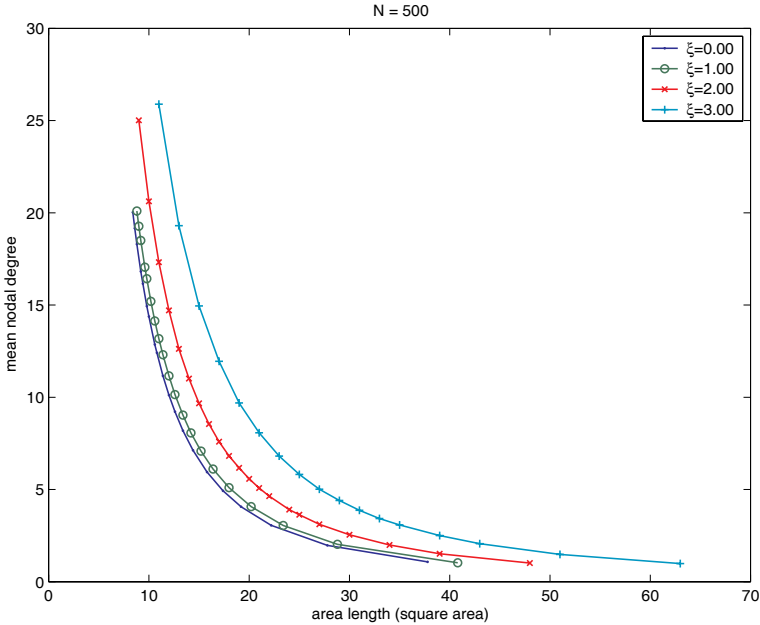


Fig. 6.4. Mean node degree for 500 nodes uniformly distributed over areas of different sizes for different values of ξ .

The giant component size not only provides information about the network being fully connect or not, but also it provides additional information about the fraction of the network which is fully connected. For practical use of ad-hoc networks it may suffice to provide conditions that, for example, only 99% of the network is connected.

This last point regarding the use of the giant component as a more suitable measure of connectivity is discussed in more details in the following section.

6.3 Giant component size

In Chapter 3 we already mentioned that in random graphs for large N the giant component size S is the non-zero solution to (3.4). In the subplots of Figure 6.1 we already showed the giant component size found through simulations for $\xi = 0, 1, 2$ and 3. In Figure 6.6 we have plotted them next to

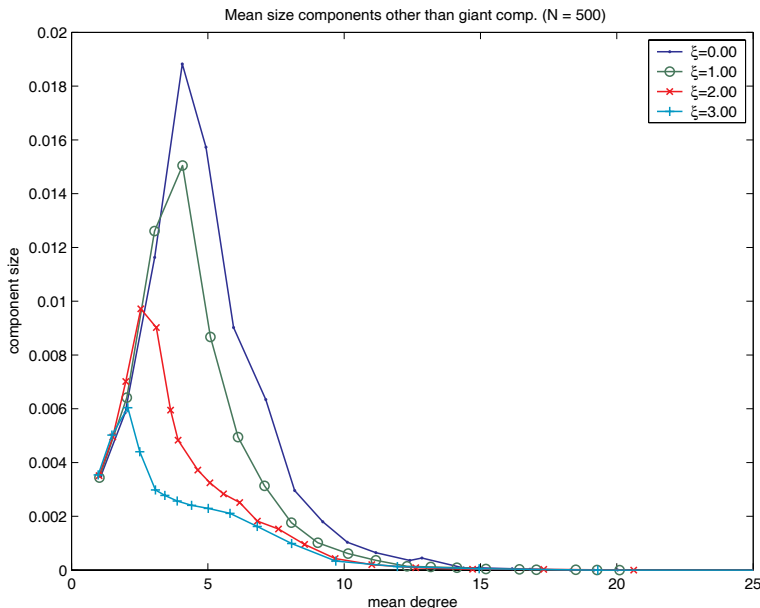


Fig. 6.5. Mean size of components other than the giant component for different values of ξ .

each other (with an additional line² for $\xi = 6$) and compared them³ with the giant component size in a random graph, found using (3.4). From Figure 6.6 we see that the lines representing the giant component size for high values of ξ get close to the values predicted by (3.4) for random graphs. However, for low values of ξ the giant component size appears to be shifted along the mean degree axis. The amount of this shift is higher for lower values of ξ . We have tried several function forms to estimate this shift. A good approximation found for this shift is: $2.64 \exp(-0.44\xi)$. Taking this into account, the size of the giant component in wireless ad-hoc networks based on our lognormal geometric random graph model, S_{lg} , is by approximation the non-zero solution to the following equation:

$$S_{\text{lg}} = 1 - \exp(-\tilde{z}S_{\text{lg}}), \quad \tilde{z} \triangleq z - 2.64 \exp(-0.44\xi) \quad (6.4)$$

² We have chosen to include a line for $\xi = 6$, although from the radio propagation point of view this value is not very likely (see Section 3.4.3). This high value for ξ is chosen only to show that in the theoretical case where radio signal power fluctuations are very severe they can dominate significantly the distance dependency of radio links, and could cause the network to behave like a random graph.

³ The giant component sizes found through simulations in Figure 6.6 are found for $N = 500$. Other simulation results for $N = 250$ and $N = 1000$ indicated no noticeable difference with these values.

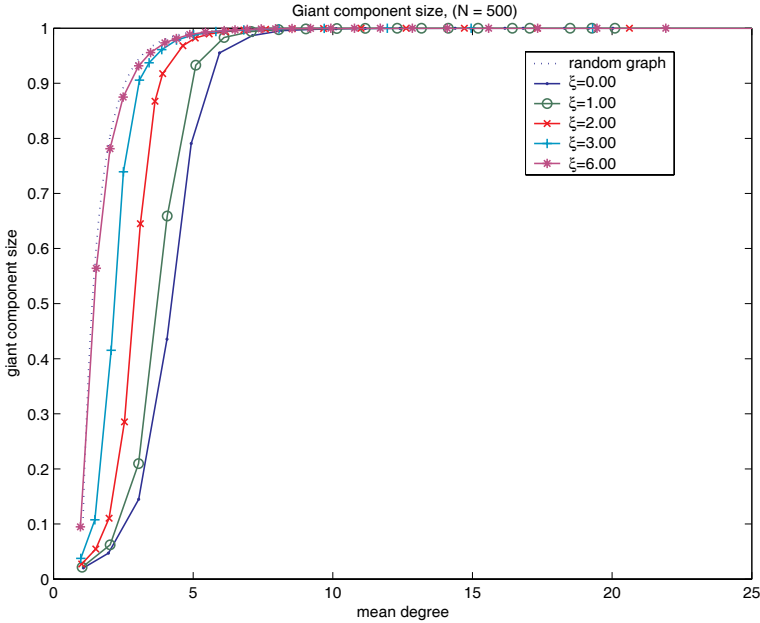


Fig. 6.6. Comparison of the giant component size in a random graph with the values found for ad-hoc networks.

where, $z = E[d]$ is the mean degree in the ad-hoc network. Figure 6.7 shows the in this way calculated giant component size in wireless ad-hoc networks for different values of ξ . For comparison, the giant component size in random graphs is drawn on each subplot of this figure. As visible in this figure, there is a good match between the simulated and the calculated values of the giant component size.

6.4 Chapter summary

In this chapter we have studied connectivity in wireless ad-hoc networks by modeling the network as an undirected geometric random graph. The novel aspect in our study is that for finding the link probability between nodes we used the lognormal propagation radio model, that takes into account statistical fluctuations of the radio signal power around its mean value. Using this model we have been able to modify the theorems for connectivity in ad-hoc networks. Our study shows:

1. The first theorem of connectivity that states for the connectivity of a network the link probability, p , needs to exceed $\log(N)/N$ is only a good test of connectivity when $N \rightarrow \infty$. In ad-hoc networks where the number of nodes is limited to tens or hundreds of nodes, the $\log(N)/N$ value is

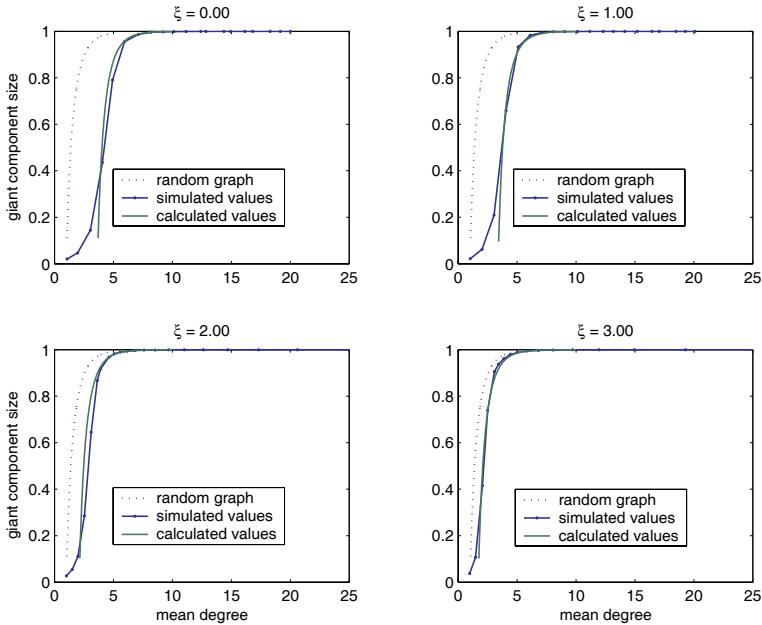


Fig. 6.7. Simulated and calculated values for the giant component size in ad-hoc networks for different values of ξ .

only an accurate indicator for the threshold where a giant component starts to appear.

- Power fluctuations of radio signals reduce the amount of correlation between links, causing the network to behave like a random graph with uncorrelated links. The second theorem of connectivity states that probability of a network to be 1-connected is equal to the probability of the minimum degree to be more than or equal to 1. This theorem has been proved to be true for the pathloss geometric random graph model only when $\Pr[d_{\min} \geq 1]$ is almost 1. However in our lognormal geometric random graph model when ξ increases, the geometric random graph approaches the random graph behavior, and the probability of 1-connectivity equals the probability $d_{\min} \geq 1$ for all values of $\Pr[d_{\min} \geq 1]$.
- Radio signal power variations increase the probability of long links, which enhances the probability of connectivity for the entire network.

Another new result in this chapter is an equation found for the calculation of the giant component size in wireless ad-hoc networks, that takes into account the level of radio signal power fluctuations. Our formula can be used to provide directives for the average required number of neighbors per node (mean degree per node) to obtain connectivity over any desired percentage of the network. Mean degree can be changed by adjusting the transmission

power of nodes or by changing the density of nodes. Results presented in this chapter also demonstrate that full connectivity is achieved at relatively high values of the mean degree, while at far lower values of the mean degree a very large portion of the network could already be connected. Therefore we argue that for practical planning and design of wireless ad-hoc networks or sensor networks 1-connectivity (full connectivity) is a too stringent condition, and suggest to use the giant component size as a measure for "connectivity".

MAC Protocols for Packet Radio Networks

Study of the Medium Access Control (MAC) protocols does not belong to the primary topics considered in this book (see Figure 2.1). However, MAC protocol characteristics affect directly interference levels, as well as capacity in ad-hoc networks. In this chapter we specify these characteristics and introduce a method of classification for the MAC protocols. This classification method facilitates our study of the interference and the capacity of ad-hoc networks in Chapters 8 and 10.

7.1 The purpose of MAC protocols

MAC protocols are needed to regulate communication between nodes through a shared medium. It corresponds to the data link layer (layer 2) of the ISO Open System Interconnect (OSI) reference model [78]. Many MAC protocols have been developed for communication in wired networks as well as wireless networks. For example IEEE 802.3 based on CSMA/CD for wired Ethernet and IEEE 802.11 for WLANs [79]. Sharing a medium by many users unavoidably restricts system performance for users in average [80]. A well-designed MAC protocol is essential to maximize the performance and the efficiency of the network.

In wireless ad-hoc networks, MAC protocols are needed as well to ensure successful operation of the network. With the increased international attention to ad-hoc and sensor networks many MAC protocols have been suggested for these networks in the past few years. Each of these MAC protocols may have different priorities for problems to solve, depending on the applications to be supported on higher OSI layers. For example, in sensor networks MAC protocols may primarily attempt to minimize energy consumption [81], whereas in ad-hoc networks intended for mobile multimedia, the emphasis is put on packet delay minimization and throughput maximization. As mentioned in Chapter 2, in this book we are not considering power consumption and energy efficiency, although this topic by itself has been the center of much attention

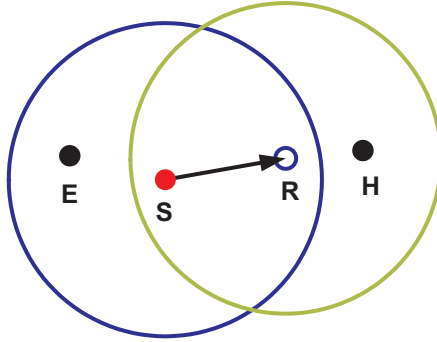


Fig. 7.1. Schematic view of Sending, Receiving, Hidden and Exposed nodes (terminals) in packet radio communication networks.

([82], [83], [84], [85]). In our study, effects of the MAC protocols on the interference, delay and throughput are relevant. These parameters are affected directly by the way that the MAC protocol deals with the *hidden terminal* and the *exposed terminal* problems.

In the Section 7.2 we describe the hidden and the exposed terminal problems and analyze the way that they affect the performance of packet radio networks in general. In Section 7.3 we will see how MAC protocols for ad-hoc networks can be categorized based on the way that they handle the hidden and the exposed terminal problems. We will use this classification in our study of the interference and the capacity of ah-hoc networks in Chapters 8 and 10.

7.2 Hidden terminal and exposed terminal problems

The hidden terminal and the exposed terminal problems are well-known problems in packet radio transmission and are commonly described in telecommunications text books and various articles ([86], [87], [88] and [89]). For the understanding of our classification of the MAC protocols we need to explain the hidden and the exposed terminal problem briefly.

The hidden terminal problem was first mentioned by Kleinrock and Tobagi in [90]. In radio communications, the radio signal strength decreases with distance, limiting the range of radio transmission. In Figure 7.1, there are four nodes, S (sender), R (receiver), H (hidden terminal), and E (exposed terminal). For simplicity in visualization of the problem, these four nodes are assumed to have the same radio transmitting range and circular coverage areas. The left and the right circles represent, respectively, the coverage area of nodes S and R . Terminals E and R are within the coverage area of node S and terminals H and S are within the coverage area of node R . This means

that S can transmit and receive signals from E and R , and similarly, R can transmit and receive signals from S and H .

To avoid collision of packets over the wireless channel, there is a basic rule in MAC protocols: a node does not attempt a transmission when it senses the medium to be busy. This principle is called *carrier sensing* and is achieved through listening to the radio channel. Suppose that S is sending a packet to R . The medium (i.e. radio channel) between S and R is determined to be busy by all nodes within the coverage area of S , therefore no other node within this region would ideally cause a collision with the packet being transmitted from S to R . However, if at roughly the same time or in an overlapping time interval, H would have a packet to send to either R or to another node in its own range, it will sense the medium as idle, because S and H cannot hear each other (H is hidden to S). If H would proceed with sending its packet, at node R the two transmitted packets will collide. As a result, one or both of the packets may be lost. As we see, the hidden terminal problem causes collision of packets and packet losses. This directly affects the throughput of the system, rendering the system less effective.

The second major issue is the exposed terminal problem. The problem is quite the opposite of the hidden terminal problem. In the exposed terminal case, when S is transmitting to R , E is also aware of the transmission. If E has a packet to send to another node outside the radio range R , it will unnecessarily postpone its transmission. It means that there is a lost transmission opportunity due to the exposure of E (hence, the name exposed terminal) to S , while there is no need for waiting. The consequence of the exposed terminal problem is that the radio channel is utilized less effectively, which in turn also reduces the throughput of the system. It is also affecting the average packet delay, which will be increased because of the unnecessary waiting time.

It is obvious that hidden and exposed terminal problems that occur in MAC protocols based on carrier sensing alone are less desirable if radio channel needs to be used more efficiently. There have been various MAC protocol suggestions to solve these problems. These solutions come at the expense of additional complexity in protocol design and signaling overhead. Although these solutions offer more efficient use of the shared medium, any MAC protocol still has to restrict the number of simultaneous transmissions per unit of area and consequently affect the aggregate interference power and the network capacity. It is beyond the scope of this book to describe all concepts used in MAC protocol design to improve the radio channel utilization. Preferably, we classify MAC protocols based on their ability to solve the hidden terminal and/or the exposed terminal problems. Our method of classification enables us to predict inference in ad-hoc networks for all MAC protocols, without getting into details of each protocol individually. For any MAC protocol it is sufficient to know to which class of protocols it belongs.

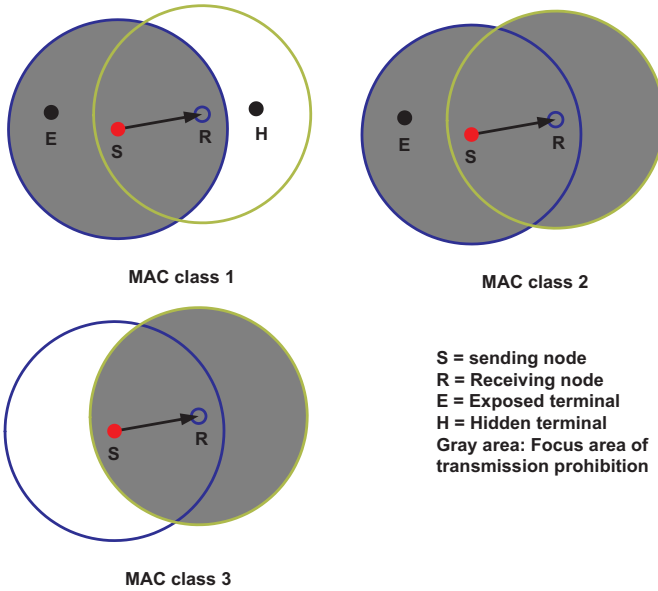


Fig. 7.2. Schematic view showing the working of the three MAC protocol classes. For simplicity, we have assumed a circular coverage area for each node ($\xi = 0$). The gray areas show the regions where each MAC protocol class attempts to restrict simultaneous transmissions.

7.3 Classification of MAC protocols

In Figure 7.2 we have depicted how MAC protocols can be classified into three distinct classes based on the method that they handle the hidden and the exposed terminal problems:

Class 1: MAC protocol prohibits simultaneous transmissions within the sender's radio range. This class leaves the hidden node as well as the exposed node problem unsolved. CSMA/CA without reservation [6] is a typical example of MAC protocols that fall into this category.

Class 2: MAC protocol prohibits simultaneous transmissions within the sender's as well as receiver's radio range. This class solves the hidden node problem but leaves the exposed node problem unsolved. CSMA/CA with reservation [6] is an example of this category. Other examples are MARCH [91], S-MAC [92], EMAC [93] and CATS [94].

Class 3: MAC protocol prohibits simultaneous transmissions within the receiver's radio range and simultaneous transmissions towards nodes within the sender's radio range. This class solves both the hidden node as well as

Table 7.1. Prohibited and allowed transmission/reception possibilities for different classes of the MAC protocols.

	nodes inside S but outside R coverage (denoted as E)		nodes inside R but outside S coverage (denoted as H)		nodes in overlapping S and R coverage	
	may send	may receive	may send	may receive	may send	may receive
MAC class 1	no (1)	yes (2)	yes (3)	yes (4)	no	yes (2)
MAC class 2	no (1)	no (5)	no	no	no	no
MAC class 3	yes (6)	no	no	yes (7)	no	no

- 1: This could have been allowed as long as destination node is outside the coverage area of **R**.
- 2: From nodes outside the coverage area of node **S**.
- 3: To any node.
- 4: From nodes outside the coverage area of node **S**.
- 5: If **E** was allowed to receive, the packet intended for it would have collided with data coming from **S**.
- 6: To nodes outside the coverage area of node **R**.
- 7: From nodes outside the coverage area of **R**.

the exposed node problems, but requires e.g. the deployment of an additional signaling channel. Two MAC protocols that fall into this category are multichannel RBCS [95] and DBTMA [96].

This method of classification is based on the way that a MAC protocol allows or prohibits nodes in the coverage area of nodes *S* and *R* to send or receive data while a packet is being transmitted from node *S* to node *R*. Figure 7.2 gives a schematic view but does not show the details regarding nodes being able either to send data to or receive data from other nodes. A more detailed description of the operation of the three MAC protocol classes is given in Table 7.1.

7.4 Chapter summary

In this chapter we have highlighted the importance of the MAC protocols in our study of fundamental properties of wireless ad-hoc networks. Specifically interference and capacity of wireless ad-hoc networks are directly affected by the working of the MAC protocols. We have studied many MAC protocols and have come to the conclusion that for the purpose of our study MAC protocols can best be classified in three different groups [72]. This classification is based on the way that MAC protocols solve the hidden and the exposed terminal problems. Our method of classification enables us to take the impact of MAC protocols into account in our studies (see Chapters 8 and 10) without getting into details of each protocol individually. For any MAC protocol it is sufficient to know to which class of protocols it belongs.

We have not described working of the MAC protocols in general, because we have assumed familiarity of the reader with this topic. Neither have we provided detailed description of the working of any of the MAC protocols mentioned in this chapter. It has not been our intention to provide a survey of the MAC protocols here.

Interference in Ad-hoc Networks

For the performance evaluation and determination of the capacity in any wireless network, it is important to have good calculation models to estimate interference power statistics. To our best knowledge, till now there has been no accurate calculation model to estimate the expected interference power and its distribution function in ad-hoc and sensor networks with realistic assumptions regarding radio propagation. We believe that we have provided such a model in this chapter.

It needs to be mentioned that already since a few decades we have good mathematical works, like [97], [98] and [99] that have investigated interference power in distributed packet radio networks with multi-hop character. For ad-hoc networks, the "order of magnitude" of the interference and the network capacity have also received attention, for example in [22] and [25]. However, these works are based on the pathloss propagation law that does not take the statistical variation of radio signal powers into account (see Section 3.4.1).

For fixed topology networks like cellular networks there exist interference calculation methods that indeed take the statistics of radio propagation into account (see e.g. [100]). However, these models assume that the interfering sources are all at fixed positions with known distances to the point where the aggregate interference power statistics is supposed to be calculated. It is obvious that combining radio signal power variations with random movement of nodes make mathematical modeling of interference a challenging task. In this chapter we use the method for the estimation of the interference statistics in fixed topology networks and add required features to enable us to calculate, with good accuracy, the interference power statistics in wireless ad-hoc networks with random position of interference sources. Our interference calculation model takes into account radio propagation conditions, the density of nodes, the size of the network, MAC protocol characteristics and the traffic load per node. The accuracy of our approach has been verified by simulations.

Section 8.1 of this chapter illustrates how the MAC protocol restricts the interfering node density, and consequently the interference power sum. In Section 8.2 we explain our calculation method. There we describe also two

important aspects, specific to ad-hoc and sensor networks, that should be taken into account for the correct estimation of the interference power sum.

8.1 Effect of MAC protocols on interfering node density

MAC protocols restrict the number of simultaneous signal transmissions per unit of area and consequently curb the aggregate interference power in ad-hoc networks. The density of interfering nodes depends (among other factors) on the MAC protocol classes described in Chapter 7. Figure 8.1 shows an example. In this example the lognormal radio propagation parameter $\xi = 0$, which results in a circular coverage area per node. On this figure we see that the interfering node density for each of the MAC classes is a different value.

The procedure for finding the interfering node density is as follows. A receiving node is placed in the center of the service area of arbitrary size and shape. Other nodes with the given density ρ are uniformly distributed around the center node. One of the nodes inside the coverage area of the center node is chosen at random to function as a sending node. These two nodes form a sending-receiving node pair. The coverage area for each node includes all nodes that according to (3.13) can be connected to it. Using the restrictions dictated by each class of the MAC protocols, new sending-receiving node pairs are formed one by one till no other combination is possible. Here we assume that the nodes always have data to send (activity ratio 100%). Selection of a new sending-receiving node pair occurs at random. This means that each time from the nodes that are not prohibited from transmission a node at random is chosen to be a sending node. From the neighbors of this new sending node, one node that is not prohibited from reception is chosen at random to be the receiving node. At the end of this procedure some nodes will be left that can neither be a sender nor a receiver. All sending nodes, except for the first sending node that is transmitting a wanted signal to the center node, are experienced as interference sources at the center node. The number of interfering sources found for each MAC class determines the interfering node density.

For the calculation of the interference power in ad-hoc and sensor networks, the density and the distribution of the interfering nodes must be known. When the density of nodes increases, more nodes will fall within the prohibited transmission areas. As a result, the density of interfering nodes is not expected to increase linearly with the increase in the density of nodes. We argue here that the interfering nodes density, ν , depends not only on the density of nodes forming the network, ρ , but also on the MAC protocol class and the radio propagation factor ξ . Factor ξ determines the link probability between nodes and consequently the shape and the extent of the coverage area around each node.

For a wide range of ξ and ρ values we have performed simulations to find the interfering nodes density. In each simulation we have placed one receiving

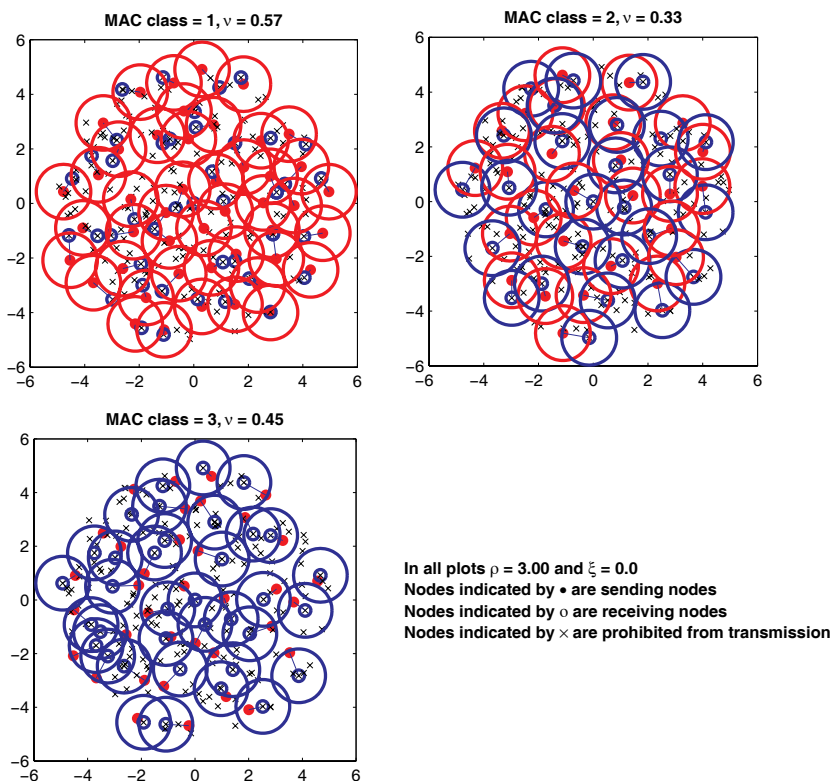


Fig. 8.1. The working of MAC classes 1, 2 and 3 on randomly distributed nodes with the density of 3 nodes per normalized area of 1×1 in a circular service area of normalized radius 5 with $\xi = 0$.

node in the center of a sufficiently large circular area and have followed the procedure described above to find the interfering node density. The normalized radius of the circular service area has been set to 3 times the distance where the link probability (3.13) drops to 5%. Therefore, the normalized radius of the area depends on the factor ξ . As an example, the normalized radius of the service area is 9.6 in case of $\xi = 3$, in other words 9.6 times the distance R defined in Section 3.4.2.

Results regarding the obtained interfering node density for different MAC classes are shown in Figure 8.2. For each combination of ξ and ρ we have performed 100 simulations¹. The values shown in this figure are the mean

¹ We have observed little variations in the obtained values of interfering node densities between simulation runs. Therefore repeating simulations for each combination of ξ and ρ for only 100 times provides already an accurate estimate for the mean value.

values. For better inspection of results a part of the simulation data is redrawn in Figure 8.3. It can be seen from these figures that, as expected, the interfering node density is highest in MAC class 1 and lowest in MAC class 2, with MAC class 3 in-between². We see also that when the node density ρ increases, the interfering node density ν increases as well but tends to level off for large values of ρ . In fact, in our simulations, the interfering node density always remains under 0.8. Further, because the mean node degree (neighbors per node) depends on ξ , the interfering node density depends on ξ as well. By increasing ξ the mean node degree increases (see Chapter 4), thus for each sending-receiving pair formed, the number of nodes falling within the prohibited transmission areas increases as well. Therefore, as observed in Figure 8.3, the number of potential interfering nodes tends to decrease for the highest values of ξ in comparison to the case $\xi = 0$.

To be precise, our simulations have shown situations where by changing ξ from 0 to 3, the interfering node density increases slightly at first before starting to decrease. This only happens for MAC classes 1 and 3 at high values of ρ (notice the slight bending of the interfering node density for MAC class 1 and 3 at $\rho = 10$ in Figure 8.2). The explanation for this effect is that in MAC classes 1 and 3, in contrast to MAC class 2, a node inside the prohibited areas still may receive data from nodes outside these areas. When ξ increases the number of nodes that fall inside the prohibited areas increases as well. On the one hand, this increases the number of potential receivers and makes new sending-receiving node pair combinations possible. On the other hand, for each sending-receiving pair formed, the number of nodes not allowed to send increases. Simulations seem to indicate that the combined outcome of these two effects is the decrease of interfering node density for the highest values of ξ .

Using simulation results, we have found 2-dimensional fitting formulas³ for the interfering node density:

$$\nu \simeq \begin{cases} 0.3466 + 0.1658 \log(\rho) - 0.0283\xi & \text{MAC class 1} \\ 0.2403 + 0.0910 \log(\rho) - 0.0453\xi & \text{MAC class 2} \\ 0.2634 + 0.1741 \log(\rho) - 0.0130\xi & \text{MAC class 3} \end{cases} \quad (8.1)$$

The root-mean-square error in the fit is 0.04, 0.02 and 0.03 for, respectively, MAC classes 1, 2 and 3. Based on (8.1) we may conclude that ν is by approximation a linear function of $\log(\rho)$, at least for the range of ρ values

² We base this expectation on the fact that the area of prohibited transmission or reception in MAC class 2 includes the entire coverage area of the sending and the receiving nodes. Therefore, MAC class 2 is the most stringent protocol class and allows the least number of simultaneous transmissions. MAC class 1 is the least stringent class and MAC class 3 is between these two classes. This point can be verified by counting the number of "yes" and "no"-s in table 7.1.

³ We have used the `rstool` of Matlab® for the 2-dimensional fitting [101].

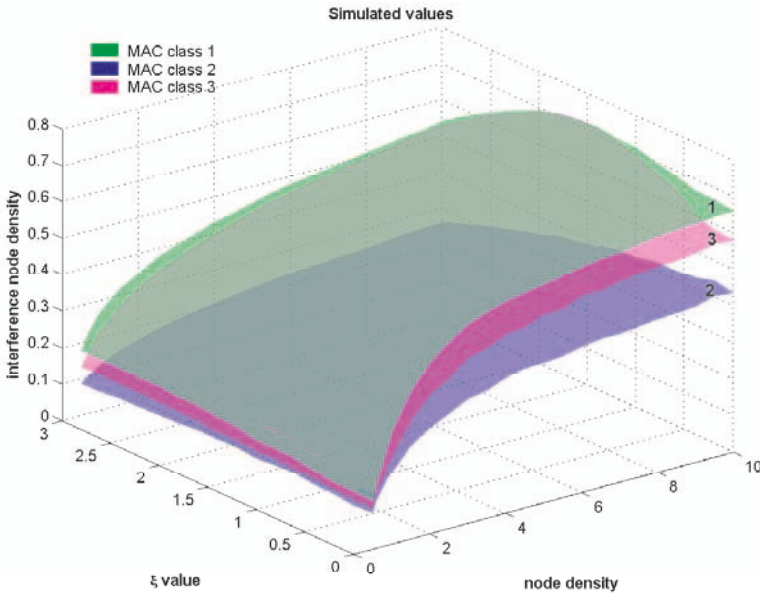


Fig. 8.2. Density of interfering nodes found by simulations for MAC classes 1, 2 and 3 ($0 \leq \xi \leq 3$ and $0.5 \leq \rho \leq 10$).

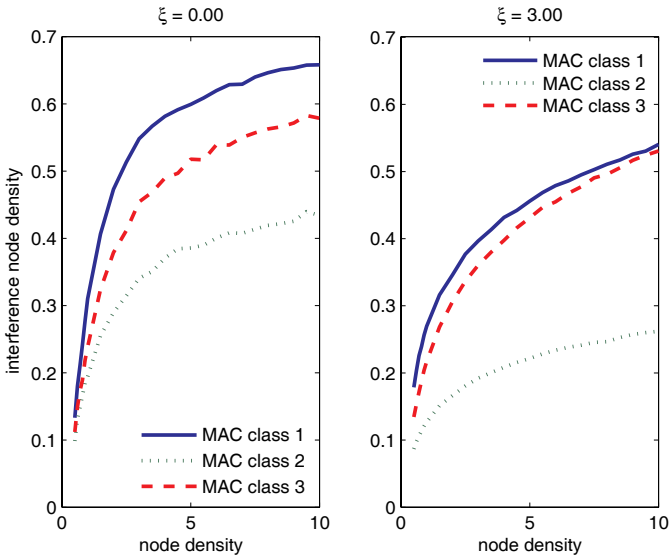


Fig. 8.3. Density of interfering nodes found by simulations for MAC classes 1, 2 and 3. Left subplot: $0.5 \leq \rho \leq 10$ and $\xi = 0$, right subplot: $0.5 \leq \rho \leq 10$ and $\xi = 3$.

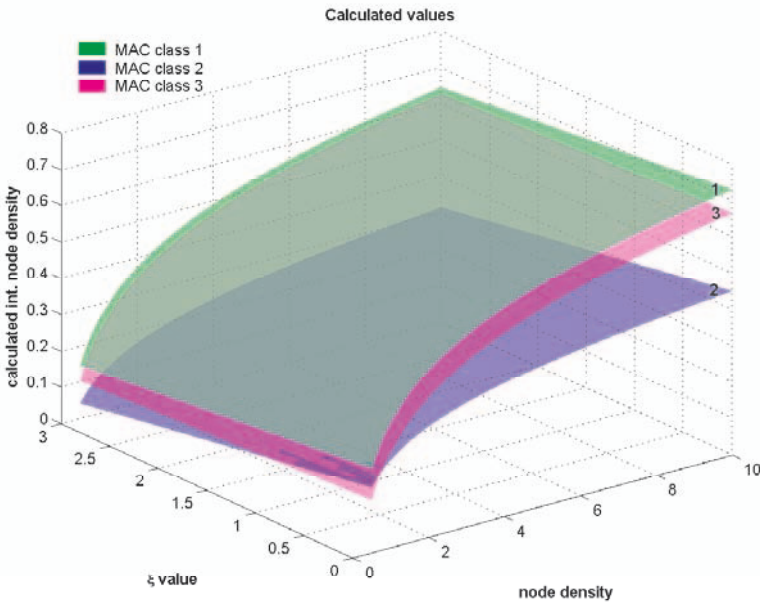


Fig. 8.4. Estimated interfering nodes densities using (8.1) for MAC classes 1, 2 and 3.

included in our simulations ($0.5 \leq \rho \leq 10$). Figure 8.4 shows the interfering nodes densities calculated using (8.1).

As mentioned before our simulations are based on the assumption that all nodes in the ad-hoc or the sensor network always have data to send to any of their neighbors. In reality this is not the case. At any moment in time only a portion of nodes forming the network are active. If the activity ratio is indicated by $\tau \in [0, 1]$, we can use (8.1) to estimate the interfering node density by replacing ρ with $\tau\rho$.

8.2 Interference power estimation

As described in Section 3.4.3 we are assuming lognormal distributed powers, which implies that the interference consists of lognormal components. The sum of lognormal components is a well-studied topic in cellular networks with fixed topology (see e.g. [102]). Here we expand the summation method of lognormal components, to our best knowledge for the first time, to ad-hoc and sensor networks. We will explain that this expansion for the estimation of the sum of interference power in ad-hoc networks is not trivial. Our approach is described stepwise in Sections 8.2.1, 8.2.2 and 8.2.3. In Section 8.2.4 we evaluate our approach with simulations.

8.2.1 Sum of lognormal variables

A lognormal random variable is characterized by the property that its logarithm has a Gaussian distribution. Let L_i be a lognormal random variable and let

$$X_i = 10 \log_{10} L_i.$$

The probability density function (PDF) of X_i is:

$$f_{X_i}(x) = \frac{1}{\sqrt{2\pi}\sigma_{x_i}} \exp\left(-\frac{(x - \mu_{x_i})^2}{2\sigma_{x_i}^2}\right),$$

where μ_{x_i} and σ_{x_i} are the mean and the standard deviation of X_i . For calculation it is more convenient to use the natural logarithm of L_i . We define $Y_i = \log(L_i)$ with the PDF:

$$f_{Y_i}(x) = \frac{1}{\sqrt{2\pi}\sigma_{y_i}} \exp\left(-\frac{(x - \mu_{y_i})^2}{2\sigma_{y_i}^2}\right)$$

and mean μ_{y_i} and standard deviation σ_{y_i} . The random variables X_i and Y_i are related as:

$$\begin{aligned} Y_i &= \beta X_i, \\ \mu_{y_i} &= \beta \mu_{x_i}, & \beta &\triangleq \log(10)/10. \\ \sigma_{y_i} &= \beta \sigma_{x_i}, \end{aligned}$$

We are interested to find the PDF of the sum of t lognormal random variables: $L = L_1 + L_2 + \dots + L_t$. Unfortunately, there is no exact mathematical solution found for this distribution. However, there exist two widely accepted good approximation methods. The first method is the Fenton-Wilkinson (FW) approximation [103], [104]. The second method is the Schwartz-Yeh (SY) approximation [105]. Both methods assume that the power sum of lognormal components has a lognormal distribution with a mean and a variance that can be calculated directly from the mean and the variance of each individual component (and if applicable, the correlation factor between the components). These methods approximate the sum of t lognormal random variables as:

$$L = \sum_{i=1}^t L_i = \sum_{i=1}^t e^{Y_i} \simeq e^Z, \quad (8.2)$$

where Z is a Gaussian random variable with mean and standard deviation of respectively μ_z and σ_z .

Working with lognormal signals often requires conversion between logarithm base 10, natural logarithm and non logarithmic values. The mean and the variance of variables change due to these conversions. The conversion rules, although simple, must be followed meticulously. We have summarized these rules here. Let μ_x and σ_x be the mean and the standard deviation of a

random variable X ; and μ_y and σ_y be the mean and the standard deviation of random variable Y :

$$\begin{aligned} \text{if } Y = \log(X) \text{ then} & \begin{cases} \mu_y = 2 \log(\mu_x) - 0.5 \log(\sigma_x^2 + \mu_x^2) \\ \sigma_y^2 = \log(\sigma_x^2 + \mu_x^2) - 2 \log(\mu_x) \end{cases} \\ \text{if } Y = \exp(X) \text{ then} & \begin{cases} \mu_y = \exp(\mu_x + \sigma_x^2/2) \\ \sigma_y^2 = \exp(2\mu_x + 2\sigma_x^2) - \exp(2\mu_x + \sigma_x^2) \end{cases} \\ \text{if } Y = 10 \log_{10}(X) \text{ then} & \begin{cases} \mu_y = \beta^{-1} [2 \log(\mu_x) - 0.5 \log(\sigma_x^2 + \mu_x^2)] \\ \sigma_y^2 = \beta^{-2} [\log(\sigma_x^2 + \mu_x^2) - 2 \log(\mu_x)] \end{cases} \\ \text{if } Y = 10^{X/10} \text{ then} & \begin{cases} \mu_y = \exp(\beta\mu_x + \beta^2\sigma_x^2/2) \\ \sigma_y^2 = \exp(2\beta\mu_x + 2\beta^2\sigma_x^2) - \exp(2\beta\mu_x + \beta^2\sigma_x^2) \end{cases} \end{aligned} \quad (8.3)$$

where $\beta \triangleq 0.1 \log(10)$.

In the following we describe the FW and SY approximation methods. It should be mentioned that the original approximation methods published in [103] and [105] have considered the sum of t independent lognormal random variables. The approximation methods have been expanded later by others to include the case of correlated variables as well [106]. In this book we will assume that lognormal random variables are independent.

Fenton-Wilkinson (FW) approximation

In the Fenton-Wilkinson approach μ_z and σ_z are found by matching the first two moments of L with the first two moments of e^Z . The k -th moment of e^Z is:

$$E[e^{kZ}] = \exp\left(k\mu_z + k^2 \frac{\sigma_z^2}{2}\right).$$

Matching the first moment provides:

$$\begin{aligned} E[L] &= E[e^Z] = E[e^{Y_1} + e^{Y_2} + \dots + e^{Y_t}] \\ &= \exp(\mu_z + \sigma_z^2/2) = \sum_{i=1}^t \exp(\mu_{y_i} + \sigma_{y_i}^2/2) \triangleq u_1. \end{aligned}$$

Matching the second moment provides:

$$\begin{aligned} E[L^2] &= E[e^{2Z}] = E\left[(e^{Y_1} + e^{Y_2} + \dots + e^{Y_t})^2\right] \\ &= \exp(2\mu_z + 2\sigma_z^2) = \sum_{i=1}^t E\left[(e^{Y_i})^2\right] + 2 \sum_{i=1}^{t-1} \sum_{j=i+1}^t E[e^{Y_i+Y_j}] \triangleq u_2. \end{aligned}$$

In the FW method of calculation, knowing the mean and the standard deviation of L_i components, the values for u_1 and u_2 are calculated first. Solving the above two equations for μ_z and σ_z then provides:

$$\mu_z = 2 \log(u_1) - \frac{1}{2} \log(u_2), \quad \sigma_z^2 = \log(u_2) - 2 \log(u_1). \quad (8.4)$$

Using (8.3) and (8.4) we find the mean and the standard deviation of L , the sum of the lognormal components. The distribution form is of course, as assumed lognormal.

It is known from the literature that the FW approximation is applicable with good accuracy when the standard deviation of lognormal components are less than 4 dB ([102], [103], [104]).

Schwartz-Yeh (SY) approximation

Schwartz and Yeh [105] also approximate the sum of lognormal variables by a lognormal distribution. However in their method the first and the second moment of the random variable Z are not obtained based on this assumption. They rather find exact expressions for the first two moments of the sum of two lognormal random variables. By assuming that this sum is again a lognormal random variable a recursive technique is used to find the first two moments of the sum of $t > 2$ lognormal random variables. The calculation method in the original paper of Schwartz and Yeh is complex and, as we have seen, prone to round-off errors when programmed on a computer. For our calculations we have used a modified method presented by Ho [107]. The expressions for finding the exact mean and variance of the sum of two lognormal random variables $Z_2 = \log(e^{Y_1} + e^{Y_2})$ are summarized here ([102], [107]):

$$\mu_{z_2} = \mu_{y_1} + G_1, \quad \sigma_{z_2}^2 = \sigma_{y_1}^2 - G_1^2 - 2\sigma_{y_1}^2 (I_0 + I_2) + G_2, \quad (8.5)$$

where,

$$\begin{aligned} G_1 &= A_0 + I_1, \\ G_2 &= I_3 + 2I_4 + \sigma_w^2 I_0 + \mu_w A_0, \\ \mu_w &= \mu_{y_2} - \mu_{y_1}, \\ \sigma_w^2 &= \sigma_{y_2}^2 + \sigma_{y_1}^2 \\ A_0 &= \frac{\sigma_w}{\sqrt{2\pi}} \exp\left(-\frac{\mu_w^2}{2\sigma_w^2}\right) + \mu_w I_0, \\ I_i &= \int_0^1 h_i(v) v^{-1} dv, \\ h_i(v) &= \begin{cases} \frac{1}{\sqrt{2\pi}} \exp\left(-\left(\log v + \frac{\mu_w}{\sigma_w}\right)^2 / 2\right), & i = 0 \\ [f_w(\log v) + f_w(-\log v)] \log(1+v), & i = 1 \\ [f_w(\log v) - f_w(-\log v)] (1+v^{-1})^{-1}, & i = 2 \\ [f_w(\log v) + f_w(-\log v)] \log^2(1+v), & i = 3 \\ -f_w(-\log v) \log v \log(1+v), & i = 4 \end{cases} \\ f_w(w) &= \frac{1}{\sqrt{2\pi\sigma_w^2}} \exp\left[-\frac{(w - \mu_w)^2}{2\sigma_w^2}\right]. \end{aligned}$$

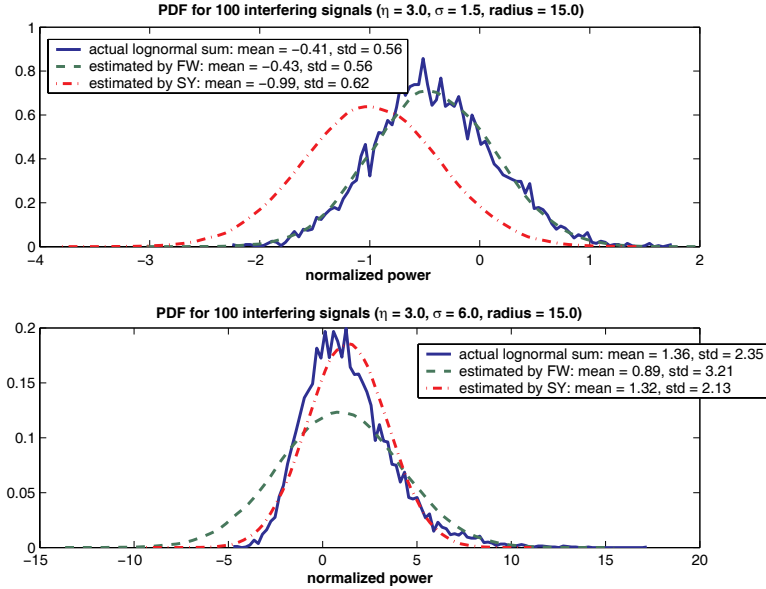


Fig. 8.5. Test of the FW and SY interference power estimation for lognormal distributed interference signals coming from known distances spread over a circular area.

It is known from the literature that the SY approximation is applicable with good accuracy when the standard deviation of lognormal components are between 4 and 12 dB ([102], [104]).

Example using FW and SY methods

Both the FW and the SY estimation methods are very fast when implemented on a computer, as they consist of a set of closed mathematical expressions. Figure 8.5 shows an example of interference power estimation with the FW and SY methods. Here we have used the FW and SY methods to approximate the interference power at the center of a circular area with normalized radius 15 and 100 nodes at random positions but with well-known distances to the center. The signal coming from each node is assumed to have a lognormal distribution according to (3.12). In other words, each interfering signal is of the form $X_i = 10 \log_{10} L_i$ with $\mu_{x_i} = 10 \log_{10}(\hat{r}_i^{-\eta})$ and $\sigma_{x_i} = \sigma$, where \hat{r}_i is the normalized distance of the i -th node to the center. The pathloss exponent η and the standard deviation σ of lognormal signals are indicated on each plot. Actual PDFs are found by taking 10000 times independent interference samples from each interference source. As we can see from Figure 8.5, the FW and SY are very accurate estimation methods for, respectively, low and high σ values.

Adapting FW and SY methods to ad-hoc networks

The FW and SY methods can be used to derive the PDF of the interference power when the number of interfering nodes, the mean power and the standard deviation of each individual interfering component is known. In ad-hoc networks we can use (8.1) to estimate the number of interfering components. The standard deviation σ of lognormal interference components is a characteristic feature of the propagation environment and is given. However, the challenge in using the FW and SY approximation methods for ad-hoc networks lies in estimating the mean power of each individual component. This task is not trivial due to the following two reasons:

1. The mean interference power experienced at node i from node j is directly linked to the distance between i and j . Because of the random distribution and the movement of nodes this distance is subject to changes. In Section 8.2.2 we describe a method to find the expected position of interfering nodes.
2. Because of lognormal power variations, for any fixed distance r_{ij} between nodes i and j there is a probability that these two nodes are "visible" to each other (see link probability in Figure 3.10). If node j is visible to node i , depending on the MAC protocol, it may be prohibited⁴ from interfering with node i . This phenomenon, which does not exist in cellular networks, implies that knowing the distance to an interfering node (that provides us with the mean expected power coming from that node) and the variance of the interfering signal components is not enough to make an accurate estimation of the aggregate interference power. In Section 8.2.3 we provide a solution for this issue.

8.2.2 Position of interfering nodes

Let us assume that interfering nodes are uniformly distributed with density ν around a center node in a circular area. We order these nodes according to their distance, r_m , to the center node. In other words, r_1 is the distance of the nearest interfering node to the center, r_2 denotes the distance of the second nearest interfering node to the center, and etc. The probability density function of the radius r_m of the m -th nearest interfering node to the center is [108]:

$$f_{r_m}(r) = \frac{2\pi r \nu}{(m-1)!} (\pi r^2 \nu)^{m-1} e^{-\pi r^2 \nu} \quad , m = 1, 2, 3, \dots \quad (8.6)$$

The expected distance of the m -th interfering node to the center node is then:

⁴ It is realistic to assume that MAC protocol is fast enough to catch up with medium scale power variations of the lognormal radio model.

$$E[r_m] = \int_0^\infty r f_{r_m}(r) dr = \frac{\Gamma(m + \frac{1}{2})}{\sqrt{\pi\nu}(m-1)!} = \frac{(2m)!}{2^{2m}\sqrt{\nu}m!(m-1)!} \simeq \sqrt{\frac{m}{\pi\nu}}. \quad (8.7)$$

In (8.7) we have used Gamma function duplication formula [109, 6.1.18]:

$$\Gamma(2m) = (2\pi)^{-\frac{1}{2}} 2^{2m-\frac{1}{2}} \Gamma(m)\Gamma(m + \frac{1}{2}),$$

and Stirling's formula [109, 6.1.38]:

$$m! = \sqrt{2\pi} m^{m+\frac{1}{2}} \exp(-m + \frac{\theta}{12m}). \quad 0 < \theta < 1$$

The approximation in (8.7) is valid for large m .

In general, the moments of r_m are:

$$E[r_m^k] = \int_0^\infty r^k f_{r_m}(r) dr = \frac{\Gamma(m + \frac{k}{2})}{(m-1)! (\pi\nu)^{k/2}},$$

where $f_{r_m}(r)$ is given by (8.6). The variance of r_m is then:

$$\begin{aligned} Var[r_m] &= E[r_m^2] - (E[r_m])^2 \\ &= \frac{1}{\pi\nu} \left(m - \left(\frac{\Gamma(m + \frac{1}{2})}{\Gamma(m)} \right)^2 \right). \end{aligned}$$

Using the approximation [109, 6.1.49]:

$$\frac{\Gamma(m + \frac{1}{2})}{\Gamma(m + 1)} \simeq \frac{1}{\sqrt{m}} \left[1 - \frac{1}{8m} + \frac{1}{128m^2} - \dots \right] \quad m \rightarrow \infty$$

we obtain:

$$\begin{aligned} Var[r_m] &\simeq \frac{1}{\pi\nu} \left(m - m \left[1 - \frac{1}{8m} + \frac{1}{128m^2} - \dots \right]^2 \right) \\ &\simeq \frac{1}{4\pi\nu} \left(1 - \frac{1}{8m} + O\left(\frac{1}{m^2}\right) \right) \quad m \rightarrow \infty \end{aligned}$$

From the above we may conclude that the variance in the position of interfering nodes is only negligible when $\nu \gg 1$. However, the simulation results in Figure 8.2 indicate that $\nu < 0.8$ for all MAC classes. This means that the variance in the position of interfering nodes in ad-hoc networks is not negligible.

In our calculations of the interference power sums we have used (8.7) to estimate the expected distance of each interfering node to the center node.

In other words, we have assumed that interfering nodes have a uniform distribution around the center node. The validity of this assumption is verified by simulations. Figure 8.6 shows an example for a network with node density 3.0, pathloss exponent $\eta = 3.0$, $\sigma = 2.4$, and $r = 4$ (normalized radius of the service area). With a MAC class 3 protocol, the interfering node density is 0.44. In Figure 8.6, the dotted vertical lines indicate the distance of the first to the 6th interfering node calculated by (8.7). The marked curves show the actual distribution of the position of interfering nodes that are found by simulations. As we can see there is a good match between the expected position (mean values) of interfering nodes found through simulations and the second to the 6th calculated positions. However, (8.7) predicts an interfering node at distance 0.72 to the center node (the left most dotted vertical line in Figure 8.6) that never seems to appear in simulations. The explanation is that a node at distance 0.72 would be connected to the center node with high probability⁵. Due to the MAC class 3 restrictions, this node is then not allowed to transmit a signal while the center node is receiving data from another node. Therefore, assuming any interference power originated from this distance would provide erroneous results. This matter which is related to point 2 mentioned on page 87 is dealt with by weighting the interference powers. The weighting method is described in the next section.

8.2.3 Weighting of interference mean powers

As mentioned above, in ad-hoc and sensor networks for any interfering node m at distance r_m there is a probability that it is excluded from the sum of interference powers. This probability is proportional to the link probability $p(r_m)$, given by (3.13).

In order to take this effect into account in the estimation of interference power sum, we suggest to weight the mean power of the m -th interfering signal with a factor proportional to $1 - p(r_m)$. Heuristically we have found out that a weight factor $w = (1 - p(r_m))^\sigma$ provides good results. This weight factor takes into account not only the probability of the node being prohibited from transmission, but also the severity of radio signal power variations represented by σ . The weight factor w varies between 0 and 1. As r_m increases $p(r_m)$ decreases, causing the weight factor to tend towards 1. At short distances the opposite occurs.

Figure 8.7 shows an example with the weighted and non-weighted area mean powers. At short distances the weighting procedure reduces the strength of interfering signals (as in reality the MAC protocol would have done by not allowing strong interference from short distances) while at long distances there is no difference between the weighted and the non-weighted case.

⁵ The exact probability is calculated using (3.13): With $\xi = 2.4/3.0 = 0.8$ we obtain $p(\hat{r}) = 0.95$.

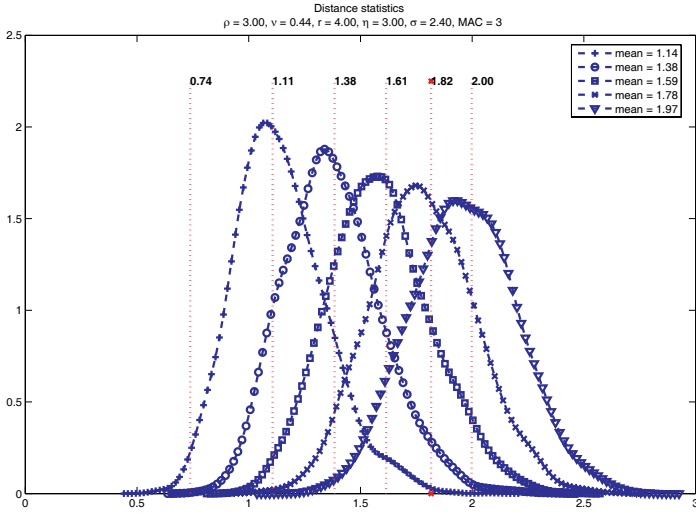


Fig. 8.6. Calculated distances of interfering nodes to the center node and the simulated probability density function of the distance of interfering nodes to the center node in an ad-hoc network with $r = 4$, $\rho = 3$, $\eta = 3$, $\sigma = 2.4$ and MAC class 3.

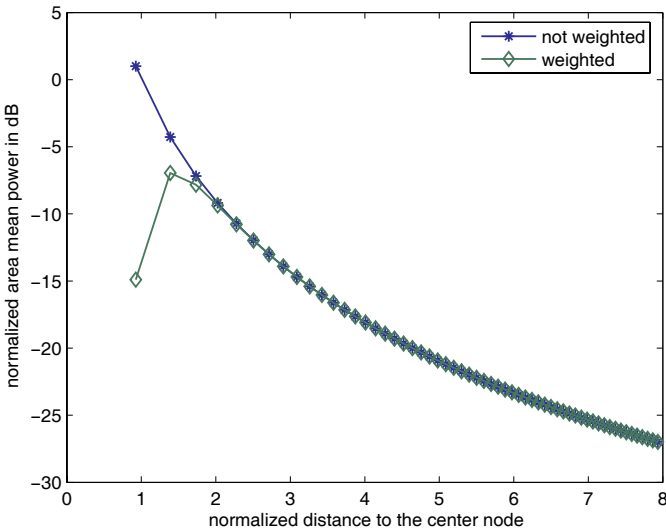


Fig. 8.7. Expected distance of interfering nodes to the center node and weighted as well as non-weighted area mean power expected from those distances in an ad-hoc network with MAC class 2, $r = 8$, $\rho = 3$, $\eta = 3.0$, $\sigma = 4.0$. The number of interfering nodes is 58 ($\nu = 0.28$).

8.2.4 Interference calculation results

Using our proposed method to find the distance of interfering nodes and the weighted mean power of individual interfering signals we now calculate the distribution function of interference power sum. The input parameters are the area size (circular area with normalized radius r), node density ρ , pathloss exponent η , standard deviation σ of the radio signal power variations, and the MAC protocol class. In this section we present our calculated values in a few representative examples and compare them with simulated results to verify the accuracy of our calculation method. The calculation procedure is as follows:

1. The interfering node density is estimated using (8.1).
2. The expected positions of interfering nodes are found using (8.7).
3. The mean value of the interference power coming from each interference source is weighted as described in Section 8.2.3.
4. The aggregate interference mean power and variance is estimated using the FW or SY method. The FW method is used when $\sigma \leq 4$ and the SY method is used for $4 < \sigma < 12$.
5. The distribution function of the interference power is derived from the mean and the variance values assuming a lognormal distribution for the power sum.

The simulation procedure is:

1. Nodes with density ρ are uniformly distributed over a circular area with radius r .
2. Sending and receiving node pairs are formed taking the MAC protocol restrictions into account. In our simulations we have assumed that nodes always have data to send to any of their neighbors⁶.
3. Each individual interference component is found using the lognormal propagation model (see (3.12)).
4. The aggregate interference power experienced at the center is obtained by adding all individual interference components.
5. To obtain the distribution function of the interference power, the above steps have been repeated 1000 times.

We need to point out here that the calculation procedure stated above is very fast. The most computational extensive part of the calculation procedure is the FW or SY method. However, on a personal computer it takes only a few seconds to go through the calculation procedure. The simulation procedure however, depending on the radius of the coverage area and node density, can last several hours even days.

⁶ This 100% activity assumption for nodes can be considered as a worst-case interference scenario. If the activity ratio of nodes is less than 1, our simulation as well as calculation method still can be used by multiplying the node density with the actual activity ratio.

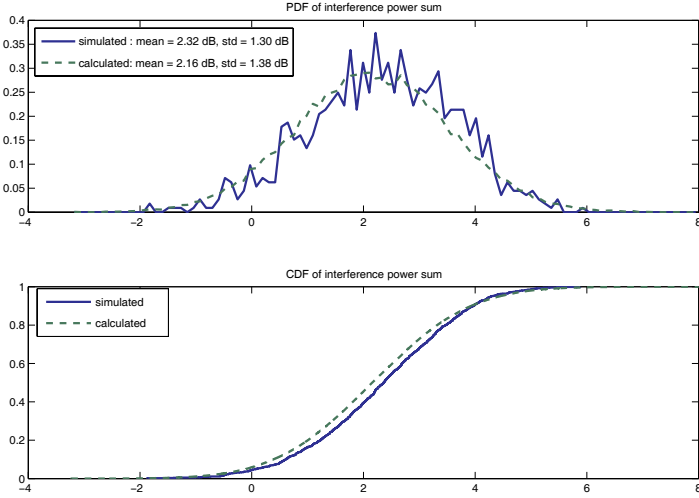


Fig. 8.8. Simulated and calculated PDF and CDF of normalized interference power in the center of a circular area with the same parameters as in Figure 8.7.

Table 8.1. Calculated and simulated interference power statistics for several values of area radius r , node density ρ , pathloss exponent η , standard deviation of shadowing σ and MAC classes 2 and 3.

Parameters	sim. mean (dB)	calc. mean (dB)	sim. std (dB)	calc. std (dB)
$r = 4.0, \rho = 8.0, \eta = 3.0, \sigma = 2.0, \text{MAC } 2$	2.78	2.76	1.10	0.76
$r = 6.0, \rho = 5.0, \eta = 2.4, \sigma = 1.5, \text{MAC } 3$	6.84	6.45	0.68	0.35
$r = 10.0, \rho = 1.0, \eta = 4.0, \sigma = 4.0, \text{MAC } 2$	-2.82	-2.31	2.57	2.13
$r = 8.0, \rho = 3.0, \eta = 4.0, \sigma = 9.0, \text{MAC } 3$	3.40	3.04	1.62	2.59
$r = 7.0, \rho = 3.0, \eta = 2.5, \sigma \approx 0, \text{MAC } 3$	5.71	5.57	0.63	0.00

Figure 8.8 shows one set of results. Other results are shown in Table 8.1. We have not presented any simulation results for MAC class 1, because due to the hidden node problem in this MAC class the interference power can explode. Note that the interference power values shown here are all **normalized** values according to the convention described in Section 3.4.3. Based on these results we argue that our calculation method is accurate in estimating the mean interference signal powers especially in situations where interference is not very weak. The standard deviation of interference power is estimated with less accuracy, as can be seen from Table 8.1. This is due to the spreading in the actual position of interfering nodes around their expected positions (see Figure 8.6) which is not included in our model. The variance of r_m for low values of ν is not negligible.

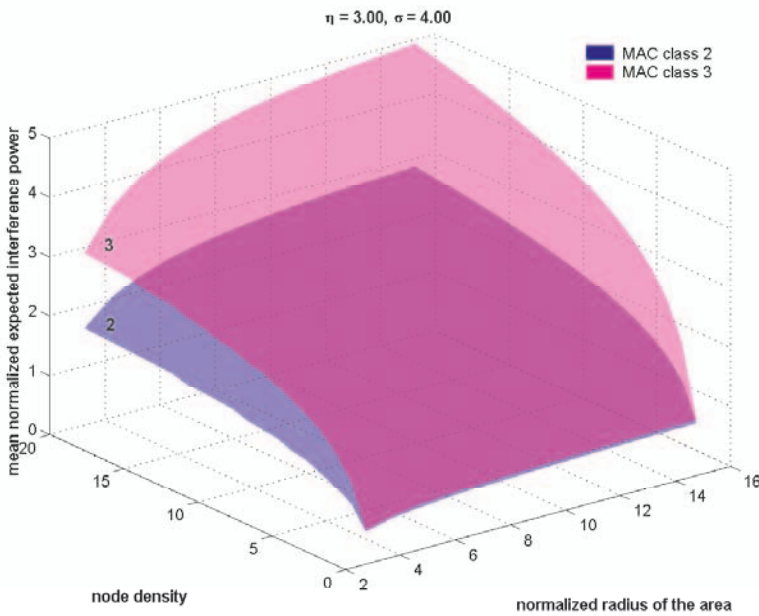


Fig. 8.9. Expected mean interference power as function of the network node density and area size for $\eta = 3.0$ and $\sigma = 4.0$.

Using our calculation method, we have plotted in Figures 8.9 and 8.10 two examples of the mean normalized interference power sum as function of the area size and the node density. As we see, interference tends to level off when the node density or the area size increases. In other words, in ad-hoc and sensor networks increasing the area size or the node density does not necessarily imply an unacceptable increase in interference power. We also notice by comparing Figures 8.9 and 8.10 that, as expected, the interference power is lower for higher values of the pathloss exponent η .

The interference calculation method presented here can be used to estimate the capacity of ad-hoc and sensor networks. We will consider capacity estimation in ad-hoc networks in Chapter 10.

8.3 Chapter summary

The focus of this chapter was on the estimation of interference power statistics in ad-hoc and sensor networks. First we have shown that the interfering node density depends on the MAC protocol characteristics. Each MAC protocol class restricts in its own way the number of interfering signal transmissions allowed per unit of area, regardless of the number of nodes falling within that area. Therefore, the interfering node density does not increase linearly

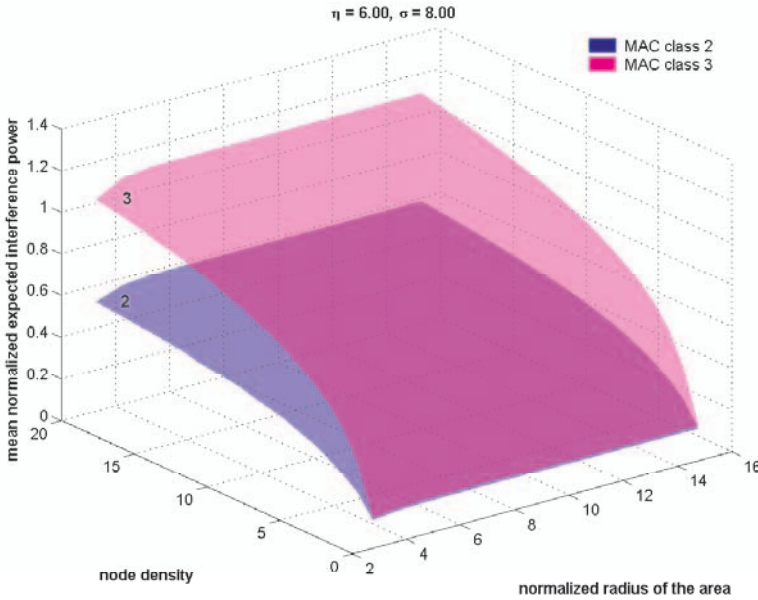


Fig. 8.10. Expected mean interference power as function of the network node density and area size for $\eta = 6.0$ and $\sigma = 8.0$.

with the density of nodes forming the network. We have found approximating formulas for calculating the expected interfering node density. These formulas show that interfering node density is, by approximation, proportional to the logarithm of the node density. We observed that interfering node density is less than 0.8 for all MAC classes.

Other result presented in this chapter is the calculation method using lognormal radio propagation model for estimation of the interference power sum statistics in ad-hoc and sensor networks. The input parameters for the calculation method are the area size, the density of the nodes, the radio propagation conditions (pathloss exponent and standard deviation), the activity ratio of nodes and the MAC protocol class. Through simulations we have verified the accuracy of our method. The value of our approach lies not only in its accuracy but also in its low computational complexity. Access to interference statistics enables us to provide good estimates for the capacity of ad-hoc networks under varying circumstances.

The calculation method presented here is a first attempt to expand interference power sum calculation from fixed topology networks to ad-hoc and sensor networks. We realize that there is room for fine-tuning and improvements in our approach. One improvement, for example, is to increase the accuracy in the estimation of the standard deviation of the interference power, as discussed in Section 8.2.4.

Simplified Interference Estimation: Honey-Grid Model

The calculation method described in Chapter 8 is an accurate estimation method for determination of interference statistics. However, this method does not provide us with a closed-form analytic formula for interference. In this chapter we find a mathematical formula for expected interference in ad-hoc networks. For this purpose we have simplified the reality of ad-hoc networks in three aspects:

1. We have used the pathloss radio propagation model,
2. We have chosen for a specific arrangement of nodes on a 2-dimensional hexagonal lattice resembling a honey-grid (which explains the name given to our model: the honey-grid model),
3. We have simplified the rules of the MAC protocol.

We describe our model along with these three simplifications in Section 9.1, and explain why these simplifications have been adopted. In Section 9.2 we use the honey-grid model and obtain an analytic formula for the expected interference in ad-hoc networks. This formula takes into account the network size, density of nodes, transmission probability per node and radio propagation pathloss exponent. We will also find a closed-form expression for an upper bound on the expected interference in ad-hoc and sensor networks. In Section 9.3 we compare the honey-grid model results with the interference calculation method presented in Chapter 8.

9.1 Model description

For simplicity of mathematical derivations, our interference calculations in this chapter will be based on the pathloss power law model for radio propagation (see 3.4.1). With the power law model for radio propagation, and the assumption that transmission power and receiver sensitivity for all nodes is the same, the coverage area of any node is a circle with radius R . A node can have direct communication with all nodes that fall inside its coverage area.

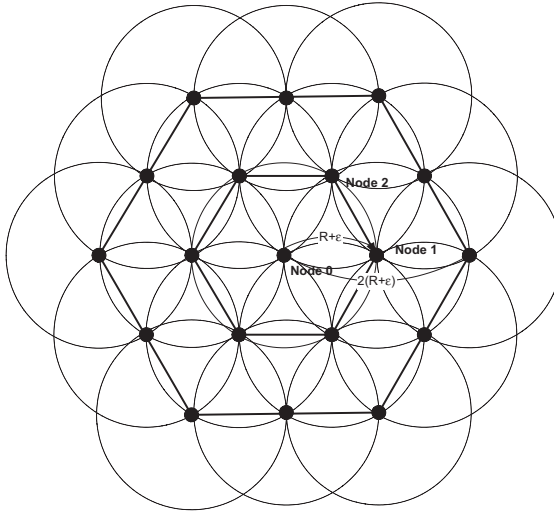


Fig. 9.1. Constellation of interfering nodes around node 0 when we arrange interfering nodes in positions to obtain the maximum number of interferers.

On the data link layer, the ad-hoc network uses a multiple access scheme for regulation of simultaneous transmissions (see Chapter 7). Our assumptions regarding the MAC protocol are as follows. We assume that when a node, say node 0, is receiving data, there will be no interference from other nodes inside the coverage area of node 0. In the worst case interference situation, the first set of interfering signals will come from other nodes closest possible to node 0. In other words, from nodes just outside the coverage area of node 0 (at distance $R + \epsilon$ to node 0, with ϵ a sufficiently small number). For example, in Figure 9.1 the first interfering signal could originate from node 1. When node 0 and node 1 are active simultaneously, the next interfering signal could only come from nodes outside the coverage areas of both these nodes. In the worst case situation, node 2 at the crossing point of the two circles with radius $R + \epsilon$ in Figure 9.1, could be the second interference source. Adding new interfering nodes in this way produces the constellation of nodes shown in Figure 9.1, with node 0 in the center of the constellation. As depicted in this figure, there are at most 6 interfering nodes at distance $R + \epsilon$ to node 0. On the next interfering ring at distance $2(R + \epsilon)$, there are at most 12 interfering nodes.

When we assume uniform distribution of nodes, inside the service area of an ad-hoc network any position (x- and y-coordinate) is equally probable to be occupied by a mobile node. However, in our approach we simplify this by introducing a regular lattice to which the position of mobile nodes is restricted. We will see later in this chapter that this restriction regarding the permissible positions for mobile nodes enables the estimation of the expected value of

interference without having accurate knowledge about the movement patterns and the exact location of all nodes at all times.

Introducing a regular lattice can be seen as enforcing a certain granularity on the 2-dimensional plane for the position of mobile nodes. On this lattice each node has a number of *adjacent* nodes, that we define as nodes in its direct vicinity and with the same distance to that node. When all positions on a regular lattice are occupied, all nodes that are not at the borders of the service area should have the same number of adjacent nodes; and adjacent nodes should be at the same distance from each other. Geometrically, on the 2-dimensional plane two lattice forms fulfill these requirements. These lattices are the rectangular lattice and the hexagonal lattice shown in Figure 9.2. In mobile ad-hoc networks communication between nodes takes place over radio channels and each node may have direct communication with all nodes inside its coverage area. It should be noticed that, depending on the transmission power and radio propagation conditions, the coverage area of a node may contain more nodes than its adjacent nodes.

From the two lattice forms shown in Figure 9.2 we have chosen to base our model on the hexagonal lattice. In this model, that we for obvious reasons will call the honey-grid model, the permissible positions of nodes on the lattice can overlap perfectly with the position of interfering nodes in the maximum interference constellation shown in Figure 9.1. Therefore, the honey-grid model allows for the maximum number of interfering signals. We have introduced the idea of using a honey-grid structure for modeling ad-hoc and sensor networks [110] and [111].

To complete the description of our assumptions in this chapter, we add that it is assumed that all nodes transmit with the same power; all nodes have the same traffic generation behavior and all data has the same priority.

When nodes are placed on a honey-grid, from the view point of a node in the center of the configuration other nodes are positioned on co-centered hexagons (see Figure 9.3). We call each of these hexagons a *ring*. The first hexagonal ring has a side of size Δ , and contains 6 nodes. The i^{th} hexagonal ring has a side of size $i\Delta$ and contains $6i$ nodes. The size of the network can be expressed in terms of k co-centered hexagonal rings around node 0, or by N the total number of nodes in this configuration. N and k are linked through the formulas:

$$N = 1 + \sum_{j=1}^k 6j = 1 + 3k(k+1), \quad (9.1)$$

$$k = \sqrt{1/4 + (N-1)/3} - 1/2.$$

In Figure 9.3 we have depicted by a circle the coverage area for node 0 in the center of the configuration. In this example we have chosen the coverage area so that it includes two hexagonal rings. The coverage area could be larger

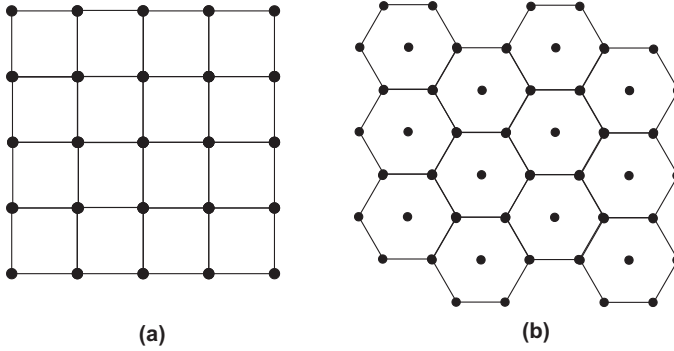


Fig. 9.2. Regular lattice forms in the 2-dimensional plane: (a) rectangular lattice, (b) hexagonal lattice.

and include more rings. This happens when the network density increases. However, the radius of the coverage area cannot be less than Δ , otherwise the network is not connected. The number of nodes inside the coverage area of each node (its degree) is indicated by d . We assume that an entire ring is either included or excluded from the coverage area. We define a node's *reach* as the number of hexagonal rings that fall inside the coverage area of that node. We indicate the reach of a node by symbol a (for example, $a = 2$ in Figure 9.3). The degree of a node that is not at the borders of the service area is

$$d = \sum_{j=1}^a 6j = 3a(a + 1). \quad (9.2)$$

Each node may communicate directly with all nodes inside its coverage area. For reaching other destinations multi-hopping must be used. There are basically two ways for reaching each destination: If node 0 in Figure 9.3 wishes to communicate with a node positioned on ring 3 (the third ring seen from the center), it either can hop through a node on ring 1 and then a node on ring 2; or it can skip ring 1 and hop directly to a node on ring 2 before reaching the destination. The first method preserves energy while the second method keeps the number of hops minimum. We will show that our model can work with both routing methods.

If we consider minimum hop routing, certain intermediate rings on the way from the source to the destination can be skipped. Figure 9.4 shows

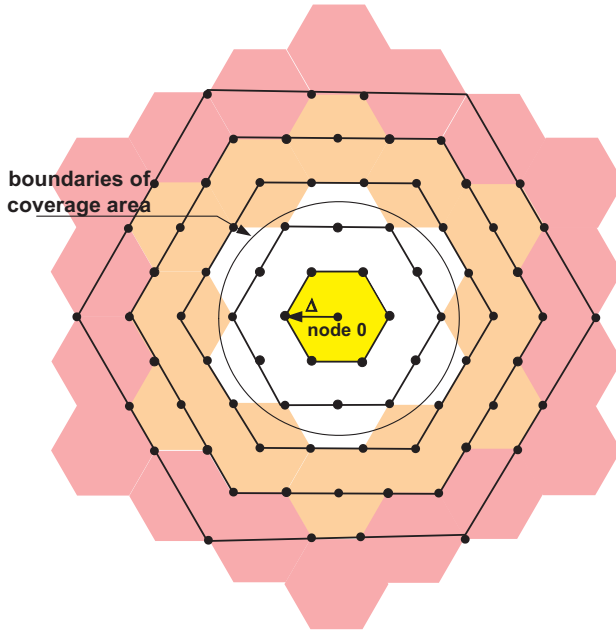


Fig. 9.3. The honey-grid model showing all nodes.

in tick lines the subset of the rings that can be used for multi-hop routing to any destination. We will call these rings *relay rings*. When packets are routing throughout the network, there may be multiple paths to the same destination. For example, the source (node 0) and the destination (node 3) shown in Figure 9.4 may be connected by the path going through nodes 0–1–3 or the path going through nodes 0–2–3. In our calculation of interference it is important to know the amount of relay traffic caused by multiple hops from source to destination, but the exact path from the source to the destination is not relevant. Therefore, for us both these paths are the same, as they both consists of two hops. In Figure 9.4 where $a = 2$, we see that the first relay ring has a side of the size 2Δ and contains 6 *relay nodes*. Relay nodes are those nodes on each relay ring that need to be used to reach any arbitrary destination (for example, when nodes 1 and 4 are relay nodes, node 2 is not chosen as a relay node because all destinations that could be reached through node 2 are already reachable through either node 1 or node 4). Generally, if a is the reach of node 0, the number of co-centered relay rings seen from node 0 is $\lfloor k/a \rfloor$, where the sign $\lfloor x \rfloor$ indicates rounding down to the nearest integer. The number of relay nodes (source node included) is then:

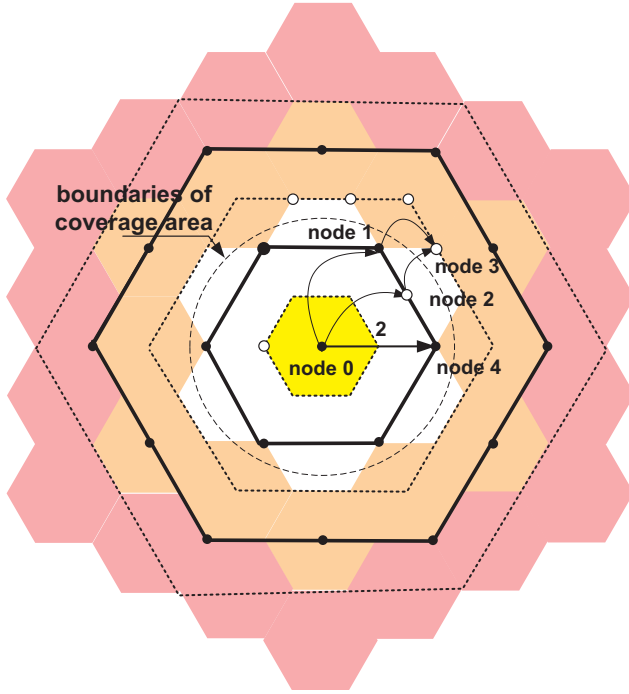


Fig. 9.4. Relay rings and relay nodes in a honey-grid. Thick lines show relay rings. Dark filled circles are relay nodes. Hollow circles are other nodes in the network.

$$N_r = 1 + \sum_{j=1}^{\lfloor \frac{k}{a} \rfloor} 6j = 1 + 3 \left\lfloor \frac{k}{a} \right\rfloor \left(\left\lfloor \frac{k}{a} \right\rfloor + 1 \right). \quad (9.3)$$

We mentioned earlier in this section that our model can handle energy efficient routing as well as minimum hop routing. If parameter $a = 1$, regardless of the reach of mobile nodes, the hopcount, traffic estimation and interference power as found in this chapter will be for energy efficient routing. If parameter a is chosen equal to the maximum radio reach of mobile nodes, the hopcount, traffic estimation and interference are found for minimum hop routing.

9.2 Interference calculation with honey-grid model

According to the honey-grid model, each node has d other nodes inside its coverage area (except for nodes at the borders of the network). As explained in Section 9.1, around node 0 the first set of interfering signals will come from signals that are transmitted from nodes just outside the coverage area

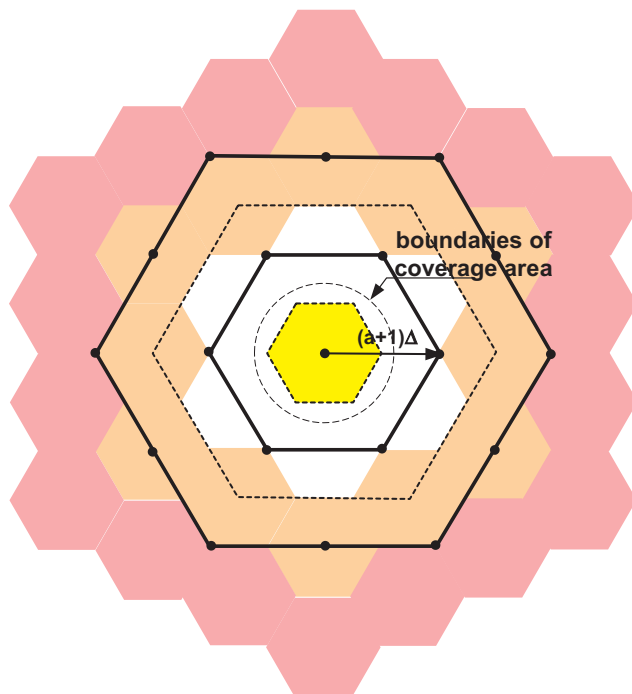


Fig. 9.5. Honey-grid with interfering rings (thick lines) for $a = 1$.

of node 0. Recalling our assumption that an entire ring is either included or excluded from the coverage area, the first ring of interference consists of 6 nodes positioned at distance $(a + 1)\Delta$ to node 0. Generally, if a is the reach of node 0, the number of co-centered interference rings seen from node 0 is $\lfloor k/(a + 1) \rfloor$, and the number of interfering nodes is:

$$N_i = \sum_{j=1}^{\lfloor \frac{k}{a+1} \rfloor} 6j = 3 \left\lfloor \frac{k}{a+1} \right\rfloor \left(\left\lfloor \frac{k}{a+1} \right\rfloor + 1 \right). \quad (9.4)$$

Figure 9.5 shows the interfering rings and the interfering nodes observed from the position of the center node in a honey-grid model with $a = 1$.

Nodes in the center of the configuration have the highest number of potential interfering nodes around them in all directions. Therefore, we choose the amount of interference experienced at node 0 as representative for the maximum level of interference inside this network. In the remainder of this section, a closed-form expression for interference at node 0 is found. If the level of interference is acceptable at node 0, we can assume that it is also acceptable for other nodes.

To calculate the amount of interference experienced at node 0, we add the interference power received at node 0 from all interfering nodes. The first interference ring contains 6 nodes at distance $(a+1)\Delta$. The second interference ring consists of 12 interfering nodes from which 6 nodes in the corners of the hexagonal ring are at the distance $2(a+1)\Delta$ to node 0 and 6 other nodes are at the distance $\sqrt{3}(a+1)\Delta$ to node 0. The distance of the nodes on each ring to node 0 can be calculated exactly. However, in our calculations in this chapter we use a simplification: we assume that the distance between all interfering nodes on each ring to node 0 is equal to the distance of the corner nodes to node 0. This is not an inaccurate approximation, especially when the service area is large. Following table shows calculation steps for finding interference power originated from the j^{th} interfering ring:

sequence number of interfering ring	j
number of interfering nodes on this ring	$6j$
approximated distance of each interfering node to the center node	$j(a+1)\Delta$
interference power coming from each interfering node on the ring	$c(j(a+1)\Delta/r_0)^{-\eta}$
interference power coming from all interfering nodes on the ring	$6jqc \left(\frac{j(a+1)\Delta}{r_0} \right)^{-\eta}$
normalized interference power coming from all interfering nodes on the ring	$6q \left(1 + \frac{1}{a} \right)^{-\eta} j^{1-\eta}$

The j^{th} interfering ring contains $6j$ nodes at approximated distance $j(a+1)\Delta$ to node 0. Let q be the probability of transmission (transmission of own signals or relay signals) per node in a given time-slot. Using (3.8), the mean power of interfering signals originating from ring j is $6jqc(j(a+1)\Delta/r_0)^{-\eta}$. According to our convention described in Section 3.4.3 we normalize this interference power to the power $\mathcal{P} = c(R/r_0)^{-\eta}$, where $R = a\Delta$ is radius of the coverage area of a node. The normalized interference power coming from ring j is then: $6q(1 + 1/a)^{-\eta} j^{1-\eta}$.

The total amount of normalized interference mean power is then:

$$\hat{I} = 6q(1 + a^{-1})^{-\eta} \sum_{j=1}^{\lfloor \frac{k}{a+1} \rfloor} j^{-(\eta-1)}. \quad (9.5)$$

When the network size increases $\lfloor \frac{k}{a+1} \rfloor \rightarrow \infty$, and the above formula can be written as:

$$\hat{I}_{\infty} = 6q(1 + a^{-1})^{-\eta} \zeta(\eta - 1)$$

where for $\text{Re}(s) > 1$, $\zeta(s) \triangleq \sum_{j=1}^{\infty} j^{-s}$ is the Riemann-Zeta function [109]. If the pathloss exponent $\eta \leq 2$, the inference power tends to explode when

the network size increases. Fortunately, as mentioned in Section 3.4.1, that pathloss exponent in outdoor environments is always more than 2. In very specific indoor environments the pathloss exponent is measured to be as low as 1.6, but a network in indoor environments is not expected to grow large in size. When the pathloss exponent $\eta > 2$, $\zeta(\eta - 1)$ is a converging series with positive terms and is upper-bounded by [112]:

$$\sum_{j=1}^{\infty} j^{-(\eta-1)} \leq 1 + \int_1^{\infty} \frac{1}{x^{\eta-1}} dx = \frac{\eta-1}{\eta-2}.$$

Based on the above formula we can conclude that the amount of interference power in a mobile ad-hoc network is upper-bounded by the following expression:

$$\hat{I} \leq 6q(1 + a^{-1})^{-\eta} \frac{\eta-1}{\eta-2}, \quad \eta > 2. \quad (9.6)$$

This conclusion is an important result and may seem contra-intuitive at the first glance. Intuitively, one may believe that adding interference power from an infinite number of interference sources, regardless of how small the interference values, may lead to an infinite sum. Above we have shown that this is not the case when radio signals decay sufficiently fast over traveled distances. To make a loose analogy, we all see that the sky at night is dark despite the virtually infinite number of stars contributing to its brightness.

From (9.6) we see that the upper bound on interference does not depend on the network size (number of nodes). But it depends on the density of the network (reflected in the value of a), the pathloss exponent η , and the probability of transmission per node q . Regardless of the total traffic per node, the probability of transmission per node, q , can never exceed 1. Hence, we may conclude that interference in mobile ad-hoc networks remains upper-bounded regardless of the offered traffic.

9.3 Comparing with previous results

In Chapter 8, Section 8.2.4 we described a method for the calculation of the expected amount of interference in ad-hoc networks with the lognormal radio model and random topology of the network. Here we compare results obtained with the calculation method presented there with the upper-bound of interference (9.6) found with the honey-grid model.

Let us assume that the node density is ρ . In the honey-grid model the reach of a node is denoted by factor a , and we have $1 + \sum_{j=1}^a 6j = 1 + 3a(a+1)$ nodes in the coverage area of a node (see (9.2)). In the honey-grid model we are assuming circular coverage areas. With normalized distances, the radius of the coverage area of each node is 1 and its area size is π . The relation between a and ρ is then by approximation:

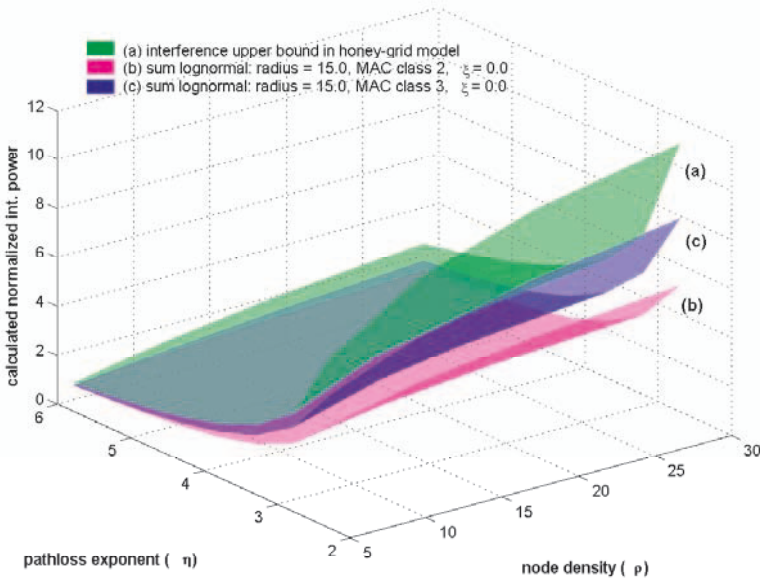


Fig. 9.6. Comparison of interference upper bound (9.6) with interference calculated using the lognormal summation method. In this plot we have assumed $\xi = 0$.

$$\rho \simeq (1 + 3a(a + 1)) / \pi,$$

$$a \simeq \left\lfloor -1/2 + \sqrt{1/4 - (1 - \pi\rho)/3} \right\rfloor.$$

For different node densities we have calculated the interference powers with the method described in Chapter 8 and have compared them with the interference power upper bound (9.6). Results for the case that $\xi = 0$ (pathloss model) are shown in Figure 9.6. As we see for $\xi = 0$ (circular coverage area around nodes), the amount of interference experienced in MAC classes 2 or 3 remains indeed under the expected upper bound. This implies that a random topology configuration, as expected, produces less interference than in the honey-grid model.

If we take the medium range radio signal power fluctuations (shadowing) into account, our calculations show that the upper bound (9.6) still applies, unless the power fluctuations are very severe. This point is verified by the plots in Figure 9.7. In this figure we see for example that the upper bound (9.6) is exceeded in the case of MAC class 3 with $\eta = 6$. Recalling that $\sigma = \xi \times \eta$, the standard deviation of radio signal power fluctuations in this case is 12 dB.

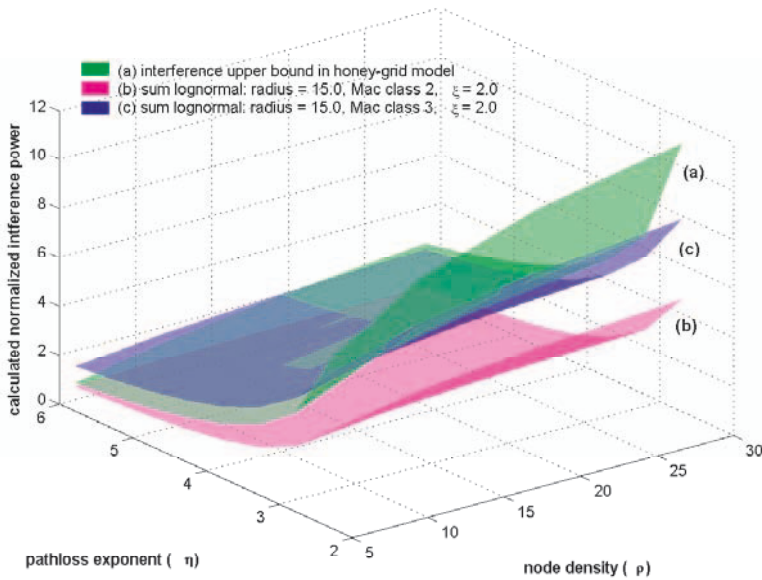


Fig. 9.7. Comparison of interference upper bound (9.6) with interference calculated using the lognormal summation method. In this plot we have taken radio signal power fluctuations into account ($\xi = 2$).

9.4 Chapter summary

In this chapter we have proposed a new model to calculate interference levels in wireless multi-hop ad-hoc networks. This model uses a regular hexagonal lattice for the location of mobile nodes. This enables us to calculate the expected values of interference without having detailed information about the movement patterns and the exact location of all nodes at all times. Assuming a simple pathloss radio model, we have found a formula for the expected interference in ad-hoc networks, and a closed-form expression for the interference upper bound. The obtained upper bound depends on the density of the network, the pathloss exponent and the probability of transmission per node. Comparison with the method of interference calculation in Chapter 8 reveals that this upper bound is still valid in networks with random topology, except when the radio signal power fluctuations are very severe (close to 12 dB and more).

Capacity of Ad-hoc Networks

In this chapter we use our findings from Chapters 8 and 9 to calculate the expected wanted carrier signal power to interference ratio in ad-hoc networks. This metric, which is called Carrier-to-Interference ratio (C/I), determines directly the capacity of the radio channel and, consequently, the ad-hoc network. Capacity is defined as the maximum possible information transfer rate over a channel. The actual information transfer rate over a channel or between two nodes is associated with the throughput of the system. Throughput measures the number of bits per second delivered over the medium.

Throughput in ad-hoc networks is affected by the routing and the offered traffic at each node. If a route cannot be found from a source to a destination, the throughput between these two nodes is virtually zero. Additionally, the offered traffic at one node determines the expected amount of relay traffic and the throughput at other nodes. Therefore, in this chapter before discussing the capacity and the throughput in ad-hoc networks, we clarify our assumptions regarding the routing and traffic generation in Sections 10.1 and 10.2, respectively.

10.1 Routing assumptions

Given a network topology, the basic function of a routing algorithm is to find an optimum path from a source to a destination. The optimum path is usually a path with the shortest length (least number of hops), although other optimization criteria like minimum delay or maximum throughput are possible as well. Well-known examples of routing algorithms are Dijkstra and Bellman-Ford algorithms. A good overview of routing algorithms can be found in [113]. Next to a routing algorithm, we need a routing protocol for coping with network dynamics when nodes and links change over time. A good overview of the routing protocols designed for ad-hoc networks can be found in [2], [4].

For the study of the capacity in ad-hoc networks we have assumed that a route between the source and the destination always can be found if it exists.

Although routing does not belong to our primary research topics (see Figure 2.1), we have studied effects of topology changes on data throughput and capacity in ad-hoc networks briefly. For this purpose we have implemented the principles of ant-routing ([114], [115]) in a software program and have run simulations. Details are to be found in Appendix A. We have noticed that data throughput reduces when due to topology changes some nodes or collection of nodes become isolated. If isolated parts of the network do not find a connection to the rest of the network during the life time of data packets intended for them, the data is lost. However, as long as the connectivity of the network is preserved, routing overhead has a less severe effect on the capacity, as we will see in Section 10.4.

10.2 Traffic model

The output traffic per node consists of the node's own traffic that is generated by the host connected to the mobile node (we will call this traffic *new* traffic) and the traffic that the node relays for other nodes (the *relay* traffic). Because of relay traffic, the total amount of traffic per node is strongly related to the multi-hop characteristics of the ad-hoc network. Our basic assumption here is that the new traffic generated by the hosts connected to mobile nodes is Poisson distributed and independent of each other. All hosts are similar and have the same traffic generation behavior. In other words, mean generated new traffic per node per time interval is the same for all nodes. We denote the mean value of new traffic per time-slot per node by λ . The length of each time-slot is denoted by t_{ts} . The average number of packet arrivals per unit time is then λ/t_{ts} . Because we assumed a Poisson arrival process, for the probability of k arrivals during a time interval of length t we have:

$$\Pr_k [t, \lambda] = \frac{(\lambda t/t_{ts})^k}{k!} e^{-\lambda t/t_{ts}}. \quad (10.1)$$

Consider two nodes i and j . When the average hopcount is $E[h]$, there are in average $E[h] - 1$ relay nodes between any source and any destination. Node i may be a relay station for node j with the probability $(E[h] - 1)/(N - 1)$, and the expected value for relay traffic arriving at node i from node j is then $\lambda(E[h] - 1)/(N - 1)$. Any node in the ad-hoc network may be a relay node for $N - 1$ other nodes. Therefore, the expected amount of relay traffic at any node is: $\lambda(E[h] - 1)$. The average total traffic per node, A , is the sum of the node's own traffic, λ , and all relay traffic that reach that node:

$$\begin{aligned} A &= \lambda + \lambda(E[h] - 1) \\ &= \lambda E[h]. \end{aligned} \quad (10.2)$$

In this formula, $E[h]$ is the expected value of the hopcount.

On page 102 we defined q , the probability of transmission per node per time-slot. The mean value of total traffic generated per node determines q . Using (10.1), for q we can write:

$$\begin{aligned} q &= 1 - \Pr_0 [t_{ts}, A] \\ &= 1 - e^{-A} \\ &= 1 - e^{-\lambda E[h]}. \end{aligned} \tag{10.3}$$

10.3 Capacity of ad-hoc networks in general

In Chapters 8 and 9 we have provided methods for the estimation of interference statistics as well as formulas for the expected interference levels in ad-hoc networks. For correct reception of radio signals, the Carrier to Interference ratio (C/I) needs to be higher than a certain threshold value (for example 7 dB)¹. C/I is the ratio between the mean power of wanted signal and the mean power of the sum of interfering signals. In radio communications the capacity of the networks is directly linked to the expected value of C/I . If we know the expected value of C/I , we can use the Shannon channel capacity formula [116, Chapter 5] to find an upper bound on the reliable data transmission speed between two nodes over the radio channel:

$$W = B \log_2 (1 + E[C/I]).$$

Here B is the channel bandwidth² in Hz and $E[C/I]$ is the expected carrier to interference ratio. W is in bits per second and indicates the upper bound on the time-averaged error free bit transmission speed over the radio channel. In other words, W is the maximum capacity of the wireless channel. When the expected value of C/I decreases, the capacity of the link between two nodes calculated with the Shannon formula decreases as well.

In ad-hoc networks an additional restriction on the capacity is imposed by the MAC protocol. As described in Chapter 7, whenever a transmission link is established between two nodes, a portion of other nodes in the network will be prohibited from simultaneous transmission, because all these nodes are sharing the same transmission medium. Under fair conditions, the capacity of

¹ In general for correct reception of radio signals, the Carrier to Interference plus Noise ratio needs to be higher than a certain threshold value. Here we are assuming that noise power is negligible in comparison to interference power.

² If a radio technology with spreading is used for radio communications, the channel bandwidth B is the channel bandwidth after despreading process. $E[C/I]$ is also the expected value of carrier to interference ratio after despreading of signals. For example, in IEEE802.11b the radio channel bandwidth before despreading is 22 MHz. With a processing gain of 11, B is equal to 2 MHz (for more information see [117]).

the radio channel is equally divided between all nodes competing to gain access to the medium. The fraction of the nodes that gain access to the medium at any time interval can be indicated by ν/ρ , where ρ is the node density and ν is the interfering node density. The relation between these two parameters is given in (8.1). In ad-hoc networks we need to multiply the Shannon capacity by ν/ρ to obtain the maximum output bit rate, $R_{out,max}$, per node:

$$R_{out,max} = \frac{\nu}{\rho} W = \frac{\nu}{\rho} B \log_2(1 + E[C/I]). \quad (10.4)$$

In this chapter we compare the output bit rate per node to $R_{out,max}$ for different network sizes, different network densities and different values of input data bit rate per node. If traffic conditions are such that the output bit rate per node tends to exceed $R_{out,max}$ the network has capacity problems.

Based on (10.2) we can find the relation between the input bit rate per node, R_{in} , and the output bit rate per node, R_{out} . However, for translation from packets per time-slot to bits per second we need the exact duration of a time-slot and the amount of overhead within each time slot. Duration of each time-slot is indicated by t_{ts} . Each time-slot consists of an overhead part, t_o , and a useful data transmission part, t_d . In other words $t_{ts} = t_o + t_d$. The overhead time is the time needed for transmission of preamble and header in each data frame. Further, the overhead time includes the required inter-frame spacing times and the required time for the reception of MAC Acknowledgments for each data frame. A typical value for t_o in IEEE 802.11b is $364 \mu s$ [6]. The length of t_d depends on data packet size, P , and data transmission speed, r . We can write $t_d = P/r$. In IEEE 802.11b, P may vary between 34 to 2346 bytes, while r is either 1 Mbps, 2 Mbps, 5.5 Mbps or 11 Mbps [6]. The input bit rate per node, R_{in} , and the output bit rate per node, R_{out} , relate to λ and Λ as:

$$\begin{aligned} R_{in} &= \frac{\lambda P}{t_{ts}}, \\ R_{out} &= \frac{\Lambda P}{t_d} = \frac{E[h]\lambda P}{t_d} = \frac{t_{ts}}{t_d} E[h] R_{in}. \end{aligned} \quad (10.5)$$

Let $R_{in,max}$ indicate the maximum input bit rate per node that can be supported by the network. Using (10.5), the maximum output bit rate per node corresponding to this maximum input bit rate is:

$$R_{out,max} = \frac{t_{ts}}{t_d} E[h] R_{in,max}.$$

Using (10.4) and the above formula we find:

$$R_{in,max} = \frac{\nu t_d}{\rho t_{ts}} \frac{W}{E[h]}. \quad (10.6)$$

Some authors call $R_{in,max}$ the per-user network capacity ([22], [118]). From (10.6) we see that the per-user network capacity is inversely proportional to the mean hopcount. This general observation explains the asymptotic values found for the capacity of ad-hoc networks in the literature. For example, in [22] it is shown that per-user network capacity with the pathloss geometric random graph model is $O\left(1/\sqrt{N}\right)$, where N is the number of nodes. We can easily explain this result noticing that the hopcount in the pathloss geometric random graph model is of the same order as the hopcount in a 2-dimensional lattice, which according to (3.6) is $O\left(\sqrt{N}\right)$.

After these considerations regarding the capacity of ad-hoc networks in general, in the next section we perform capacity calculations for the specific case of the honey-grid model.

10.4 Capacity calculation based on honey-grid model

For estimation of the capacity and the output bit rate per node we need to know the expected C/I and the mean hopcount (see (10.4) and (10.5)). Exact hopcount distribution in the honey-grid model is found in Section 10.4.1. The expected C/I is analytically obtained in Section 10.4.2. Using results from these two sections we analyze the capacity and the throughput of ad-hoc networks in Section 10.4.3.

10.4.1 Hopcount in honey-grid model

We have found the exact hop distribution for the honey-grid model. The mean and the variance are derived directly from the exact distribution of the hopcount. The method for finding hopcount distribution in the honey-grid model is discovered by finding the exact hopcount for several network configurations (from $k = 1$ to $k = 8$) and extrapolating the observed systematics to higher values of k . The algorithm found in this way is presented here. For the definition of parameters k and a please see Section 9.1.

```

begin
k = number of rings
a = a node's reach
s = k/a [note: s should be an integer, and k>a]
form matrix A(2s, s) with all values zero
form matrix B(2s, s) with all values zero
form matrix C(2s, s) with all values zero
form array h(2s) with all values zero
for j = 1 to s
  A(1, j) = 3
  A(i, j) = A(i-1, j) + 2, for i=2 to j
  A(i, j) = A(i-1, j), for i=j+1 to 2j
  B(i, j) = 2, for i=1 to 2j-1
  B(2j, j) = 2j+1
  A(i, j) = B(i, j)/2 + (A(i, j) - B(i, j)), for i=1 to 2j
  h = h + 6j A(:, j) [note: A(:, j) denotes column j of A]
end for loop
C(1, j) = C(1, j-1) + (j-1), for j=2 to s
C(i, j) = C(i-1, j-1)+C(1, j-i+1), for i=2 to s-1 and j=i to s
C(i, j) = -C(2j-i+1, j), for j=2 to s and i=j+1 to 2j
h = h + 6C(:, s) [note: C(:, s) denotes column s of C]
end

```

At the end of this procedure, array h contains the exact number of node combinations that are at distance $1, 2, \dots, 2 \lfloor k/a \rfloor$ hops from each other. As an example, Figure 10.1 shows the distribution of the hopcount for three different values of k . In all cases it is assumed that $a = 1$.

When $a = 1$, this calculation method produces the exact number of hops from any source to any other destination in the entire network. We have used the above described procedure to find the mean and variance of hopcount for different number of nodes N . The results, in logarithmic scale, are shown in Figure 10.2.

As observed in this figure, on logarithmic scale, the mean and the variance of the hopcount seem to be linear functions of the number of nodes. This is confirmed by first order curve fitting results:

$$\begin{aligned}\log E[h]_{a=1} &\simeq 0.50 \log(N) - 0.64 \\ \log Var[h]_{a=1} &\simeq \log(N) - 2.81\end{aligned}$$

These linear approximations fit almost perfectly with computed values³. Based on these formulas we find the following approximation for the average and variance of the hopcount in the honey-grid model:

³ For $k = 500$, the root mean square error (rmse) of the linear fit for the average hopcount is of the order 10^{-4} , and the rmse for the linear fit of the variance is of the order 10^{-3} .

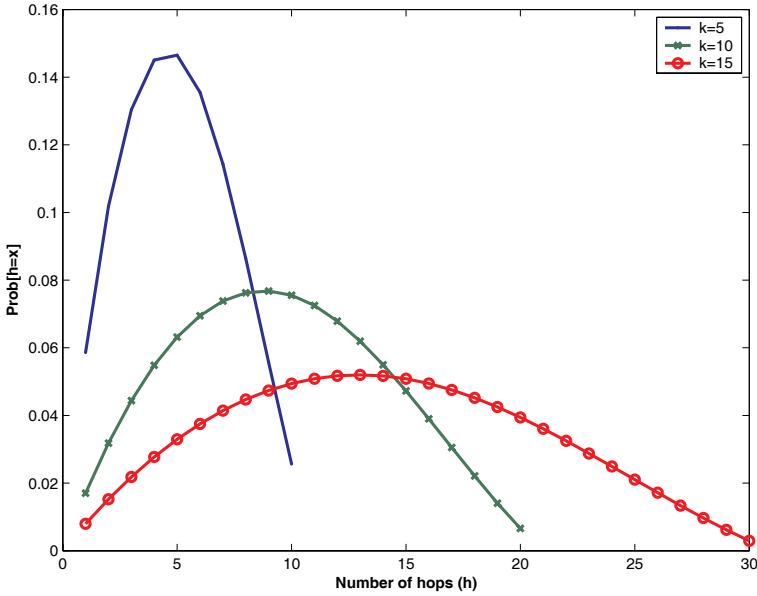


Fig. 10.1. Hopcount distribution in the honey-grid model for $k = 5$ (91 nodes), $k = 10$ (331 nodes), and $k = 15$ (721 nodes). In all cases $a = 1$.

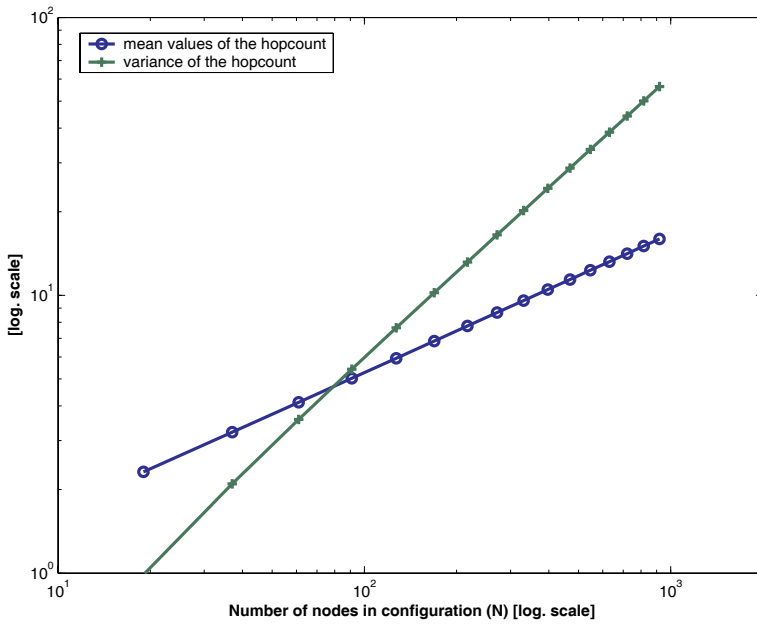


Fig. 10.2. Mean and variance of the hopcount in the honey-grid model.

$$E[h]_{a=1} \simeq 0.53 N^{0.5} \quad (10.7)$$

$$Var[h]_{a=1} \simeq 0.06 N \quad (10.8)$$

It is interesting to mention that the formulas found here for the mean and the variance of the hopcount in the honey-grid model agree with expressions found in [119] for *rectangular* d-lattice graphs. For the 2-dimensional lattice $d = 2$ in [119] we find; $E[h] \simeq 2/3 N^{1/2}$, and $Var[h] \simeq 1/9 N$. In comparison to (10.7) and (10.8) only the pre-factor due to a form difference between a hexagonal and rectangular lattice is slightly different. It should be noticed that (10.7) and (10.8) are valid for small as well as large values of N , while expressions in [119] are found for large values of N .

The mean hopcount in the entire network for the case that $a = 1$ is found directly by (10.7). However, in the case that $a \neq 1$, (10.7) produces the average hopcount over relay nodes. We assume a node that is not situated on a relay ring will hop its traffic first to a relay node positioned on a relay ring. Consequently, if both the source and the destination nodes are not on relay rings, the average hopcount from source to destination is two hops more than the average value found over relay nodes. The average hopcount is then approximately:

$$E[h]_{a>1} \simeq 0.53N_r^{0.5} + 2 \left(1 - \frac{N_r}{N}\right). \quad (10.9)$$

In this formula, N is the number of nodes in the configuration, N_r (see (9.3)) is the number of nodes on the relay rings seen from the center node and $(1 - N_r/N)$ represents the probability that either the source or destination node is not a relay node.

Figure 10.3 shows the mean value of the hopcount calculated with (10.9) for different number of nodes in a honey-grid structure.

10.4.2 Expected carrier to interference ratio

In the honey-grid model the lowest expected value for wanted signal power, C , is related to the situation that the wanted signal (signal from the source) is transmitted from the farthest neighbor of node 0 at distance $a\Delta$. The highest value of C is related to the situation that the wanted signal is transmitted from the nearest neighbor of node 0, which is at distance Δ (see Section 9.1). The total number of nodes inside the coverage area of node 0 according to (9.2) is $3a(a + 1)$. The j^{th} ring ($j \leq a$) contains $6j$ nodes at distance Δj to node 0 in the center⁴. The probability that the wanted signal is originated from distance $j\Delta$ is then $\frac{6j}{3a(a+1)}$. Using (3.8) and taking into account all

⁴ In the case that $j > 1$, assuming that all nodes on the ring are at the same distance to the center node is a simplification. As described on page 102, we consider this simplification to be acceptable.

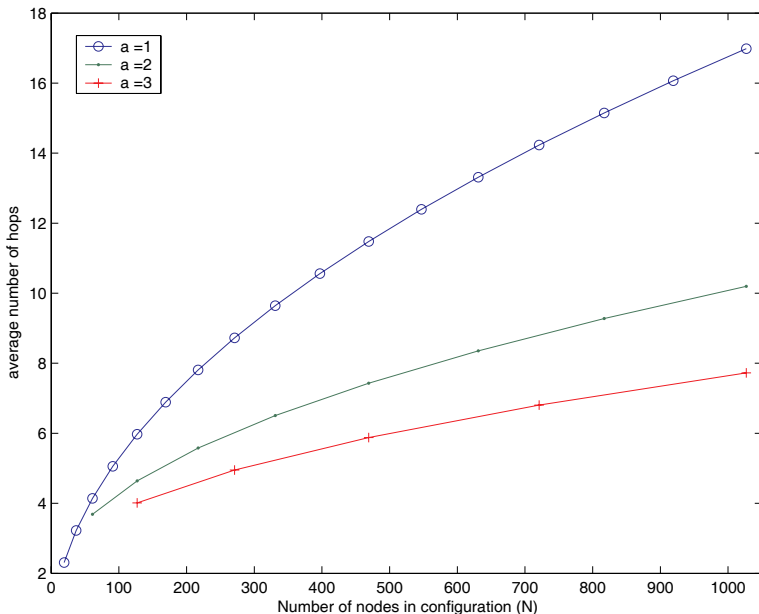


Fig. 10.3. Mean value of the hopcount in a honey-grid structure for different number of nodes (N) and different values of a (reach of a node).

possible positions for the wanted signal transmitter, the expected value for C is:

$$\begin{aligned}
 E[C] &= \sum_{j=1}^a \frac{6j}{3a(a+1)} c.(j\Delta/r_0)^{-\eta} \\
 &= \frac{2c(\Delta/r_0)^{-\eta}}{a(a+1)} \sum_{j=1}^a j^{-(\eta-1)}.
 \end{aligned}$$

According to our convention described in Section 3.4.3 we can normalize the wanted signal power to the power $\mathcal{P} = c(R/r_0)^{-\eta}$, where $R = a\Delta$ is radius of the coverage area of a node. The normalized expected power of the wanted signal is then:

$$E[\hat{C}] = \frac{2}{a^{-\eta+1}(a+1)} \sum_{j=1}^a j^{-(\eta-1)}. \quad (10.10)$$

In mobile ad-hoc networks based on WLAN technologies, mostly spread-spectrum techniques are used. In these cases we should only consider the amount of interference power that coincides with the wanted signal after de-spreading process. The reduction in interference power is indicated by *pro-*

cessing gain⁵, g . Based on (9.5) and (10.10), the following formula calculates the expected value of C/I for a node in the center of an ad-hoc network.

$$E[C/I] = \frac{g \sum_{j=1}^a j^{-(\eta-1)}}{3a(a+1)^{-(\eta-1)} q \sum_{j=1}^{\lfloor \frac{k}{a+1} \rfloor} j^{-(\eta-1)}}.$$

From the above formula we see that the expected value of carrier to interference ratio, $E[C/I]$, depends on the network size k , density of the network a , pathloss exponent η and the probability of transmission per node q . Substituting q in the above formula from (10.3) provides:

$$E[C/I] = \frac{g \sum_{j=1}^a j^{-(\eta-1)}}{3a(a+1)^{-(\eta-1)} (1 - e^{-\lambda E[h]}) \sum_{j=1}^{\lfloor \frac{k}{a+1} \rfloor} j^{-(\eta-1)}}. \quad (10.11)$$

Here, η is the pathloss exponent, g is the processing gain, a is the reach of nodes in the center of the configuration, k is the number of rings in the network, λ is the mean arrival rate of new packets per node per time-slot (node's own traffic) and $E[h]$ is the average number of hops. Relation between the number of nodes, N , and the number of rings k is given in (9.1). Average hopcount, $E[h]$, is found by (10.9).

Effect of network size and network density on C/I

Figure 10.4 shows the calculated values of $E[C/I]$ according to (10.11) for different values of the pathloss exponent and different number of nodes with $a = 1$. Figure 10.5 shows the calculated values of $E[C/I]$ according to (10.11) for a fixed value of the pathloss exponent and the node's own traffic but with different values for a . From these two figures we can conclude that for large networks the expected value of C/I tends to an asymptotic value that depends only on the pathloss exponent and the value of a . In other words, for large ad-hoc networks, the expected value of C/I depends on the network density (which is directly related to a) and the pathloss exponent. In indoor environments, with higher values of pathloss exponent, an ad-hoc network performs better than in outdoor environments where due to lower pathloss values radio signals travel to farther distances and cause more interference. Previously in (9.6) we showed that interference is upper bounded in ad-hoc networks that use carrier sensing for medium access. When interference is upper-bounded we expect $E[C/I]$ to have a lower bound. Results shown in Figures 10.4 and 10.5 confirm this claim.

⁵ In 802.11 DSSS (Direct Sequence Spread Spectrum) the processing gain is realized by modulating each data bit with an 11 bit Barker code (pseudo random sequence). Processing gain is therefore 11:1, or 10.4 dB [6].

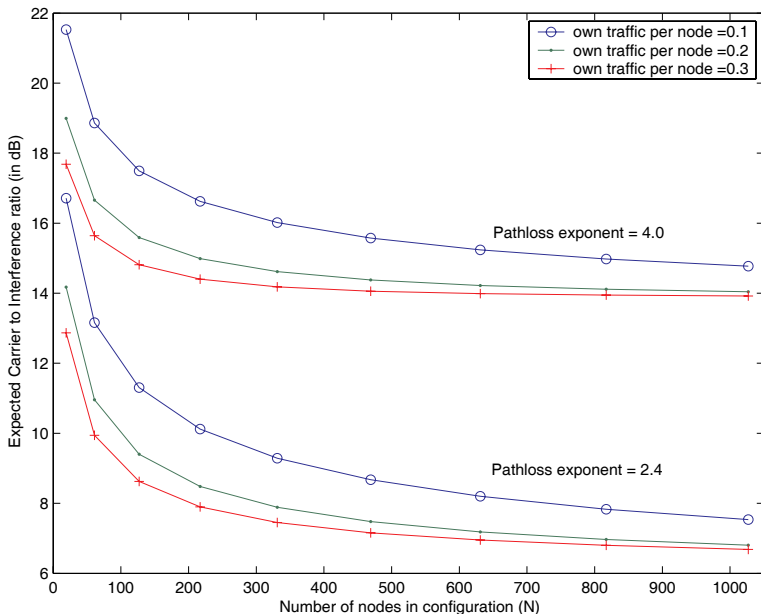


Fig. 10.4. Expected value of C/I for a node in the center of a honey-grid structure for different values of a node’s own traffic, λ . In all cases the node’s reach, a , is 1 and the processing gain is 10.4 dB.

Effect of routing overhead on C/I

New traffic per node, λ , consists of two parts: the data traffic and routing overhead. Data traffic is the actual communication data to be transmitted from a source to a destination (for example the content of an e-mail). Routing overhead consists of all traffic generated by a node for finding new routes, or for keeping routing information up-to-date. We can use (10.11) to study the effect of traffic increase due to routing overhead on the performance of a mobile ad-hoc network. Figure 10.6 shows calculated results for a few examples. In this figure, degradation of $E[C/I]$ along the y-axis is the difference between $E[C/I]$ with routing overhead and $E[C/I]$ for the same value of data traffic with zero routing overhead. From Figure 10.6 we may conclude that routing overhead does not seem to have significant influence on $E[C/I]$ in large networks with high data traffic volumes.

10.4.3 Capacity and throughput

Having access to the expected values of C/I , we can use the Shannon channel capacity formula (10.4) to find an upper bound on reliable data transmission speed between two neighboring nodes in the honey-grid model. For this, we

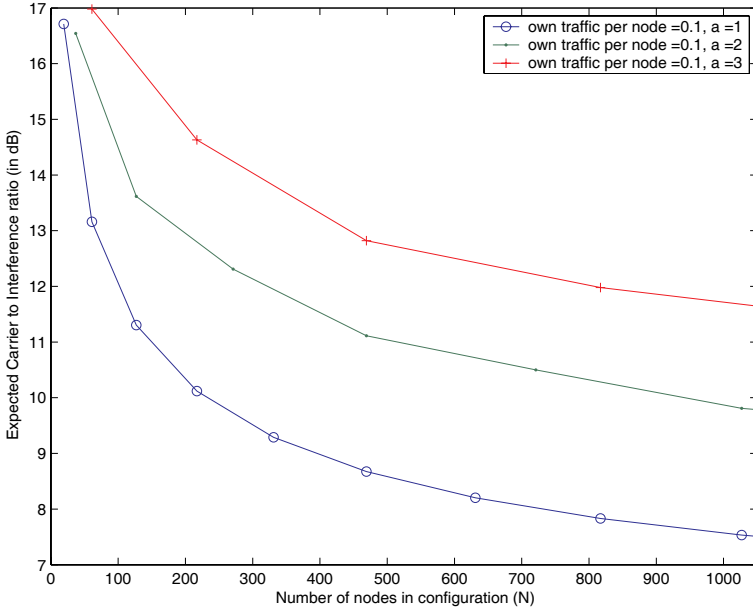


Fig. 10.5. Expected value of C/I for a node in the center of a honey-grid structure for different values of a node’s reach, a . In all cases the pathloss exponent is 2.4, the node’s own traffic rate is 0.1 packets per time-slot and the processing gain is 10.4 dB.

substitute $E[C/I]$ in (10.4) with (10.11). With the node degree d , at any moment in time only one of the $d + 1$ neighboring nodes may transmit. Therefore we substitute $\frac{\nu}{\rho}$ in (10.4) with $1/(d + 1)$. In the honey-grid model d is given by (9.2). The result is:

$$R_{out,max,hg} = \frac{B}{1 + 3a(a + 1)} \log_2 \left(1 + \frac{(a + 1)^{\eta-1} g \sum_{j=1}^a j^{-(\eta-1)}}{3a (1 - e^{-\lambda E[h]}) \sum_{j=1}^{\lfloor \frac{k}{a+1} \rfloor} j^{-(\eta-1)}} \right). \tag{10.12}$$

$R_{out,max,hg}$ in bits per second indicates the upper bound on the error free output bit rate per node for the honey-grid model.

We have used (10.12) and (10.5) to compute the available capacity and the output bit rate per node when the network size, the network density and the input traffic per node change. Figures 10.7 and 10.8 show two examples. In these figures we see when the network size increases the output bit rate generated per node increases as well. On the other hand, by increasing the network size the amount of interference increases and this will cause the available capacity per node to decrease. At the point where the increasing output bit rate intersects with the decreasing capacity per node, we say that the

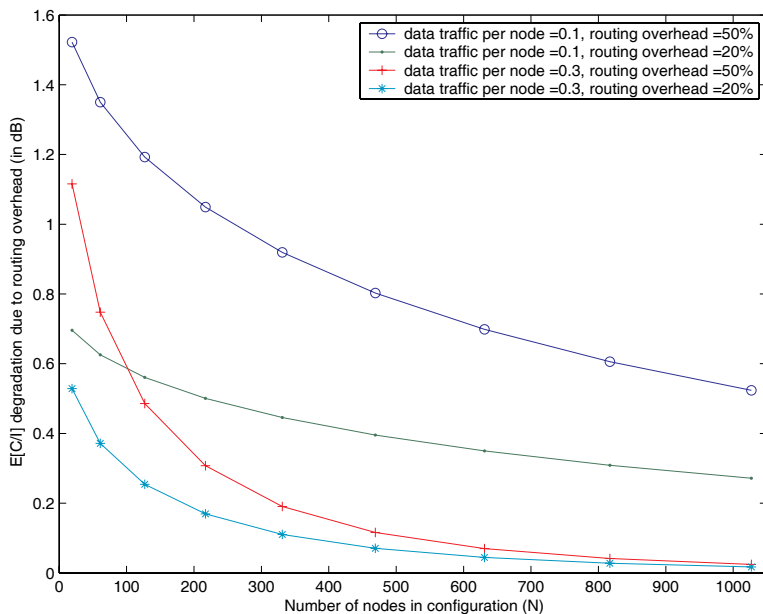


Fig. 10.6. Effect of traffic increase due to routing overhead on $E[C/I]$ in an ad-hoc network with different number of nodes. In all cases $a=1$, $\eta = 2.4$, and processing gain is 10.4 dB.

network saturation point is reached⁶. Beyond this point a node will not have time for successful transmission of any additional incoming data. As a result, the useful output bit rate per node, i.e. throughput per node, remains at a constant level even when the network size or the input data rate increase. Beyond the saturation point, increasing network size or input data rate will not increase the throughput, but will cause the delay to grow.

Another effect visible from comparing figures 10.7 and 10.8 is the effect of increase in network density. When network density increases, number of neighbors per node increases as well. We see when the network density increases (higher node's degree in Figure 10.8), the network saturation point is reached for a lower number of nodes and at lower data rates.

We mention here that our finding that the throughput in IEEE802.11b networks flattens when traffic load increases is also observed in some experimental measurement results [120].

We believe our model for calculation of the throughput per node presented in this chapter has practical applications in the design and optimization of ad-hoc and sensor networks. Figure 10.9 illustrates another set of data obtained

⁶ In figures 10.7 and 10.8 the dashed lines show the trend in the increase of the output bit rate and the decrease in the available capacity if saturation point was not reached.

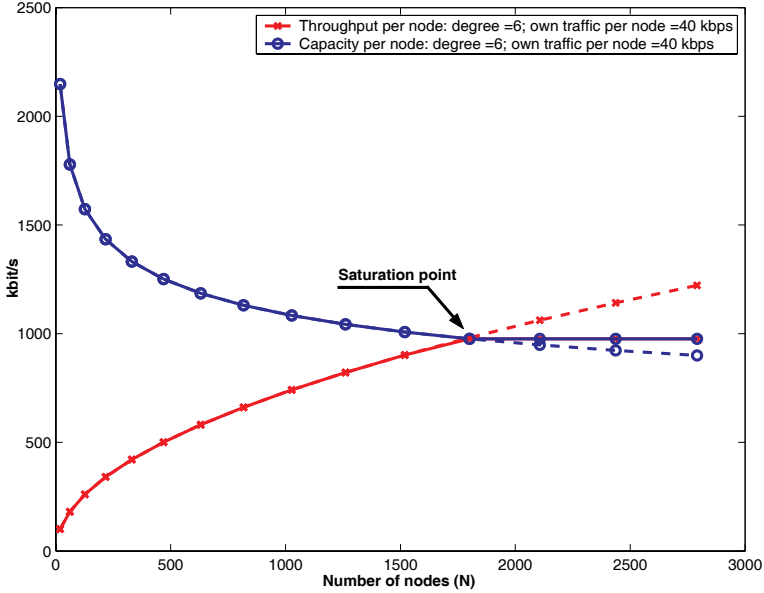


Fig. 10.7. Comparing the capacity and the output bit rate per node. In this figure the node’s reach, a , is 1 (6 neighbors per node) and each node’s own traffic equals to 40 kbps. For calculations we have assumed: channel bandwidth B is 22 MHz (before despreading), processing gain g is 11, data packets size P is 1000 bytes, transmission speed r is 2 Mbps, $t_0 = 364\mu s$ and the pathloss exponent η is 2.4.

using (10.12) and (10.5) to compute the throughput per node for different number of nodes and different values of the input bit rate per node. From this figure we can read the maximum supported input bit rate per node for different network sizes. Figure 10.10 is a different perspective on Figure 10.9. In Figure 10.10 we have shown the portion of the output per node that is the node’s own traffic, assuming that the own traffic and the relay traffic have the same priority. As we can see from Figure 10.10, when network size increases, due to the increase in multi-hop relay traffic, nodes could not get rid of their own data. The maximum allowable input data per node depends on the size of the networks, or better said on the expected hopcount. Figure 10.10 shows clearly that large ad-hoc networks with high diameter (high value of the mean hopcount) are only practical when the input data rate per node is low. For example, a multi-hop network consisting of thousands of nodes is probably a good solution for a sensor network in which each node has limited data to transmit. However, when data rates start to increase, like in multimedia applications, only ad-hoc networks of small size with few hops can support these kind of broadband applications.

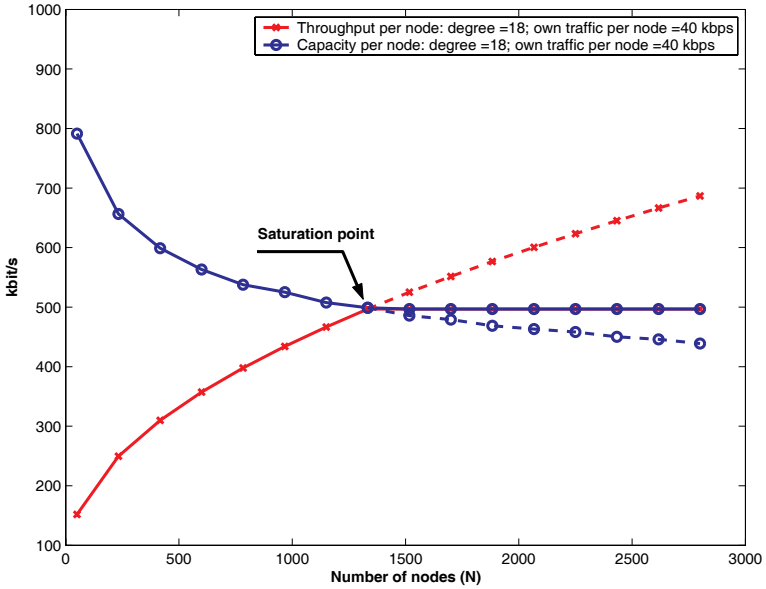


Fig. 10.8. Comparing the capacity and the output bit rate per node. In this figure the node’s reach, a , is 2 (18 neighbors per node). Other assumptions are the same as in Figure 10.7.

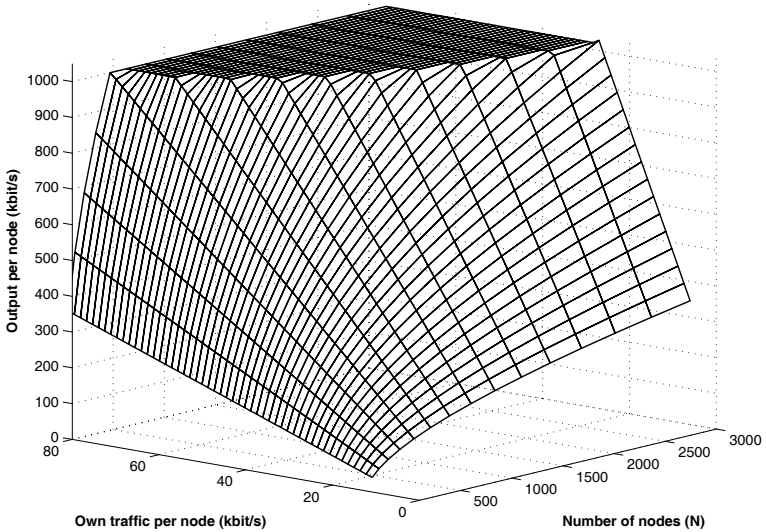


Fig. 10.9. Throughput per node for different values of input data bit rate per node and different number of nodes. Each node’s own traffic varies between 10 kbps and 80 kbps. Other values and assumptions are the same as in Figure 10.7.

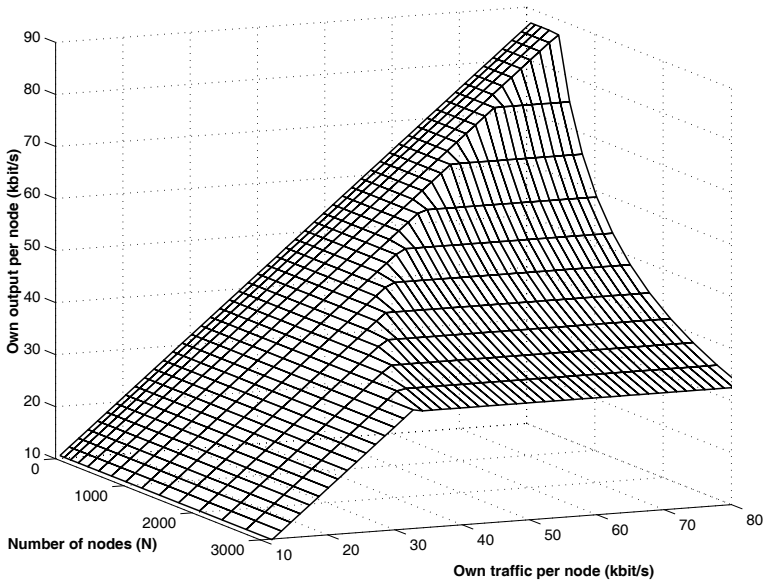


Fig. 10.10. Portion of the throughput per node assigned to a node's own traffic. All values and assumptions are the same as in Figure 10.9.

10.5 Chapter summary

In this chapter we have studied the throughput and the capacity of ad-hoc networks. We have extended the Shannon channel capacity formula for use in ad-hoc networks, where the transmission medium is shared by all users. Further, using the honey-grid model, we have derived an analytical expression for the expected value of C/I in ad-hoc networks. We have shown that the pathloss exponent η has a significant effect on the expected values of C/I in ad-hoc networks. In environments with lower values of η , ad-hoc networks perform worse, as radio signals travel to farther distances and cause more interference. For each value of η and each node density, the expected value of C/I decreases by the increase in the number of nodes. However, it tends asymptotically to a lower bound independent of the number of nodes forming the network.

We have shown that the throughput of ad-hoc networks can get saturated. Maximum throughput per node at the saturation point depends on the interference conditions and the density of the network. Once the saturation ceiling is reached, the network cannot accept any additional increase in the network size or the input bit rate per node.

In multi-hop ad-hoc networks, the output bit rate per node is proportional to the product of the node's own traffic and the mean hopcount. Output bit

rate per node cannot grow beyond the maximum capacity of the system. Therefore, the per-user network capacity (the maximum input bit rate supported per user) is inversely proportional to the mean hopcount. The mean hopcount depends on the network size and the dimensions of the service area. In the design of ad-hoc networks there is a trade-off between the network size and the input bit rate per node. For example, high bit rate multi-media applications can only be combined with an ad-hoc network limited in size, or better said, with an ad-hoc network limited in the number of hops.

Book Summary

In the diverse field of research areas related to wireless mobile ad-hoc networks, we have focused in our work on fundamental properties of ad-hoc networks. By fundamental properties we mean the connectivity, capacity, and network characteristics that significantly and directly affect the former two. In this respect, we have shown that degree distribution, hopcount distribution, and interference statistics are fundamental properties as well. We have studied all these fundamental properties using a realistic network model based on realistic assumptions for radio propagation. This book is centered around the following main themes:

- realistic modeling,
- degree distribution,
- hopcount distribution,
- connectivity, and
- capacity and interference estimation, which are closely related topics.

In this final chapter of this book we provide for each of these themes an overview of the obtained results. Whenever appropriate we include remarks regarding possible extensions of the work. The descriptions in this chapter are at a higher level of abstraction than the remarks at the end of the corresponding chapters.

Realistic modeling

We have shown that graph theory can be used for modeling ad-hoc networks. However, none of the random graph, lattice graph, scale-free graph and pathloss geometric random graph models is suitable to model wireless ad-hoc networks. In this book we introduced the lognormal geometric random graph model that matches very well all basic characteristics of wireless ad-hoc networks (see Table 3.1).

Our model for ad-hoc networks is based on the medium scale signal power fluctuation in radio communications and assumes that these power fluctuations have a lognormal distribution. The ratio of the standard deviation of radio signal power fluctuations to the pathloss exponent is denoted by symbol ξ . Throughout this book, this parameter appears to be a significant factor in determining ad-hoc network properties like degree distribution, hopcount distribution and connectivity.

Our lognormal geometric random graph model assumes that links between nodes are two-way, undirected links. There is a link connecting two nodes if a signal transmitted from one node is received at the other node above a minimum required power threshold. Whether two connected nodes can communicate with each other at the desired data communication speed at all times is a matter of interference and capacity calculation. In our modeling we have clearly separated network topology from network capacity. Whenever communication between two connected nodes drops to lower speeds or even becomes impossible we say that the link capacity has diminished, instead of saying that the network topology has changed.

Our modeling based on the lognormal assumption of medium scale radio signal power fluctuations is a step in the right direction for better and realistic modeling of ad-hoc networks. However, we emphasize at the same time that more measurements are needed for better understanding of radio channel characteristics in typical ad-hoc network environments and frequencies.

Degree distribution

Assuming uniform distribution of nodes over the service area, we have found an analytic expression for the link density in wireless ad-hoc networks. The expected node degree in ad-hoc networks is found by multiplying the link density with the number of nodes forming the network. It has been shown that link density is a function of the area size and the parameter ξ . When area size tends to ∞ , link density tends to 0, which is a direct consequence of the fact that in ad-hoc networks links are distance dependent. Further, it has been shown that the link density, and consequently the mean degree, are higher for larger values of ξ . The minimum link density occurs at $\xi = 0$, which corresponds to the pathloss model of radio propagation. We may conclude therefore that the pathloss model is the most pessimistic model for the estimation of the mean degree in ad-hoc networks.

In ad-hoc networks, the degree distribution can be considered to be binomial when the density of nodes is low and the area size large in comparison to the *maximum link distance*. By maximum link distance we mean the metric length of the distance over which two nodes can be connected with a non-negligible probability. We know that degree distribution in random graphs is also binomial. It is interesting to see that despite their totally different behavior, both the random graph and the geometric random graph have a binomial

degree distribution. It should be noticed however that binomial degree distribution in geometric random graphs is conditional on the uniform distribution of nodes over the service area.

Hopcount distribution

The hopcount behavior in ad-hoc networks for low values of ξ is similar to the hopcount in rectangular lattice networks with the same length and the width as the service area of the ad-hoc network. When ξ increases, both the mean hopcount and the network diameter reduce due to the appearance of occasional long links between nodes. For a given node density, the mean hopcount in ad-hoc networks increases with increasing service area size. Hopcount is not affected by an increase in the number of nodes (small-world property) if we keep the service area size unchanged.

We have observed that the hopcount in ad-hoc networks is a function of the parameters ξ , the number of nodes N , and the service area size. We have shown how the hopcount is affected by a change in each of these parameters. We have not presented an exact analytic formula for the hopcount distribution as function of the parameters ξ , N and the service area size. However, for a specified form of ad-hoc networks, the honey-grid model with $\xi = 0$, we have found an algorithm that provides the exact hopcount distribution. The honey-grid model, introduced by us, is a simplified way of looking at ad-hoc networks and has proved to be of value for studying not only the hopcount but also the capacity of ad-hoc networks.

Connectivity

Using our geometric random graph model we have studied connectivity probability in ad-hoc networks. Our study shows that radio signal power variations increase the probability of having long links, which in turn enhances the probability of connectivity for the entire network. In the light of this new finding we have been able to modify the theorems of connectivity for ad-hoc networks (for details please see page 63).

Our results also demonstrate that full connectivity in ad-hoc networks is achieved at relatively high values of the mean node degree, while at far lower values, a very large portion of the network could already be connected. Therefore we argue that for practical planning and design of wireless ad-hoc networks or sensor networks full connectivity is a very stringent condition to fulfill, and suggest to use the giant component size as a measure for "connectivity". We have found an equation for calculating the giant component size in wireless ad-hoc networks that takes into account the level of radio signal power variations. Our formula can be used to provide directives for the average required number of neighbors per node (mean degree per node) to obtain connectivity over any desired percentage of the network. The mean degree can be changed by adjusting the transmission power of nodes or by changing the node density.

Interference and Capacity

Interference and capacity in wireless ad-hoc networks are directly affected by the working of MAC protocols. Each MAC protocol restricts in its own way the number of interfering signal transmissions allowed per unit of area, regardless of the number of nodes falling within that area. Therefore, the interfering node density depends on the MAC protocol details. For the purpose of our study we have classified MAC protocols into three different groups. This classification, which is based on the way in which MAC protocols solve the hidden and the exposed terminal problems, has enabled us to take into account the impact of MAC protocols without going into the details of each MAC protocol individually. For each MAC protocol class, we have found approximating formulas to calculate the expected interfering node density as a function of the node density and the parameter ξ . These formulas show that the interfering node density is by approximation proportional to the logarithm of the node density.

We have presented a calculation method using the lognormal radio propagation model to estimate the interference power sum statistics in ad-hoc and sensor networks. The input parameters for the model are the area size, density of the nodes, the radio propagation conditions (pathloss exponent and lognormal fading standard deviation), the activity ratio of nodes and the MAC protocol class. The method presented here is a first attempt to expand the interference power sum calculation methods used in fixed topology networks to ad-hoc and sensor networks. Although simulations have confirmed that our method calculates the mean interference power with acceptable accuracy, there is room for fine-tuning and improvements. Especially estimation of the standard deviation of the interference power sum could be improved.

For analytic calculation of interference and capacity we have introduced the simplified honey-grid model. In this model, nodes are assumed to be placed on a hexagonal 2-dimensional lattice. Using this model with a simple pathloss radio model, we have found closed-form analytic formulas for the interference and interference upper bound in ad-hoc networks. The interference upper bound depends on the node density, the pathloss exponent η , and the probability of transmission per node, but it is independent of the number of nodes. This is an important conclusion which implies that increasing the network size in ad-hoc networks for the same node density does increase the amount of interference.

To study the capacity of wireless ad-hoc networks we have used the Shannon channel capacity formula and have extended it to include medium sharing effects of the MAC protocols on the capacity. We have shown that the pathloss exponent η has a significant effect on the expected values of C/I in ad-hoc networks. In environments with lower values of η , ad-hoc networks perform worse, as radio signals travel to farther distances and cause more interference.

The output bit rate per node in ad-hoc networks depends not only on the node's own traffic but also on the relay traffic passing through that node.

In multi-hop ad-hoc networks the output traffic per node is proportional to the product of the node's own traffic and the mean hopcount. However, the output bit rate per node cannot grow beyond the capacity limit of the system. Therefore, in the design of ad-hoc networks there is a trade-off between the network size (which affects the mean hopcount) and the input bit rate per node. Large ad-hoc networks, consisting of thousands of nodes with relatively large mean hopcount, can only support moderate bit rate applications.

Ant-routing

To study network performance metrics like throughput, delay and routing protocol overhead in wireless ad-hoc networks we have developed a software simulation tool¹. This tool has a graphical user interface that allows us to monitor changes in the node's routing table and data output variations when the network topology and the input traffic rates change. The input parameters for the simulator include:

- number of nodes in the network,
- size of the service area,
- speed of the nodes,
- capacity and transmission delay of radio link between nodes,
- input traffic statistics per node, and
- buffer capacity per node.

The routing protocol used in our simulator is a modified version of AntNet [121]. AntNet is an adaptive approach to routing in packet-switched communication networks that is inspired by the stigmergy model of communication observed in ant colonies.

In ant colonies, indirect communication among individuals takes place through modifications induced in their environment. Ants lay a trail of pheromones on their way between a source (nest) and a destination (food), as depicted in Figure A.1. Each ant choosing a branch increases the amount of pheromones on that branch, and in this way it increases the probability of choosing the same branch for following ants. Small but systematic differences are amplified to reach overall shortest path selection.

In our simulator program each node produces on regular intervals “artificial ants” that are sent to randomly chosen destinations. When a destination is reached, the ant travels back to the source node following the same route

¹ Our ad-hoc network simulator was built upon a software implementation by the team of dr. drs. L.J.M. Rothkrantz, at the Delft University of Technology, for dynamic vehicle routing in fixed networks.

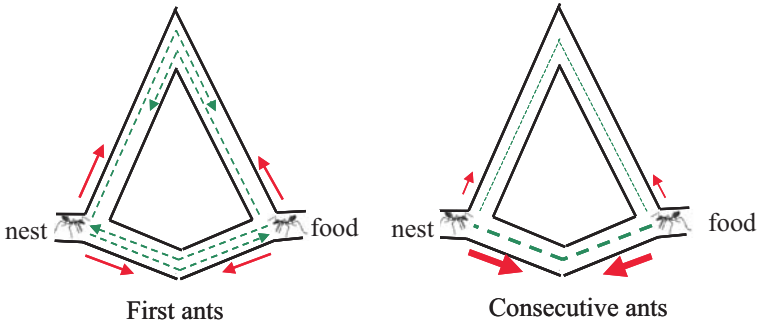


Fig. A.1. The principle of ant-routing.

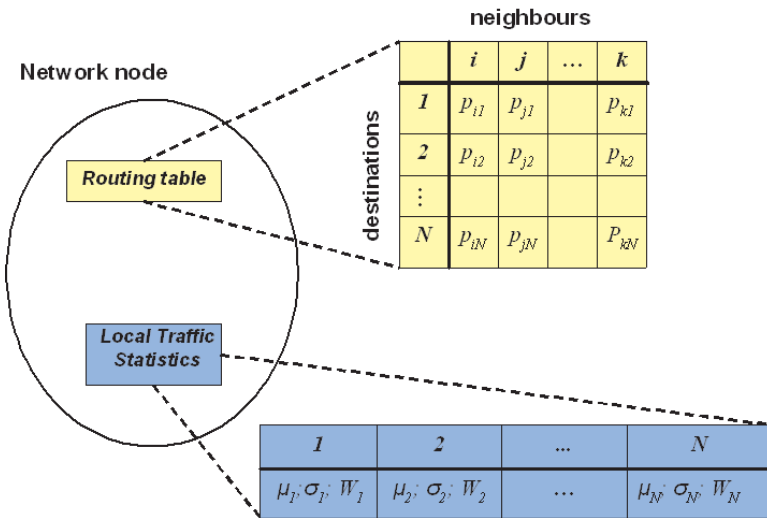


Fig. A.2. Routing table and local traffic statistics in ant-routing..

in opposite direction. Ants are handled with high priority at nodes and do not experience the same delay as data packets. However, based on the queue size at each node, ants collect information about the delay that a data packet would experience using the same path. This information is used to update two data structures in each node: the routing table and the local traffic statistics (see Figure A.2).

In a network of N nodes, the routing table at each node contains the probabilities to reach any of the possible $N - 1$ destinations through each of the k neighbors of that node. Local traffic statistics at each node are the sample mean and the variance of the trip time to all other destinations in the network; plus the best trip time to each destination. This information, which is collected and updated by ants, is used to refresh routing tables continuously.

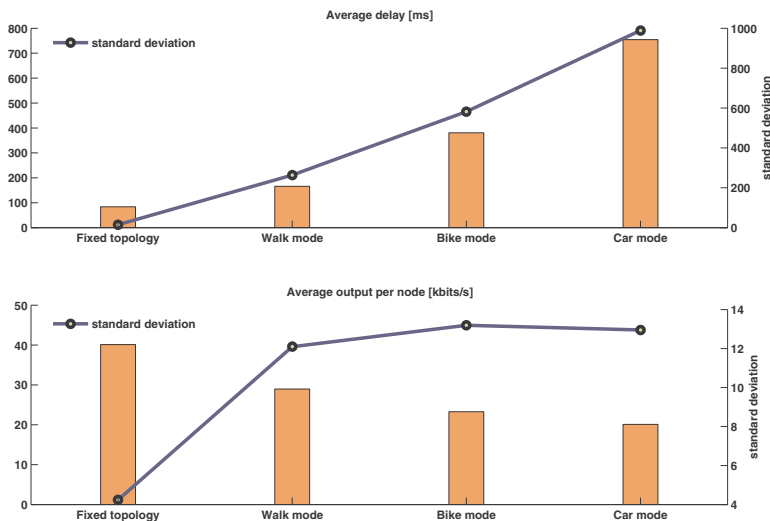


Fig. A.3. A set of simulation results found using ant-net simulator. The walk mode, bike mode and car mode correspond to node speeds of, respectively, 5 km/h, 15 km/h and 75 km/h.

On the graphical user interface of the simulator one can follow changes in the network topology and its direct effects on the throughput, delay and utilization factor in the entire network. Therefore, this simulator helps to get a realistic feeling about the behavior of ad-hoc networks under varying circumstances. Figure A.3 depicts some simulation results that show changes in the throughput and the packet delay as function of the speed of the network nodes. These results are found for a Poisson traffic arrival rate with an average of 40 kbit/s data input per node.

From this figure we see that the throughput of systems reduces and the delay increases when the topology of the network changes more rapidly. The reduction in data throughput is mainly due to lost packets when the destination of some packets are not reachable.

B

Symbols and Acronyms

α	signal amplitude
β	constant equal to $\log(10)/10$
γ	exponent of power-law degree in scale free graphs
Δ	distance between two adjacent nodes in honey-grid model
$\zeta(\cdot)$	zeta function
η	pathloss exponent
$\kappa(G)$	vertex-connectivity of graph G
λ	mean value of a node's own traffic in packets per time-slot
Λ	mean value of a node's own traffic and relay traffic in packets per time-slot
μ	mean value
ν	interfering node density
ξ	σ/η in the lognormal radio model
ρ	node density
σ	standard deviation of radio signal power fluctuations
τ	activity ratio
v	constant equal to $10/(\sqrt{2}\log 10)$
$\varkappa(G)$	edge-connectivity of graph G
a	reach of a node (number of rings falling inside a node's coverage area) in honey-grid model
a_{ij}	element (i, j) in matrix A
A	adjacency matrix
B	radio channel bandwidth
c	constant depending on the transmitted power, antenna gains and wavelength

c_i	clustering coefficient of node i
C	carrier power
C/I	carrier to interference ratio
C_G	clustering coefficient of graph G
d	degree
d_{\min}	minimum degree
E	edge set in graph G
$E[x]$	expected value of x
g	processing gain
G	notation for a graph
$G_{m,n}$	lattice graph on a square grid of size $m \times n$
$G_p(N)$	random graph with link probability p and N nodes
$G_{p(r_{ij})}(N)$	geometric random graph with link probability $p(r_{ij})$ between nodes and N nodes
h	hopcount
L	number of links (edges) in a graph
\mathcal{L}	link density
\mathcal{L}_{\lg}	link density with lognormal radio model
L	lognormal random variable
\log	natural logarithm
\log_{10}	logarithm in base 10
\log_2	logarithm in base 2
N	number of nodes (network size)
$O(\cdot)$	<i>big-O</i> asymptotic order notation
p	link probability between two nodes in a graph
\mathbf{P}_a	area mean power
P	packets size
$\mathbf{P}(r)$	received power at distance r from a transmitter
$\hat{\mathbf{P}}(\hat{r})$	normalized power (normalized to \mathcal{P}) at normalized distance \hat{r} (normalized to R)
p	instantaneous power of a Rayleigh faded signal
\bar{p}	average power of a Rayleigh faded signal
\mathcal{P}	receiver power threshold for correct detection of signals
$\Pr[x = y]$	probability of $x = y$
q	transmission probability per node in a time-slot
r	distance between two nodes
r	data transmission speed
r_0	reference distance
\hat{r}	normalized distance r/R
R	coverage radius of a node with the pathloss radio model

R_{in}	input bit rate per node
$R_{in,max}$	maximum input bit rate possible per node
R_{out}	output bit rate per node
$R_{out,max}$	maximum output bit rate possible per node
$R_{out,max,hg}$	maximum output bit rate possible per node in honey-grid model
\mathcal{S}	the set of the lengths of the shortest paths between all pairs of nodes in a graph
S	fraction of a graph occupied by the giant component
S_{lg}	S with lognormal radio model
t_d	length of the data part for a packets transmitted in a time-slot
t_o	length of the overhead part for a packets transmitted in a time-slot
t_{ts}	length of a time-slot
V	Vertex set in Graph G
$Var[x]$	variance of x
w	weight factor between 0 and 1
W	maximum capacity of a wireless channel
x	a zero-mean normal distributed random variable
z	mean degree

AODV	Ad hoc On-Demand Distance Vector (routing protocol)
DBTMA	Dual Busy Tone Multiple Access (MAC protocol)
CATS	Collision Avoidance Transmission Scheduling (MAC protocol)
CDF	Cumulative Distribution function (also called Distribution Function)
CIP	Cellular IP
CDMA	Code Division Multiple Access
CS	Coding Scheme
CSMA	Carrier Sense Multiple Access
CSMA/CA	Carrier Sense Multiple Access with Collision Avoidance
CSMA/CD	Carrier Sense Multiple Access with Collision Detection
dBm	dB referencing 1 milliwatt (mW)
dBW	dB referencing 1 Watt
DSSS	Direct Sequence Spread Spectrum
EMAC	Energy-efficient MAC
FDD	Frequency Division Duplex
FHSS	Frequency Hopping Spread Spectrum
FW	Fenton-Wilkinson lognormal power sum approximation method
GPRS	General Packet Radio Service

GPS	Global Positioning System
GSM	Global System for Mobile Communications
Hawaii	Handoff-aware Wireless Access Internet Infrastructure
IETF	The Internet Engineering Task Force
IP	Internet Protocol
ISM	Industrial, Scientific and Medical (ISM) Frequency Bands
kbps	kilo bits per second
LAN	Local Area Network
LOS	Line of Sight
MAC	Medium Access Control
MANET	Mobile Ad-hoc Networks (an IETF working group)
MARCH	Multiple Access with ReduCED Handshake (MAC protocol)
ns-2	Network Simulator version 2
OFDM	Orthogonal Frequency Division Multiplexing
OFDMA	Orthogonal Frequency Division Multiple Access
OLSR	Optimized Link State Routing (routing protocol)
OSI	Open System Interconnection
OSPF	Open Shortest Path First
RBCS	Receiver-Based Channel Selection
PDF	Probability Density Function (also called Density Function)
RIP	Routing Information Protocol
RMS	Root-Mean-Square
S-MAC	Sensor-MAC
S/A	Selective Availability
SY	Schwartz-Yeh lognormal power sum approximation method
TBRPF	Topology Dissemination Based on Reverse-Path Forwarding (routing protocol)
TDMA	Time Division Multiple Access
THSS	Time Hopped Spread Spectrum
UMTS	Universal Mobile Telecommunications System
UWB	Ultra-WideBand
W-CDMA	Wideband Code Division Multiple Access
WLAN	Wireless Local Area Network
WGS84	World Geodetic System 1984
WiFi	the 802.11 family is referred to as WiFi
WiMAX	the 802.16 family is referred to as WiMAX
WMAN	Wireless Metropolitan Area Network
WPAN	Wireless Personal Area Network

References

- [1] C. E. Perkins, *Ad Hoc Networking*. Addison Wesley Professional, December 2000.
- [2] M. Ilyas, ed., *The Handbook of Ad hoc Wireless Networks*. CRC Press, December 2002.
- [3] F. Akyildiz, W. Su, Y. Sankarasubramaniam, and E. Cayirci, "Wireless sensor networks: a survey," *Computer Networks*, vol. 38, pp. 393–422, March 2002.
- [4] C. S. R. Murthy and B. Manoj, *Ad Hoc Wireless Networks: Architectures and Protocols*. Prentice Hall PTR, May 2004.
- [5] W. Mohr, "Further developments beyond third generation mobile communications," *Proceedings of International Conference on Communication Technology 2000, WCC - ICCT 2000*, vol. 2, pp. 1001–1008, 21-25 August 2000.
- [6] IEEE 802.11 WIRELESS LOCAL AREA NETWORKS - The Working Group for WLAN Standards, "ANSI/IEEE Std 802.11, part 11: Wireless LAN medium access control (MAC) and physical layer (PHY) specifications," tech. rep., IEEE 802 LAN/MAN Standards Committee, 1999.
- [7] J. Solomon, *Mobile IP the Internet Unplugged*. Prentice Hall PTR, January 1998.
- [8] H. Soliman, *Mobile IPv6: Mobility in a Wireless Internet*. Addison Wesley, June 2004.
- [9] C. Huitema, *IPv6: The New Internet Protocol*. New Jersey: Prentice Hall, 1998.
- [10] IETF Mobile IP Working Group, "Mobility support in IPv6," tech. rep., IETF Mobile IP Working Group, December 2003.
- [11] A. Campbell, J. Gomez, K. Sanghyo, W. Chieh-Yih, Z. Turanyi, and A. Valko, "Comparison of IP micromobility protocols," *IEEE Wireless Communications*, vol. 9, pp. 72–82, February 2002.
- [12] C. Huitema, *Routing in the Internet, second edition*. New Jersey: Prentice Hall PTR, January 2000.

- [13] S. A. Thomas, *IP Switching and Routing Essentials: Understanding RIP, OSPF, BGP, MPLS, CR-LDP, and RSVP-TE*. Wiley Computer Publishing, December 2001.
- [14] P. Samar, M. Pearlman, and Z. J. Haas, "Independent zone routing: an adaptive hybrid routing framework for ad hoc wireless networks," *IEEE/ACM Transactions on Networking*, vol. 12, pp. 595 – 608, August 2004.
- [15] Z. Haas and M. Pearlman, "The performance of query control schemes for the zone routing protocol," *IEEE/ACM Transactions on Networking*, vol. 9, pp. 427–438, August 2001.
- [16] E. Royer and C.-K. Toh, "A review of current routing protocols for ad-hoc mobile wireless networks," *IEEE Personal Communications*, vol. 6, pp. 46–55, April 1999.
- [17] "IETF mobile ad-hoc networks (MANET) working group", IETF, <http://www.ietf.org/html.charters/manet-charter.html>.
- [18] IETF MANET Working Group, "Topology dissemination based on reverse-path forwarding (TBRPF), (RFC 3684)," IETF-Draft, IETF, February 2004.
- [19] IETF MANET Working Group, "Ad hoc on-demand distance vector (AODV) routing, (RFC 3561)," IETF-Draft, IETF, July 2003.
- [20] IETF MANET Working Group, "Optimized link state routing protocol (OLSR), (RFC 3626)," IETF-Draft, IETF, October 2003.
- [21] J. Hsu, S. Bhatia, M. Takai, R. Bagrodia, and M. J. Acriche, "Performance of mobile ad hoc networking routing protocols in realistic scenarios," *IEEE Military Communications Conference, MILCOM 2003*, vol. 2, pp. 1268 – 1273, October 2003.
- [22] P. Gupta and P. R. Kumar, "The capacity of wireless networks," *IEEE Transactions on Information Theory*, vol. 46, pp. 388–404, March 2000.
- [23] G. A. Gupta, S. Toumpis, J. Sayir, and R. R. Muller, "On the transport capacity of gaussian multiple access and broadcast channels," *Proceedings of the 3rd international symposium on modeling and optimization in mobile, ad hoc, and wireless networks (WiOpt05)*, Riva del Garda, Italy, pp. 10–20, 3-7 April 2005.
- [24] R. Negi and A. Rajeswaran, "Capacity of power constrained ad-hoc networks," *Proceedings of IEEE Infocom 2004*, 2004.
- [25] A. Zemlianov and G. de Veciana, "Capacity of ad hoc wireless networks with infrastructure support," *IEEE Journal on Selected Areas in Communications*, vol. 23, pp. 657–667, March 2005.
- [26] P. Marbach and R. Pang, "Transmission costs, selfish nodes, and protocol design," *Proceedings of the 3rd international symposium on modeling and optimization in mobile, ad hoc, and wireless networks (WiOpt05)*, Riva del Garda, Italy, pp. 31–40, 3-7 April 2005.
- [27] "The network simulator - ns-2", Information Sciences Institute, University of Southern California, <http://www.isi.edu/nsnam/ns/>.

- [28] M. Wellens, M. Petrova, J. Riihijarvi, and P. Mahonen, "Building a better wireless mousetrap: need for more realism in simulations," *Second Annual Conference on Wireless On-demand Network Systems and Services, WONS 2005*, pp. 150 – 157, 19-21 January 2005.
- [29] M. E. J. Newman, S. H. Strogatz, and D. J. Watts, "Random graphs with arbitrary degree distributions and their applications," *Physical Review E*, vol. 64, 026118, July 2001.
- [30] G. Nemeth and G. Vattay, "Giant clusters in random ad hoc networks," *Physical Review E (Statistical, Nonlinear, and Soft Matter Physics)*, vol. 67, pp. 036110/1–036110/6, March 2003.
- [31] I. Glauche, W. Krause, R. Sollacher, and M. Greiner, "Continuum percolation of wireless ad-hoc communication networks," *Physica A*, vol. 325, pp. 577–600, 2003.
- [32] M. Acharya, J. Girao, and D. Westhoff, "Performance measurements of the saturation throughput in IEEE 802.11 access points," *Proceedings of the 3rd international symposium on modeling and optimization in mobile, ad hoc, and wireless networks (WiOpt05), Riva del Garda, Italy*, pp. 129–138, 3-7 April 2005.
- [33] S. Bohacek, A. Ilic, and V. Sridhara, "On the predictability of link lifetimes in urban MANETs," *Proceedings of the 3rd international symposium on modeling and optimization in mobile, ad hoc, and wireless networks (WiOpt05), Riva del Garda, Italy*, pp. 209 – 218, 3-7 April 2005.
- [34] B. Bollobas, *Random Graphs*. Academic Press, 1985.
- [35] B. Bollobas, *Modern Graph Theory*. Springer-Verlag New York, 1998.
- [36] T. Emden-Weinert, "Graphs: Theory-algorithms-complexity", <http://people.freenet.de/Emden-Weinert/graphs.html>.
- [37] W. T. Tutte, *Graph Theory as I Have Known It*. Oxford, England: Oxford University Press, August 1998.
- [38] D. J. Watts, *Small World, the dynamics of networks between order and randomness*. Princeton University Press, Princeton, New Jersey, 1999.
- [39] D. J. Watts and S. H. Strogatz, "Collective dynamics of 'small-world' networks," *Nature*, vol. 393, pp. 440–442, 1998.
- [40] A. Broder, R. Kumar, F. Maghoul, P. Raghavan, S. Rajagopalan, R. Stata, A. Tomkins, and J. Wiener, "Graph structure in the web," *Computer networks, Proceedings of the 9th international World Wide Web conference on Computer networks*, vol. 33, pp. 309 – 320, May 2000.
- [41] T. Blass, *The Man Who Shocked the World: The Life and Legacy of Stanley Milgram*. Basic Books, March 2004.
- [42] P. Erdos and A. Renyi, "On the evolution of random graphs," *Publications of the Mathematical Institute of the Hungarian Academy of Sciences*, vol. 5, pp. 17–61, 1960.
- [43] H. G. S. E. Stefan Bornholdt (Editor), *Handbook of Graphs and Networks: From the Genome to the Internet*. Wiley-VCH, January 2003.

- [44] R. Albert and A. L. Barabasi, "Statistical mechanics of complex networks," *Review of Modern Physics*, vol. 74, pp. 47–97, January 2002.
- [45] G. Hooghiemstra and P. Van Mieghem, "On the mean distance in scale free graphs," *Submitted to Methodology and Computing in Applied Probability*, 2004.
- [46] R. V. der Hofstad, G. Hooghiemstra, and P. Van Mieghem, "Distances in random graphs with finite variance degrees," *Random Structures and Algorithms*, accepted, 2004, <http://www.nas.its.tudelft.nl/people/Piet/teljournal.html>.
- [47] K. Huang, *Introduction to Statistical Physics*. Taylor and Francis, 2001.
- [48] M. Molloy and B. Reed, "The size of the giant component of a random graph with a given degree sequence," *Combinatorics, Probability and Computing*, vol. 7, pp. 295–305, 1998.
- [49] P. Van Mieghem, "The asymptotic behaviour of queueing systems: Large deviations theory and dominant pole approximation," *Queueing Systems*, vol. 23, pp. 27–55, 1996.
- [50] P. Van Mieghem, *Performance Analysis of Communications Systems and Networks*. Cambridge University Press, 2005.
- [51] G. H. Hardy and E. M. Wright, *An Introduction to the Theory of Numbers*. Oxford University Press; 5th edition, February 1980.
- [52] M. Newman, D. Watts, and S. Strogatz, "Random graph models of social networks," *Proc. Natl. Acad. Sci. USA* 99, pp. 2566–2572, 2002.
- [53] S. Dorogovtsev and J. Mendes, *Evolution of Networks: From Biological Nets to the Internet and WWW*. Oxford University Press, January 2003.
- [54] A. L. Barabasi and R. Albert, "Emergence of scaling in random networks," *Science*, vol. 286, pp. 509–512, 1999.
- [55] B. Bollobas, O. Riordan, J. Spencer, and G. Tusnady, "The degree sequence of a scale-free random graph process," *Random Structure Algorithms*, vol. 18, pp. 279 – 290, 2001.
- [56] H. Bertoni, *Radio Propagation for Modern Wireless Systems*. Prentice-Hall PTR, 2000.
- [57] J. B. Anderson, T. S. Rappaport, and S. Yoshia, "Propagation measurements and models for wireless communication channels," *IEEE Communications Magazine*, vol. 33, pp. 42–49, January 1995.
- [58] B. H. Fleury and P. E. Leuthold, "Radiowave propagation in mobile communications: an overview of european research," *IEEE Communications Magazine*, vol. 34, pp. 70–81, February 1996.
- [59] D. Molkdar, "Review on radio propagation into and within buildings," *Microwaves, Antennas and Propagation, IEE Proceedings H*, vol. 138, pp. 61–73, February 1991.
- [60] R. Prasad, *Universal Wireless Personal Communications*. Artech House Publishers, 1998.
- [61] T. Rappaport, *Wireless Communications, Principles and Practice*. Upper Saddle River Prentice-Hall PTR, 2002.

- [62] “Lord rayleigh - biography”, The Nobel Foundation, <http://nobelprize.org/physics/laureates/1904/strutt-bio.html>.
- [63] A. B. Carlson, P. B. Crilly, and J. Rutledge, *Communication Systems, Forth edition*. McGraw-Hill, 2001.
- [64] E. J. Gumbel, *Statistics of Extremes*. Columbia University Press, 1967.
- [65] J. Diaz, J. Petit, and M. Serna, “Random geometric problems on $[0,1]^2$,” *Randomization and Approximation Techniques in Computer Science*, vol. 1518 of Lecture Notes in Computer Science, pp. 294–306, 1998. Springer-Verlag Berlin.
- [66] M. D. Penrose, “On k -connectivity for a geometric random graph,” *Random Structures and Algorithms*, vol. 15, pp. 145–164, 1999.
- [67] C. Bettstetter, “On the minimum node degree and connectivity of a wireless multihop network,” *Proc. 3rd ACM International Symposium on Mobile Ad Hoc Networking and Computing (MobiHoc), Lausanne, Switzerland*, pp. 80–91, June 9–11 2002.
- [68] C. Bettstetter, “On the connectivity of wireless multihop networks with homogeneous and inhomogeneous range assignment,” *Proceedings IEEE 56th Conference on Vehicular Technology*, vol. 3, pp. 1706 – 1710, September 2002.
- [69] R. Hekmat and P. Van Mieghem, “Degree distribution and hopcount in wireless ad-hoc networks,” *Proceeding of the 11th IEEE International Conference on Networks (ICON 2003), Sydney, Australia*, pp. 603–609, Sept. 28–Oct. 1 2003.
- [70] R. Hekmat and P. Van Mieghem, “Study of connectivity in wireless ad-hoc networks with an improved radio model,” *Proceeding of the 2nd workshop on modeling and optimization in mobile ad hoc and wireless networks (WiOpt04), Cambridge, UK*, pp. 142–151, March 28–26 2004.
- [71] C. Bettstetter and C. Hartmann, “Connectivity of wireless multihop networks in a shadow fading environment,” *Proceedings of the 6th ACM international workshop on Modeling analysis and simulation of wireless and mobile systems (MSWiM), San Diego, CA, USA*, pp. 28–32, September 2003.
- [72] R. Hekmat and P. Van Mieghem, “Interference power sum with log-normal components in ad-hoc and sensor networks,” *Proceeding of the 2nd workshop on modeling and optimization in mobile ad hoc and wireless networks (WiOpt05), Trentino, Italy*, April 2005.
- [73] P. Van Mieghem, “Paths in the simple random graph and the waxman graph,” *Probability in the Engineering and Informational Sciences (PEIS)*, vol. 15, pp. 535–555, 2001.
- [74] L. Sachs, *Applied Statistics, a handbook of techniques*. Springer-Verlag New York, second edition, 1982.
- [75] R. Hekmat and P. Van Mieghem, “Connectivity in wireless ad hoc networks with a log-normal radio model,” *Accepted paper for Mobile Networks and Applications, The Journal of Special Issues on Mobility of Systems, Users, Data and Computing*, 2005.

- [76] O. Dousse, F. Baccelli, and P. Thiran, "Impact of interference on connectivity in ad hoc networks," *IEEE Infocom2003*, April 2003.
- [77] S. Janson, D. E. Knuth, T. Luczak, and B. Pitel, "The birth of the giant component," *Random Structures and Algorithms*, vol. 4, no. 3, pp. 231–358, 1993.
- [78] A. S. Tanenbaum, *Computer Networks*. London: Prentice-Hall International, Inc., third ed., 1996.
- [79] J. Walrand, *Communication Networks, A First Course*. Boston: McGraw-Hill, second ed., 1998.
- [80] J. Capone and I. Stavrakakis, "Achievable QoS in an interference/resource-limited shared wireless channel," *IEEE Journal on Selected Areas in Communications*, vol. 17, pp. pp. 2041–2051, November 1999.
- [81] W. Ye, J. Heidemann, and D. Estrin, "Medium access control with coordinated adaptive sleeping for wireless sensor networks," *IEEE/ACM Transactions on Networking*, vol. 12, pp. 493–506, June 2004.
- [82] C.-K. Toh, "Maximum battery life routing to support ubiquitous mobile computing in wireless ad hoc networks," *IEEE Communications Magazine*, vol. 39, pp. 138 – 147, June 2001.
- [83] V. Kawadia and P. Kumar, "Power control and clustering in ad hoc networks," *IEEE Infocom 2003*, 2003.
- [84] V. Rodoplu and T. Meng, "Minimum energy mobile wireless networks," *IEEE Journal on Selected Areas in Communications*, vol. 17, pp. 1333–1344, August 1999.
- [85] C. E. Jones, K. M. Sivalingam, P. Agrawal, and J. C. Chen, "A survey of energy efficient network protocols for wireless networks," *Wireless Networks*, vol. 7, August 2001.
- [86] J. H. Schiller, *Mobile Communications, Second Edition*. Addison-Wesley, 2003.
- [87] R. Prasad and L. Munoz, *WLANs and WPANs towards 4G Wireless*. Artech House, 2003.
- [88] A. Sikora, *Wireless personal and local area networks*. England: John Wiley and Sons Ltd., 2003.
- [89] S.-L. Wu, Y.-C. Tseng, and J.-P. Sheu, "Intelligent medium access for mobile ad hoc networks with busy tones and power control," *IEEE Journal on Selected Areas in Communications*, vol. 18, pp. 1647–1657, September 2000.
- [90] L. Kleinrock and F. Tobagi, "Packet switching in radio channels: Part ii - the hidden terminal problem in carrier sense multiple-access and the busy-tone solution," *IEEE Transactions on Communication*, vol. COM-23, pp. 1417–1433, December 1975.
- [91] C.-K. Toh, V. Vassiliou, G. Guichal, and C.-H. Shih, "MARCH: a medium access control protocol for multihop wireless ad hoc networks," *MILCOM 2000, 21st Century Military Communications Conference Proceedings (IEEE MILCOM)*, vol. 1, pp. 512–516, Oct 22-25 2000.

- [92] W. Ye, J. Heidemann, and D. Estrin, "An energy-efficient MAC protocols for wireless sensor networks," *Proceedings of the IEEE Infocom 2002*, pp. 1567–1576, June 2002.
- [93] P. Havinga, "EMACs - EYES MAC protocol for sensor networks," *7th Wireless World Research Forum*, December 2002.
- [94] Z. Tang and J. Garcia-Luna-Aceves, "Collision-avoidance transmission scheduling for ad-hoc networks," *IEEE International Conference on Communications*, vol. 3, pp. 1788–1794, June 18–22 2000.
- [95] N. Jain, S. Das, and A. Nasipuri, "A multichannel MAC protocol with receiver-based channel selection for multihop wireless networks," *Proceedings of the 9th International Conference on Computer Communications and Networks (IC3N)*, October 2001.
- [96] Z. Haas and J. Deng, "Dual busy tone multiple access (DBTMA) - a multiple access control scheme for ad hoc networks," *IEEE Transactions on Communications*, vol. 50, pp. 975–985, June 2002.
- [97] E. S. Sousa and J. A. Silvester, "Optimum transmission range in direct-sequence spread-spectrum multihop packet radio networks," *IEEE journal on selected areas in communications*, vol. 8, pp. 762–771, June 1990.
- [98] T. J. Shepard, "A channel access scheme for large dense packet radio networks," *Proceedings of ACM SIGCOMM'96, Stanford University, California*, pp. 219–230, August 26–30 1996.
- [99] L. Kleinrock and J. A. Silvester, "Optimum transmission radii for packet radio networks or why siz is a magic number," *Proceedings of National Telecommunications conference*, pp. 4.3.1–4.3.5, December 1978.
- [100] F. Graziosi and F. Santucci, "Analysis of second order statistics of the SIR in cellular mobile networks," *50th IEEE Vehicular Technology Conference*, vol. 3, pp. 1316–1320, September 19–22 1999.
- [101] "Matlab ®", The MathWorks Inc., <http://www.mathworks.com>.
- [102] P. Pirinen, "Statistical power sum analysis for nonidentically distributed correlated lognormal signals," *The 2003 Finnish Signal Processing Symposium (FINSIG'03), Tampere, Finland*, pp. 254–258, May 19 2003.
- [103] L. F. Fenton, "The sum of log-normal probability distributions in scatter transmission systems," *IEEE Transactions on Communications Systems*, vol. 8, pp. 57–67, March 1960.
- [104] A. A. Abu-Dayya and N. C. Beaulieu, "Outage probabilities in the presence of correlated lognormal interferers," *IEEE Transactions on Vehicular Technology*, vol. 43, pp. 164–173, February 1994.
- [105] S. C. Schwartz and Y. S. Yeh, "On the distribution function and moments of power sums with log-normal components," *The Bell systems technical journal*, vol. 61, pp. 1441–1462, September 1982.
- [106] A. Safak and M. Safak, "Moments of the sum of correlated log-normal random variables," *IEEE 44th Vehicular Technology Conference*, vol. 1, pp. 140–144, June 8–10 1994.

- [107] C. L. Ho, "Calculating the mean and variance of power sums with two log-normal components," *IEEE transactions on Vehicular Technology*, vol. 44, pp. 756–762, November 1995.
- [108] A. Mawira, "Estimate of mean C/I and capacity of interference limited mobile ad-hoc networks," *2002 International Zurich Seminar on Broad-band Communications, Access, Transmission, Networking*, pp. 51–51–6, February 19–21 2002.
- [109] M. Abramowitz, *Handbook of Mathematical Functions*. Dover Publications, 1970.
- [110] R. Hekmat and P. Van Mieghem, "Interference in wireless multi-hop ad-hoc networks," *Proc. Med-hoc-net 2002 Conference, Sardegna, Italy*, Sept. 4–6 2002.
- [111] R. Hekmat and P. Van Mieghem, "Interference in wireless multi-hop ad-hoc networks and its effect on network capacity," *Wireless Networks Journal*, vol. 10, pp. 389–399, July 2004.
- [112] C. Edwards, *Calculus : with analytic geometry*. Upper Saddle River Prentice-Hall, 1998.
- [113] R. K. Ahuja, T. L. Magnanti, and J. B. Orlin, *Network flows: Theory, algorithms, and applications*. New Jersey: Prentice Hall, February 1993.
- [114] R. Beckers, J. L. Deneubourg, and S. Goss, "Trails and u-turns in the selection of the shortest path by the ant *lasius niger*," *Journal of theoretical biology*, no. 159, pp. 397–415, 1992.
- [115] M. Dorigo and T. Stutzle, *Ant Colony Optimization*. New Jersey: The MIT Press, July 2004.
- [116] J. Wozencraft and I. Jacobs, *Principles of Communication Engineering*. John Wiley & Sons, 1965.
- [117] J. Massey, "Information theory aspects of spread-spectrum communications," *IEEE Third International Symposium on Spread Spectrum Techniques and Applications, IEEE ISSSTA '94*, vol. 1, pp. 16–21, 1994.
- [118] M. J. Neely and E. Modiano, "Capacity and delay tradeoffs for ad hoc mobile networks," *IEEE Transactions on Information Theory*, vol. 51, pp. 1917–1937, June 2005.
- [119] P. Van Mieghem, G. Hooghiemstra, and R. W. van der Hofstad, "Scaling law for the hopcount," *Delft University of Technology, report2000125*, January 2000.
- [120] T. Pagtzis, P. Kirstein, and S. Hailes, "Operational and fairness issues with connection-less traffic over IEEE802.11b," *IEEE International Conference on Communications 2001*, vol. 6, pp. 1905–1913, 2001.
- [121] G. Di Caro and M. Dorigo, "Antnet: Distributed stigmergetic control for communications networks," *Journal of Artificial Intelligence Research (JAIR)*, vol. 9, pp. 317–365, 1998.